

AD-751 505

DEVELOPMENT OF WEAPON DELIVERY MODELS
AND ANALYSIS PROGRAMS. VOLUME I. SYSTEM
MODELING AND PERFORMANCE OPTIMIZATION

A. Ferit Konar

Honeywell, Incorporated
Minneapolis, Minnesota

April 1972

DISTRIBUTED BY:

NTIS

National Technical Information Service
U. S. DEPARTMENT OF COMMERCE
5285 Port Royal Road, Springfield Va. 22151

AD751505

AFFDL-TR-71-123
Volume I

DEVELOPMENT OF WEAPON DELIVERY MODELS AND ANALYSIS PROGRAMS

Volume I. System Modeling and Performance Optimization

A. FERIT KONAR

HONEYWELL INC.

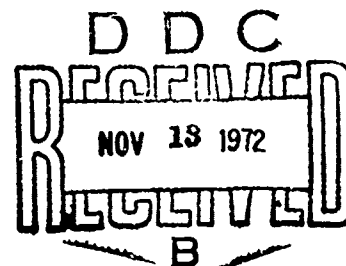
TECHNICAL REPORT AFFDL-TR-71-123, VOLUME I

APRIL 1972

Reproduced by
NATIONAL TECHNICAL
INFORMATION SERVICE
U S Department of Commerce
Springfield VA 22151

Approved for public release; distribution unlimited.

AIR FORCE FLIGHT DYNAMICS LABORATORY
AIR FORCE SYSTEMS COMMAND
WRIGHT-PATTERSON AIR FORCE BASE, OHIO



R
206

NOTICE

When Government drawings, specifications, or other data are used for any purpose other than in connection with a definitely related Government procurement operation, the United States Government thereby incurs no responsibility nor any obligation whatsoever; and the fact that the government may have formulated, furnished, or in any way supplied the said drawings, specifications, or other data, is not to be regarded by implication or otherwise as in any manner licensing the holder or any other person or corporation, or conveying any rights or permission to manufacture, use, or sell any patented invention that may in any way be related thereto.

ACCESSION for	
NTIS	White Section <input checked="" type="checkbox"/>
DOC	Half Section <input type="checkbox"/>
UNANZONCED	<input type="checkbox"/>
JUSTIFICATION	
BY	
DISTRIBUTION/AVAILABILITY CODES	
Dist.	AVAIL. and/or SPECIAL
<input checked="" type="checkbox"/>	<input type="checkbox"/>

Copies of this report should not be returned unless return is required by security considerations, contractual obligations, or notice on a specific document.

Unclassified

Security Classification

DOCUMENT CONTROL DATA - R & D		
(Security classification of title, body of abstract and indexing annotation must be entered when the overall report is classified)		
1. ORIGINATING ACTIVITY (Corporate author)		2a. REPORT SECURITY CLASSIFICATION
Honeywell Inc. Systems and Research Division, Research Dept. Minneapolis, Minnesota 55413		Unclassified
		b. GROUP
		NA
3. REPORT TITLE		
DEVELOPMENT OF WEAPON DELIVERY MODELS AND ANALYSIS PROGRAMS Volume I. System Modeling and Performance Optimization		
4. DESCRIPTIVE NOTES (Type of report and inclusive dates)		
Final Technical Report - 5 October 1970 - 5 October 1971		
5. AUTHOR(S) (First name, middle initial, last name)		
A. Ferit Konar		
6. REPORT DATE	7a. TOTAL NO. OF PAGES	7b. NO. OF REFS
April 1972	206	57
8a. CONTRACT OR GRANT NO.	9a. ORIGINATOR'S REPORT NUMBER(S)	
F33615-71-C-1059	12261-FR1, Vol. I	
b. PROJECT NO.	9b. OTHER REPORT NO(S) (Any other numbers that may be assigned this report)	
8219	AFFDL-TR-71-123 , Vol. I	
c. Task No. 821911		
d.		
10. DISTRIBUTION STATEMENT		
Approved for public release; distribution unlimited.		
11. SUPPLEMENTARY NOTES		12. SPONSORING MILITARY ACTIVITY
		Air Force Flight Dynamics Laboratory Air Force Systems Command Wright-Patterson Air Force Base, Ohio
13. ABSTRACT		45433
<p>The concern in the work reported is the development of a dynamic precision weapon delivery system model for analyzing the effects of system parameters and disturbances on delivery performance. In addition, a methodology of precision weapon delivery flight control design is developed, without considering the pilot as a control element. The aircraft model accommodates a wide variety of airframe nonlinear dynamics, control points and methods and measurement systems. The bomb model is general enough for a variety of dive-bomb angles, release altitudes and release speeds. The circular error probable (CEP) at impact is chosen as a measure of weapon delivery performance, and a technique is developed for relating the effects of flight control parameters, airframe dynamics, measurement errors and gust disturbances to this measure by using the system model. Demonstration analysis is performed to show how to identify critical system parameters with regard to the delivery of an iron bomb and to illustrate how the method of analysis can be used. Digital computer subprograms (in Fortran IV language) were developed and documented implementing the mathematical models. Extensive use of subroutines were made to provide flexibility. Development and documentation of the computer programs and the demonstration example are presented in Volume II of this report. Finally, by consolidating the subprograms, an efficient and versatile "Armament Delivery Analysis Programming System (ADAPS) was developed for the analysis and design of weapon delivery systems.</p>		

DD FORM 1473

REPLACES DD FORM 1473, 1 JAN 64, WHICH IS OBSOLETE FOR ARMY USE.

Unclassified

Security Classification

Unclassified

Security Classification

14 KEY WORDS	LINK A		LINK B		LINK C	
	ROLE	WT	ROLE	WT	ROLE	WT
Weapon Delivery modeling Error analysis CEP Optimal control Program						

Unclassified

Security Classification

DEVELOPMENT OF WEAPON DELIVERY MODELS AND ANALYSIS PROGRAMS

Volume I. System Modeling and Performance Optimization

A. FERIT KONAR

Approved for public release; distribution unlimited.

FOREWORD

This document is the first of the three volumes of the final report of a study conducted for the United States Air Force Under the Contract F33615-71-C-1059, "Development of Weapon Delivery Models and Analysis Programs." Approximately one man year of effort was covered by the contract. It was initiated under Project No. 8219, "Stability and Control Investigations," Task No. 821911, "Flight Control System Analysis," and administered by the Air Force Flight Dynamics Laboratory, Wright-Patterson Air Force Base, Ohio. Major Harvey M. Paskin (FGC), and Mr. Alonzo J. Connors (FGC) were project engineers.

The technical work reported was conducted by the Research Department of the Systems and Research Division of Honeywell Inc. Dr. A. Ferit Konar was the principal investigator; Mr. M. D. Ward was the programmer analyst. Dr. G. B. Skelton and Dr. E. E. Yore were program managers. Technical consultation was provided by Dr. Gunter Stein and Mr. C. R. Stone of Honeywell Inc.

The reporting period was October 1970 to July 1971. The report was first submitted in August 1971. The contractor's report number is Honeywell document 12261-FR1.

The author of this study would like to thank Major Harvey H. Paskin for his enthusiastic support, for his technical leadership, and for his assistance in obtaining bomb data. The author would also like to thank Mr. Alonzo J. Connors for providing direction and assistance in testing the analysis programs.

This work has benefited considerably from the past efforts of the colleagues of the author in Honeywell. They are too numerous to be named individually here. However, the author would like to acknowledge the works of Drs. G. B. Skelton, C. A. Harvey on quadratic optimization, Dr. E. E. Yore for his simulation setup of F-4, Mr. K. D. Graham for fire control, and Mr. H. E. Bean for the THRUST program.

This technical report was reviewed and is approved.



C.B. Westbrook
Chief, Control Criteria Branch
Flight Control Division
Air Force Flight Dynamics Laboratory

TABLE OF CONTENTS

	Page
SECTION I	
INTRODUCTION	1
SECTION II	
PERFORMANCE ANALYSIS AND OPTIMAL DESIGN OF WEAPON DELIVERY PROCESSES	3
Air-to-Ground Delivery Processes	3
Mathematical Models	7
Dive and Pull-up Phases	7
Release Phase	13
Release Transient Phase	14
Weapon Free-Fall Phase	15
Optimal Control of Perturbation Models	16
Overall Organization of ADAPS	19
SECTION III	
DEVELOPMENT OF A NONLINEAR DYNAMICAL MODEL FOR RIGID-BODY MOTIONS	21
Development of the Differential Equations of Motion	21
Reference Frames	21
The Dynamics of Motion	23
The Kinematics of Motion	25
Gravity Components in the Body Axes	35
Summary of the Analysis	36
Development of Integration Algorithm for the Equations of Motion	40
SECTION IV	
DEVELOPMENT OF TOTAL FORCE AND MOMENT SYSTEM FOR RIGID BODIES MOVING IN UNSTEADY AIRMASS	42
Aerodynamic Forces and Moments for Aircraft	42
The Functional Form of the Aerodynamic Forces and Moments	42
Usage of Aerodynamic Data	43
Total Aerodynamic Coefficient Model for Aircraft	47
Aerodynamic Force and Moment Model for Bomb	49
Simplified Aerodynamic Model for Bomb	49
Development of a Model for Thrust Forces and Moments	52
AGEometrical Model of Thrust Producers	53
Dynamical Model for Thrust Magnitudes	56
Dynamical Model for Thrust Orientation Actuators	57
Effect of Moving Air Mass on the Aerodynamics of a Rigid Body	58

TABLE OF CONTENTS -- CONTINUED

	Page
Modeling for the Influence of Unsteady Air Mass	58
Modeling for the Equivalent Linear and Angular Velocities	60
SECTION V DEVELOPMENT OF MEASUREMENT SYSTEM MODEL	72
Development of a Geometric Model for Measurements	72
Geometrics of Control Measurements	73
Air Data Measurements	77
Fire Control Measurements	80
Development of a Dynamical Model for Sensors	84
SECTION VI LINEARIZATION OF THE WEAPON DELIVERY PROCESS	88
Linearization Process	89
Development of the Perturbation Equations	89
Development of the Nominal Solution	92
Development of the First Partial	94
Mixed Linearization Approach	96
Pure Numerical Linearization Approach	100
Transformation of the Perturbation States	104
SECTION VII DEVELOPMENT OF THE NOMINAL STATE AND PARAMETER (TRIMMING)	111
Algebraic Trimming	111
Algebraic Trimming for Dive and Pull-up Trajectory	112
Development of the Finite Iteration Algorithm	120
Finite Iteration Algorithm versus Newton- Raphson Process	122
Trimming with an Autopilot	123
SECTION VIII DEVELOPMENT OF A PERFORMANCE MEASURE FOR OPTIMAL WEAPON DELIVERY CONTROLLER DESIGN	125
Development of the Initial State of Bomb	125
Nominal State of Bomb at Release	126
Perturbation State of Aircraft at Release	129
Perturbation State of Bomb at Release	131
Perturbation State Transition During Release Transient	132

TABLE OF CONTENTS -- CONTINUED

		Page
	Perturbation State of Bomb at Impact Planes	134
	Development of Statistical Performance Measure for Weapon Delivery Processes	135
	Approximation to Weapon Delivery Performance	141
	Development of Design Performance Index	143
	Development of the Release Error Propagation Process	144
	Development of the Variance Contribution Matrix	147
SECTION IX	DEVELOPMENT OF A METHOD FOR NON- STATIONARY OPTIMAL WEAPON DELIVERY CONTROLLER DESIGN	149
	Statement of the Problem	149
	Solution of the Problem	150
	Minimization of the Continuous Model	150
	State Estimation	154
	Combining the Results	154
	Discretization of the Continuous Process and Optimization of the Discretized System	155
	Discretization by Rectangular Rule	156
	Discretization by a Matrix Exponential	157
	Solution for the Discretized Model with Piecewise Constant Controller	158
SECTION X	DEVELOPMENT OF A METHOD FOR STATIONARY OPTIMAL CONTROLLER DESIGN	164
	Description of Algorithm LYAK	164
	Method of Solution	164
	Choice of the Parameter α	165
	Convergence Criteria	165
	Description of Algorithm DIAK	165
	Stationary Optimization Problem for Controller Gains	165
	Method of Solution	167
	Stationary Optimization Problem for the Estimator Gains	168
	The Steady-State Covariance with the Optimal Estimator	169
SECTION XI	CONCLUSIONS AND RECOMMENDATIONS	173
	Significant Qualitative Results	173
	Recommendations for Future Analysis and Modeling Work	173
	Conclusions	174

TABLE OF CONTENTS -- CONCLUDED

	Page
APPENDIX I DEVELOPMENT OF A METHOD FOR FIXED- FORM OPTIMAL CONTROLLER DESIGN	175
APPENDIX II DEVELOPMENT OF THE NOMINAL RELEASE EQUATIONS	180
REFERENCES	187

LIST OF ILLUSTRATIONS

Figure		Page
1	Basic Dive-Bombing Trajectories for the Manual Release	4
2	Angles for the Iron-Sight Delivery	4
3	High-Approach Dive Toss (with automatic release)	6
4	Overall System Diagram	8
5	Overall Organization of Armament Delivery Analysis Programming System (ADAPS)	19
6	Earth-Fixed and Moving Coordinate Frames	22
7	Body Orientation and Euler Angles	26
8	Relations Between Fixed and Moving Frames	32
9	Body and Stability Axes Systems	45
10	Aerodynamic Force Resolution	45
11	Moment Reference Center with Respect to Mass Center	46
12	Definition of Stability-Like Axes for Bomb	50
13	Geometry of a Thrust Producer	53
14	Dynamical Model for a Thrust Producer	56
15	Rigid Body in an Unsteady Air Mass	58
16	Description of the Mean Wind	60
17	Structure of the Equivalent-Linear and Angular Velocity Gust Generator (Dryden Model)	67
18	State Equation of the Gust Generator	68
19	State Diagram for Side Gust Filter	70

LIST OF ILLUSTRATIONS -- CONTINUED

20	General Structure of Perfect-Measurement Model	73
21	Axes Systems for Linear Velocity and Acceleration Measurements: (a) Body Axes, (b) Instrument Axis	74
22	Radar Measurement Geometry: (a) Body Axes, (b) Radar Axes, (c) Earth Axes	81
23	Dynamical Significance Radius	85
24	Measurement Dynamics of i^{th} Scalar Signal	85
25	General Measurement Model	87
26	Nominal Trajectory for Dive-Toss Maneuver: (a) Dive Phase, (b) Pull-up Phase, (c) Free-Fall Phase, (d) Release Transient Phase	88
27	Development of Nominal Trajectories and Linearized Equations of Motion for an Aircraft Weapon Pair for a Dive-Toss Maneuver in xz Plane	90
28	State Diagram of the Nonlinear Equations of Motion of a Rigid Body	97
29	"Data Increment" and "Parameter Perturbation" Cubes	103
30	Linearized State Equations of Airframe with Nominal State Component Assignment	105
31	Linearized State Equations of Airframe with Channeled State Component Assignment	106
32	Full-Gust Filter State Equations with Channeled State Component Assignment	109
33	Reduced-Gust Filter State Equations	110
34	Nominal Dive and Pull-Up Trajectory	113
35	Finite Iteration Algorithm	124
36	Newton-Raphson Process	124
37	Trim by Autopilot	124

LIST OF ILLUSTRATIONS -- CONCLUDED

38	Discrete Nonlinear Transition of the State at Release	127
39	Bomb Station Geometry	127
40	Linearization About the Nominal Release Point [$x(t_r)$, t_r]	129
41	Weapon State Transition During Release Transient Phase	133
42	Structure of Perturbation State of Bomb Just After Release	133
43	Linearization About the Nominal Impact Point [$x(t_f)$, t_f]	134
44	Evolution of the Region D	138
45	Regions for Horizontal and Vertical CEP Evaluations	139
46	CEP Parameter versus Standard Deviation Ratio	140
47	HPA Parameter versus Standard Deviation Ratio	142
48	Bomb Dynamics with a Wind Driver	144
49	Decomposition of the State Vector	156
50	Discretized Dynamics of Overall System	163
51	Weapon-Release Geometry in the $x_e - z_e$ Plane	182

LIST OF TABLES

I	Effective Thrust Output Coefficients, $j = 1, 2$	57
II	Wind-Filter Coefficients	69
III	Terminology for the Radius of Half Probability Ball	139

LIST OF SYMBOLS

A, B	Linear dynamics and control matrices
b	Wing span (ft)
c	Mean aerodynamic chord (ft)
ΣC_D	Drag coefficient, drag/ $(\bar{q}S)$
ΣC_L	Lift coefficient, lift/ $(\bar{q}S)$
ΣC_l	Rolling moment coefficient, $(L/\bar{q}Sb)$
ΣC_m	Pitching moment coefficient, $(M/\bar{q}Sb)$
ΣC_n	Yawing moment coefficient, $(N/\bar{q}Sb)$
ΣC_y	Side-force coefficient, $(Y/\bar{q}S)$
ΣC_z	Downward force coefficient, $(Z/\bar{q}S)$
X, Y, Z	Aerodynamic x, y, z forces acting on aircraft (lbs)
g	Acceleration of gravity, (ft/sec^2)
h	Altitude (ft)
I_x, I_y, I_z, I_{xz}	Moments and product of inertia (with respect to body axes, slug ft ²)
M	Mach number
L, M, N	Aerodynamic moments about x, y, z axes (ft-lbs)
p, q, r	Roll, pitch and yaw angular velocity (rad/sec)
\bar{q}	Dynamic pressure (lb/ft ²)
S	Wing surface area (ft ²)
T_1, T_2	Effective thrust of engine 1, and 2 respectively (lbs)
T_{c1}, T_{c2}	Throttle commands to engine 1, and 2 respectively (percent)
Pow	Maximum thrust level indicator, (0 or 1)

V_a	Speed of cg with respect to air mass
V	Speed of cg with respect to earth-fixed frame
W	Speed of airmass with respect to earth-fixed frame
u	Control input vector
u, v, w	Translational velocities along axes x, y, z (ft/sec)
u_g, v_g, w_g	Gust components in body axes (ft/sec)
x	Aircraft state
x, y, z	Body-fixed vehicle axes or coordinates
x_e, y_e, z_e	Earth axes or coordinates (ft) (origin at the impact point)
X_s, Y_s, Z_s	Aerodynamic force components along stability axes (lbs)
X_T, Y_T, Z_T	Thrust force components in body axes (lbs)
α	Angle of attack (rad)
α_w	Angle of attack of wing (deg)
β	Angle of sideslip (rad)
γ	Flight path angle (rad)
δ_a	Aileron deflection (deg)
δ_{lg}	Landing gear deflection (deg)
δ_r	Rudder deflection (deg)
δ_s	Stabilator deflection (deg)
δ_{sb}	Speed brake deflection (deg)
δ_{sp}	Spoiler deflection (deg)
θ	Pitch attitude (rad)
ϕ	Roll attitude (rad)
ψ	Yaw attitude (rad)

SECTION I

INTRODUCTION

For aircraft weapon systems which deliver unguided armament (guns, rockets, bombs), small improvements in delivery accuracy can result in substantial reductions of weapon dispersion [1]. The net result is a reduced number of sorties required per target and hence less exposure of aircraft to enemy defenses. Consequently, the analysis of precision weapon delivery has become an area of extreme interest. Two approaches to the problem have evolved. The first is to analyze the precision weapon delivery task by detailed simulation of the tactical situation and the second is to investigate the effects of initial condition errors, release point errors, and gust disturbance errors by propagating them along the weapons trajectories to impact. For the latter approach, a method of analysis is needed which considers the effects of flight control parameters, airframe dynamics, measurement errors and gust disturbances on the release parameters and then propagates these release errors to impact to obtain a meaningful measure of weapon system performance.

Such an analysis tool can then be used in connection with the former approach to establish critical measurement requirements as well as to evaluate the effects of various control points and methods prior to large-scale simulation or flight tests.

In this study, a dynamic precision weapon delivery system model, a method of performance analysis, and a set of computer programs are developed to evaluate effects of various process parameters on overall weapon system performance, with particular emphasis on flight control parameters, airframe dynamics, measurement points and errors, and gust environments. The model of the process assumes precision control without considering the dynamics of the operator as a control element. The controller is in the form of an optimal controller consisting of an optimal estimator and optimal feedback gains. The model is general enough, however, to consider existing controllers as well as the operator in the loop. For the latter case (i. e., pilot weapon delivery) mathematical models of the operator have to be incorporated into the present model [2, 3, 4, 5]. Since the operator tracking error is one of the major contributors to impact dispersion, the piloted delivery deserves separate attention. The model is also flexible enough for considering alternate airframe dynamics/control points/measurement system combinations. The developed armament model is for the delivery of iron bombs. It is sufficiently general to treat a variety of dive angles and release altitudes and bomb characteristics. The delivery of other weapons can be considered also by minor modifications.

The impact covariance and the circular error probable (CEP) are used as measures of delivery performance.

A simplified variance analysis is given in [5] by ignoring cross-covariance terms. The elimination of the cross-variance terms was pursued in [2] by choosing random variables which are uncorrelated.

In this work the full impact covariance matrix is developed and retained in the analysis using the complete dynamical model. The concepts of half-probability circle and circular error probable are extended to half-probability ball and spherical error probable. These are thought to be more meaningful performance measures in air-to-air delivery.

The complete report is divided into three volumes. Volume I contains the works on the weapon delivery system modeling and optimization. Volume II documents the programs which implement the analysis developed in Volume I. Volume III contains a demonstration example to illustrate how these programs are used.

In this volume the presentation begins with a brief description of the weapon delivery process and the approach taken for the performance analysis of the overall system. In addition, the synthesis of the optimal weapon delivery controller is outlined and the overall organization of the analysis program is given. In Section III the development of a mathematical model for the six-degree-of-freedom motion of aircraft and weapon is presented. In Section IV the development of the total force and moment system for the aircraft and weapon moving in an unsteady airmass is given. The wind model is developed in that section also. The development of the measurement system model is presented in Section V. The nonlinear observation geometry as well as sensor dynamics are considered. In Section VI the process of linearization is treated. The transformation of the perturbation states is presented in that section also. The development of the nominal states and parameters (trimming) for the linearization is discussed in Section VII. The methods of algebraic as well as the autopilot trim are presented. The performance measure development for the analysis and design of the weapon delivery controller is given in Section VIII. The circular error probable performance index is generalized to the spherical error probable for the air-to-air weapon delivery. In Section IX a method for nonstationary optimal weapon delivery controller design is presented. Both deterministic and stochastic disturbances are considered. This is followed by the presentation of a stationary controller design method in Section X. The iterative solutions of the Lyapunov as well as the Riccati equations are given in that section also. Section XI summarizes the analysis and modeling work and lists recommendations for additional areas of study and extensions.

The reduced controller (fixed-form) design method is given in Appendix I. The development of the fire control equations for the nominal release time is given in Appendix II.

SECTION II

PERFORMANCE ANALYSIS AND OPTIMAL DESIGN OF WEAPON DELIVERY PROCESSES

This section provides an overview of the approach taken for the system analysis and the optimal design of weapon delivery processes. First, a brief description of the air-to-ground weapon delivery processes is presented; then the mathematical models of the subsystems and the overall delivery system are described. Subsequently the optimal perturbation control of the delivery model is discussed, and finally, the overall organization of the "Armament Delivery Analysis Programming System (ADAPS)" is given.

AIR-TO-GROUND DELIVERY PROCESSES

Air-to-ground delivery is currently accomplished with a limited number of well-defined attack maneuvers, each designed for a particular tactical situation (i. e., for given target type and defenses, aircraft type, armaments and electronic aids). Figure 1 shows some of the basic dive-bombing trajectories used mostly for manual (iron-sight) delivery [7]. In this delivery technique, the pilot flies a fairly consistent preplanned flight path which brings the aircraft to an initially set release condition, e. g., release altitude, ground speed and dive angle. The weapon is released when these three conditions are satisfied simultaneously in the ideal cases and the target passes through the center of a depressed reticle sight. The depressed reticle sight display system is used most often for target tracking during conventional air-to-ground weapon delivery.

The aim dot (pipper) of the reticle image, which the pilot attempts to position onto the target by steering the aircraft, is "depressed" below the velocity vector of the aircraft as shown in Figure 2 in order to display the nominal bomb impact point corresponding to the preselected nominal release condition.

The setting of the sight angle is determined from the nominal trajectory line-of-sight angle, γ_{los} . The sight depression angle, η , is the angle of the line of sight below the fuselage line (x-axis) of the aircraft. The pilot determines from tabulated data the correct fixed sight depression angle for the selected pickle (release) conditions, and adjusts the sight depression mechanism to this setting. He dives towards the target in such a way as to achieve the nominal release conditions at the time the pipper is on the target.

When using fire control computers, achieving the same accurate dive conditions is not necessary. Instead, the target is held on the center of an "undeepressed" reticle sight throughout the dive, and the weapon system is pickled at the desired release altitude. This initiates the weapon system computer for automatic release.

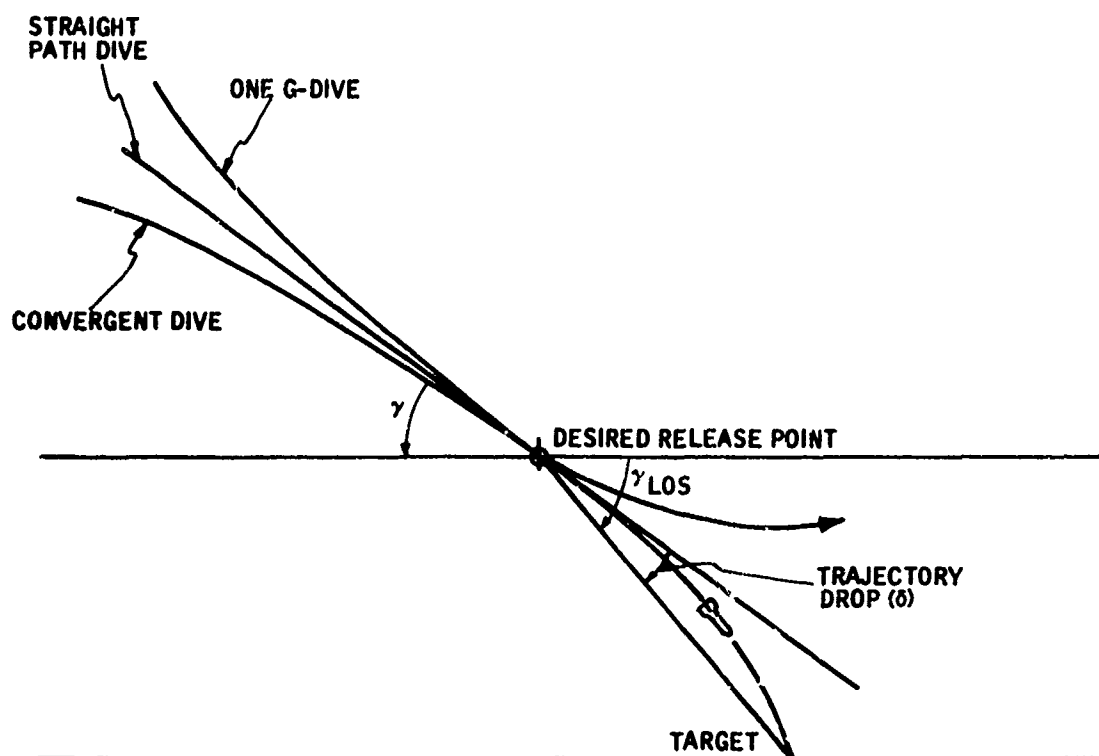


Figure 1. Basic Dive-Bombing Trajectories for the Manual Release

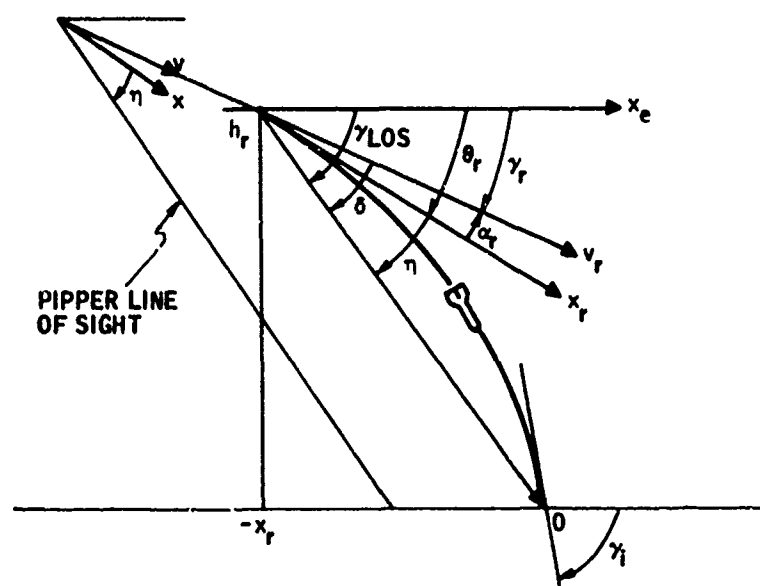


Figure 2. Angles for the Iron-Sight Delivery

The automatic release capability increases the number of possible delivery maneuvers. Figure 3 shows a typical example, the "high-approach dive-toss" maneuver with automatic release [8]. After target acquisition, this maneuver may be broken into four phases:

- Dive -- The aircraft is aligned with the target and flown to a desired release altitude, ground speed, and dive angle. The automatic weapon release computer set (WRCS) is (pickled at the desired altitude) for starting the pull-up. This initiates the weapons system computer for automatic release.
- Pull-up -- Following the release or pickle command, a constant-g pull-up is initiated. This serves the obvious purpose of reducing exposure to enemy defenses and also provides for clean aircraft-bomb separation. With fire control, weapon release will occur automatically during the pull-up maneuver.
- Release Transient -- Weapons are commonly released from their mounting racks with explosive charges that inject them into the airflow near wings or fuselage with uncertain linear and angular velocities. The resulting short-lived but poorly understood transients establish initial conditions for the weapon's free fall.
- Weapon Free-Fall -- The weapon follows a ballistic trajectory toward the target. This may be single-stage, as for iron bombs, or multi-stage, as for dispenser-type weapons. This work deals primarily with free-falling weapons, subject only to aerodynamic and gravity forces. The analysis program, however, is sufficiently general to accept nonballistic trajectories for, say, guided bombs or missiles.

While the dive-toss is a specialized attack maneuver, it can easily be parameterized with respect to acquisition altitude, dive angle, speed, release altitude and pull-up g's to generate various other maneuvers. For example, letting the dive angle γ vanish and executing a zero-g increment pull-up (and depressing the sight reticle appropriately) leads to the standard "low-level approach and laydown" maneuver. Similarly, $\gamma = 0$ with positive-g pull-up and automatic weapon release gives a "loft bombing" maneuver.

Because of this inherent generality, the discussions to follow are built around the dive-toss maneuver as a typical nominal trajectory.

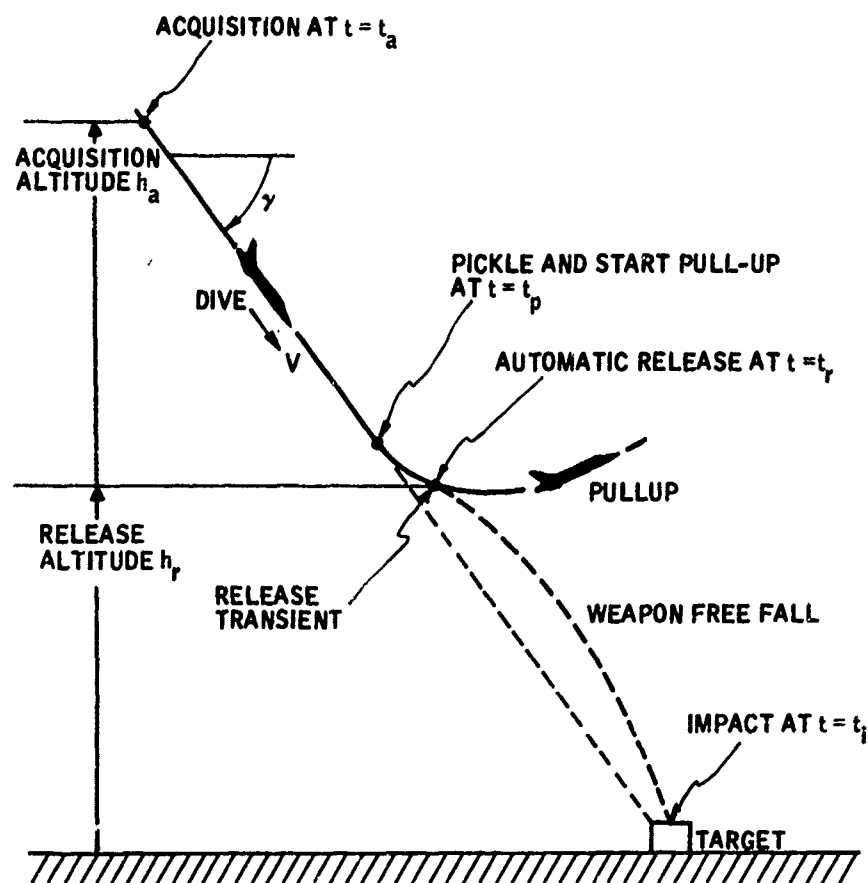


Figure 3. High-Approach Dive Toss (with automatic release)

MATHEMATICAL MODELS

The weapon delivery processes in this work are treated as nonlinear stochastic phenomena. This is both realistic and computationally attractive. For each phase of the attack maneuver, the process is linearized. CEP performance is evaluated with standard covariance analyses, and optimization is accomplished with linear-quadratic control theory. No repeated runs or Monte Carlo methods are required. Discussed below are the models applicable to each trajectory phase -- dive, pull-up, release transient, and weapon free-fall.

Dive and Pull-up Phases

The mathematical model for the dive and pull-up phases includes aircraft equations of motion, measurement equations with measurement noises and biases, and wind model equations for gusts and mean winds. The model also includes simple fire control equations which define the nominal pull-up and release times. The overall system contains both linear and nonlinear dynamics (Figure 4).

Airframe Model -- To handle arbitrary trajectories, various control points, and methods, the aircraft mode is described by a set of nonlinear, time-varying differential equations of the form

$$\dot{x}_p = f(x_p, \dot{x}_p, y_T, y_\delta, w, \bar{v})$$

where

- x_p = state vector of the aircraft
- y_T = vector of effective thrust inputs to the aircraft
- y_δ = vector of effective surface deflection inputs to the aircraft
- w = vector of disturbances (gusts) on the aircraft
- \bar{v} = vector of deterministic inputs (mean winds) to the aircraft

Actuator and Thrust System Model -- To allow variations in the effectiveness of thrust and aerodynamic surfaces, the actuator and thrust system outputs are assumed to be nonlinear functions of their states.

The actuator and thrust dynamics are modeled as follows:

$$\begin{aligned}\dot{x}_\delta &= F_\delta x_\delta + G_\delta u_\delta + K_{\gamma\delta} y_m \\ \dot{x}_T &= F_T x_T + G_T u_T + K_{\gamma T} y_m\end{aligned}$$

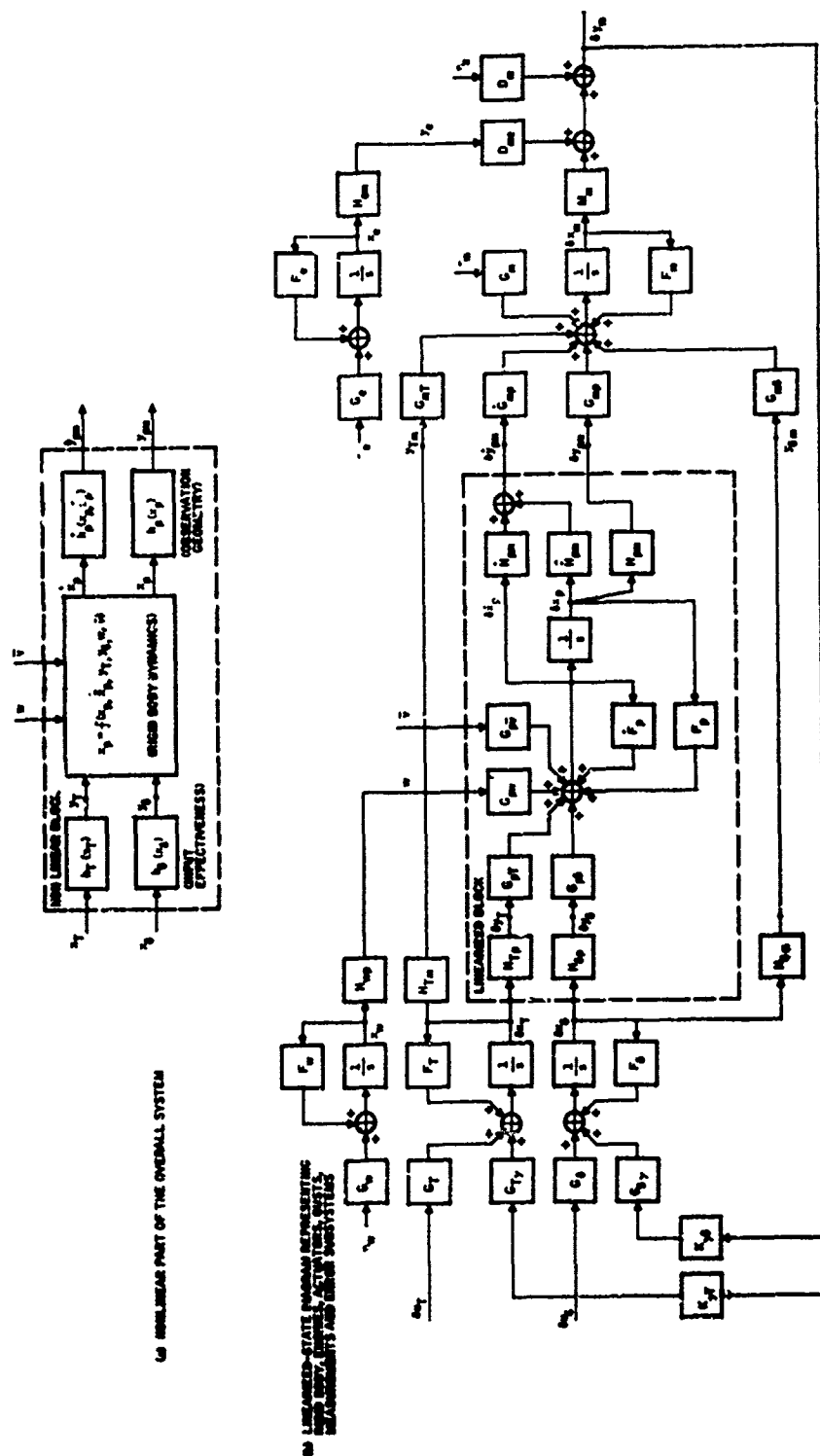


Figure 4. Overall System Diagram

with nonlinear outputs

$$y_{\delta} = h_{\delta}(x_{\delta})$$

$$y_T = h_T(x_T)$$

where

x_{δ} = actuator system state vector

x_T = thrust system state vector

y_{δ} = effective aerodynamic surface deflection output vector

y_T = effective thrust magnitude and deflection output vector

$K_{y_{\delta}}, K_{y_T}$ are arbitrary feedback gains and y_m is the measured signals as modeled below.

Measurement System Model -- To allow various measurement points and methods, the measurement system model is represented by a set of linear differential equations (i.e., sensor dynamics) with linear and nonlinear inputs. The nonlinear inputs correspond to the observation geometry of the state measurements

$$\begin{aligned} \dot{x}_m &= F_m x_m + G_{mp} y_{pm} + \dot{G}_{mp} \dot{y}_{pm} + G_{mT} y_{Tm} + G_{m\delta} y_{\delta m} \\ &+ G_m \eta_m \end{aligned}$$

$$y_m = M_m x_m + D_{me} \dot{y}_e + D_m \eta_a$$

where

x_m = measurement system state vector

y_{pm} = sensed signal vector for aircraft states

\dot{y}_{pm} = sensed signal vector for aircraft state derivatives

y_{Tm} = sensed signal vector for the thrust magnitude and thrust deflection states

$y_{\delta m}$ = sensed signal vector for the actuator states

η_m = white noise input vector to the measurement system

y_m = measured signals

y_e = output vector from the bias error process

η_a = additive, white measurement noise

The sensed signal vectors for the aircraft states are assumed to be nonlinear (i. e., observation geometry) functions of the states and its derivatives:

$$\dot{y}_{pm} = h(\dot{x}_p, \dot{x}_p)$$

$$y_{pm} = h(x_p)$$

The sensed signal vectors for the thrust and actuator states are assumed to be linear functions of the thrust and actuator states

$$y_{Tm} = H_{Tm} x_T$$

$$y_{\delta m} = H_{\delta m} x_{\delta}$$

The measurement system model not only contains those measurements for controlling the aircraft in flight (such as gyro and accelerometer outputs used for augmenting pilot control and for flexure control), but also those measurements necessary to estimate the states for the fire control equations (such as radar range, azimuth and elevation, and altimeter outputs to determine time of weapons release). Error sources in the measurement system are also included. Examples of these are gyro biases, accelerometer noise due to engine vibrations, and radar angle errors due to misalignment.

Linear Equations -- For small perturbation analysis the nonlinear part of the overall system (i. e., the nonlinear equations of motion, the effective input equations and the observation equations) is linearized about the nominal flight path to the form

$$\delta \dot{x}_p = \left(\frac{\partial f}{\partial x_p} \right) \delta x_p + \left(\frac{\partial f}{\partial \dot{x}_p} \right) \delta \dot{x}_p + \left(\frac{\partial f}{\partial y_T} \right) \delta y_T + \left(\frac{\partial f}{\partial y_{\delta}} \right) \delta y_{\delta} + \left(\frac{\partial f}{\partial w} \right) w + \left(\frac{\partial f}{\partial \bar{v}} \right) \bar{v}$$

$$\delta y_T = \left(\frac{\partial h_T}{\partial x_T} \right) \delta x_T$$

$$\delta y_{\delta} = \left(\frac{\partial h_{\delta}}{\partial x_{\delta}} \right) \delta x_{\delta}$$

$$\delta y_{pm} = \left(\frac{\partial h_p}{\partial x_p} \right) \delta x_p$$

$$\delta \dot{y}_{pm} = \left(\frac{\partial \dot{h}_p}{\partial x_p} \right) \delta x_p + \left(\frac{\partial \dot{h}_p}{\partial \dot{x}_p} \right) \delta \dot{x}_p$$

The measurement perturbation equations become

$$\begin{aligned}\dot{\delta x}_m &= F_m \delta x_m + G_{mp} \delta y_{pm} + \dot{G}_{mp} \delta \dot{y}_{pm} + G_{mT} \delta y_{Tm} \\ &+ G_{m\delta} \delta y_{\delta m} + G_m \eta_m\end{aligned}$$

Letting

$$\begin{aligned}F_p &= \frac{\partial f}{\partial x_p}, \quad \dot{F}_p = \frac{\partial \dot{f}}{\partial x_p}, \quad G_{p\delta} = \frac{\partial f}{\partial y_\delta}, \quad G_{pT} = \frac{\partial f}{\partial y_T}, \\ G_{pw} &= \frac{\partial f}{\partial w}, \quad G_{p\bar{v}} = \frac{\partial f}{\partial \bar{v}}, \quad H_{Tp} = \frac{\partial h_T}{\partial x_T}, \quad H_{\delta p} = \left(\frac{\partial h_\delta}{\partial x_\delta} \right) \\ H_{pm} &= \frac{\partial h_p}{\partial x_p}, \quad \dot{H}_{pm} = \frac{\partial \dot{h}_p}{\partial x_p}, \quad \ddot{H}_{pm} = \frac{\partial \ddot{h}_p}{\partial x_p}\end{aligned}$$

the state perturbation equations become

$$\begin{aligned}\dot{\delta x}_p &= F_p \delta x_p + \dot{F}_p \delta x_p + G_{pT} H_{Tp} \delta x_T + G_{p\delta} H_{\delta p} \delta x_\delta + G_{pw} w + G_{p\bar{v}} \bar{v} \\ \dot{\delta x}_m &= F_m \delta x_m + (G_{mp} H_{pm} \delta x_p + \dot{G}_{mp} \dot{H}_{pm}) \delta x_p + \dot{G}_{mp} \ddot{H}_{pm} \delta x_p \\ &+ G_{mT} H_{Tm} \delta x_T + G_{m\delta} H_{\delta m} \delta x_\delta + G_m \eta_m\end{aligned}$$

The wind gust model with the Dryden spectrum is described by

$$\begin{aligned}\dot{x}_w &= F_w(t) x_w + G_w \eta_w \\ w &= H_{wp} x_w\end{aligned}$$

where

$$\begin{aligned}x_w &= \text{gust filter state} \\ w &= \text{gust filter output} \\ \eta_w &= \text{white noise input to the filter}\end{aligned}$$

The measurement bias error vector $x_e(t)$ is modeled as a differential equation with a long time constant so that it remains approximately constant over the time of the weapon delivery maneuver. That is

$$\dot{x}_e = F_e x_e + G_e \eta_e$$

$$y_e = H_{em} x_e$$

$$x_e = \text{bias error vector state}$$

$$y_e = \text{error system output}$$

$$\eta_e = \text{white noise input to error filter}$$

The matrix G_e is selected so that the steady-state rms values of x_e are equal to the rms biases.

Defining

$$x = \text{col} [x_m, x_\delta, x_T, x_p, x_w, x_e]$$

$$y = y_m$$

$$u = \text{col} [u_\delta, u_T]$$

$$\eta = \text{col} [\eta_m, \eta_a, \eta_w, \eta_e]$$

the augmented mathematical model is obtained in the form of

$$[I - \dot{F}(t)] \dot{x} = F(t)x + G_u(t)u + G_v(t)\bar{v} + G_\eta \eta$$

$$y = M(t)x + D\eta$$

where the matrices F , G_u , G_v , G_η , M and D are given as follows:

$$F = \begin{bmatrix} F_m & G_{m\delta}H_{\delta m} & G_{mT}H_{Tm} & G_{mp}H_{pm} + \dot{G}_{mp}\bar{H}_{pm} & 0 & 0 \\ G_{\delta\gamma}K_{\gamma\delta}M_m & F_\delta & 0 & 0 & 0 & G_{\delta\gamma}K_{\gamma\delta}D_{me}H_{em} \\ G_{T\gamma}K_{\gamma T}M_m & 0 & F_T & 0 & 0 & G_{T\gamma}K_{\gamma T}D_{me}H_{em} \\ 0 & G_{p\delta}H_{\delta p} & G_{pT}H_{Tp} & F_p & G_{pw}H_{wp} & 0 \\ 0 & 0 & 0 & 0 & F_w & 0 \\ 0 & 0 & 0 & 0 & 0 & F_e \end{bmatrix}$$

$$\dot{\mathbf{F}} = \begin{bmatrix} 0 & 0 & 0 & \dot{G}_{mp} \dot{H}_{pm} & 0 & 0 \\ 0 & 0 & 0 & 0 & 0 & 0 \\ 0 & 0 & 0 & 0 & 0 & 0 \\ 0 & 0 & 0 & \dot{F}_p & 0 & 0 \\ 0 & 0 & 0 & 0 & 0 & 0 \\ 0 & 0 & 0 & 0 & 0 & 0 \end{bmatrix}$$

$$G_u = \begin{bmatrix} 0 & 0 \\ G_\delta & 0 \\ 0 & G_T \\ 0 & 0 \\ 0 & 0 \\ 0 & 0 \end{bmatrix}, \quad G_{\bar{v}} = \begin{bmatrix} 0 \\ 0 \\ 0 \\ G_{p\bar{v}} \\ 0 \\ 0 \end{bmatrix}, \quad G_\eta = \begin{bmatrix} G_m & 0 & 0 & 0 \\ 0 & G_{\delta\gamma} K_{\gamma\delta} D_m & 0 & 0 \\ 0 & G_{T\gamma} K_{\gamma T} D_m & 0 & 0 \\ 0 & 0 & 0 & 0 \\ 0 & 0 & G_w & 0 \\ 0 & 0 & 0 & G_e \end{bmatrix}$$

$$M = [M_m \ 0 \ 0 \ 0 \ 0 \ D_{me} H_{em}], \quad D = [0 \ D_m \ 0 \ 0]$$

This finishes the dive phase of the modeling. Figure 4 shows the overall system linearized state diagram.

Release Phase

For the automatic release, equations predicting the nominal pull-up time and the release time are needed. They are in the form of

$$t_p = h_{t_p}[x(t)], t < t_p$$

$$t_r = h_{t_r}[x(t_p), x(t)], t_p < t < t_r$$

where

t_p = nominal pull-up time

t_r = nominal time of weapon release

x = state vector of the nonlinear model

These are linearized at the nominal release time $t = t_r$ yielding

$$\delta t_p = \frac{\partial h_{t_p}'}{\partial x} \delta x(t_p)$$

$$\delta t_r = \frac{\partial h_{t_r}'}{\partial x(t_p)} [\delta x(t_p)] + \left(\frac{\partial h_{t_r}'}{\partial x} \right)' [\delta x(t_r)]$$

where prime indicates the transpose.

If the estimate of perturbation state $\delta \hat{x}$ is available instead of δx itself then in the above equations δx is replaced by $\delta \hat{x}$. These equations define the timing errors in the release time. Computation delay and rack relay delays contribute additional timing errors. These are modeled as independent additive random variables.

Release Transient Phase

The release transient phase is defined here as the period from the actual release time of bomb to the time when it leaves the region of the wings. Although this phase is not modeled in detail in this work, it has an important influence on the weapon delivery performance. The records in some cases show that when the bomb is ejected from the wing rack, the wing moves up (flexure) while the bomb follows a trajectory without safe separation. Because of the inability to predict bomb aerodynamics and stability in the region of the wing, experimental data are used for the description of the release transient phase. At the present time, the U.S. Air Force has a program called "SEEK EAGLE" [9, 10], which is both analytically and experimentally studying the release problem. In this work, the release transient phase is taken into account by introducing at release an independent, additive, stochastic, initial-condition error.

The state of bomb at release is described by

$$x_b = h_b(x_p)$$

The perturbation state of bomb at nominal release is then given by

$$\delta x_b(t_r) = H_b \delta x_p(t_r)$$

where

$$H_b = \left. \frac{\partial h_b}{\partial x_p} \right|_{t=t_r}$$

The state of bomb immediately following release transient is given by

$$\delta x_b(t_{r+}) = H_b [\delta x_p(t_r) + f_r \delta t_r] + H_r \xi_r$$

where

$$f_r = \dot{x}_p(t_r)$$

$$\delta t_r = \text{release time error}$$

$$H_r = \text{release transient error input matrix}$$

$$\xi_r = \text{release transient error}$$

Weapon Free-Fall Phase

In evaluating weapon delivery performance, translating the dispersion errors at bomb release to the impact of the bomb on the target and introducing errors which occur during the bomb trajectory is necessary. Two possibilities exist for satisfying this requirement -- bomb tables or trajectory computation. As trajectory computation allows treatment of various weapons and permits introduction of disturbances such as winds and uncertain bomb parameters during the trajectory, this method has been chosen in this work.

The bomb model is described by

$$\dot{x}_b = f(x_b, \dot{x}_b, u, w, \bar{v})$$

where

x_b = state vector of the bomb

u = input vector due to bomb imperfections

w = vector of disturbances (gusts) on the bomb

\bar{v} = vector of deterministic inputs (mean winds) to the bomb

For small-perturbation analysis, the nonlinear equations are linearized about the nominal free-fall flight path. This yields

$$\dot{\delta x}_b = F_b(t) \delta x_b + \dot{F}_b(t) \delta x_b + G_{bw}(t) w + G_{bv} \bar{v} + G_u u$$

The perturbation state of bomb at the impact on the horizontal plane is given by

$$\tilde{\delta x}(t_f) = \delta x(t_f) + f_b(t_f) \delta t_f$$

where

$\delta x(t_f)$ = the perturbation state of bomb at the nominal impact time t_f

$$f_b(t_f) = \dot{x}_b(t_f)$$

and

$$\delta t_f = \frac{\delta h(t_f)}{H(t_f)}$$

h , being the altitude state component of the bomb.

After having modeled the delivery process from the target acquisition to the impact, various performance measures can be defined for the analysis and design of the delivery system as presented in the following subsection.

OPTIMAL CONTROL OF PERTURBATION MODELS

The mathematical models just discussed provide small perturbation descriptions of the weapon delivery process. They are incomplete, however, in that the control variables u_d and u_T for the dive and pull-up phases of the trajectory are undefined. Adding arbitrary (linear) controllers to the mathematical model is a simple matter, and the developed aircraft model provided this option. Its utility lies in quick performance evaluations of all kinds of specific bomb systems and control schemes.

Tools are needed for evaluating intrinsic properties of various constraint configurations to answer questions such as:

- For a fixed complement of sensors and a given set of control inputs (control points), what minimum CEP is attainable within these constraints?
- What maximum CEP improvements does adding a single sensor to the above configuration give?
- What performance penalty exists for replacing a sensor with a noisier, but cheaper, version?

These questions call for performance analyses of optimal controllers.

A large number of possible optimal control problems can be formulated for the weapon delivery process -- for example, computing optimal attack trajectories. This has already been avoided by saying that these are largely predetermined by the tactical situation. Another problem is that of optimally controlling velocity deviations and target deviations from the reticle of the bomb sight during the dive phase of attack, followed either by an open-loop or optimally controlled pull-up. Assuming the steady-state operation, the performance index for this formulation takes the form

$$J_1 = E \{ q_{11} \delta V^2 + q_{22} \epsilon_h^2 + q_{33} \epsilon_y^2 + u' R u \}$$

where

δV = velocity deviation from nominal

ϵ_h = vertical deviation of target from center of reticle

ϵ_y = lateral deviation of target from center of reticle

$q_{11}, q_{22}, q_{33}, R$ = weighting coefficients and prime indicates the transpose

The solution mimics a pilot's own efforts to hold target alignment and velocity during his dive. The weights q_{ij} , R can be chosen via the iterative methods of quadratic equivalence [11]

Still another optimization problem which is followed in this work involves direct minimization of the HPA. This can be done with a performance index obtained in the following manner.

Strictly speaking, HPA is the area of a 0.5 probability circle centered at the mean impact point; CEP is its radius. For normal distributions with small cross correlations, this area can be closely approximated by

$$HPA = [q_x \sigma_x^2(t_f) + q_y \sigma_y^2(t_f)]$$

where σ_x and σ_y are downrange and crossrange standard deviations, and q_x, q_y are weightings which depend on the ratio σ_x/σ_y .

This expression, in turn, can be written in terms of the bomb release covariance matrix $X(t_{r+})$ using the perturbation equations of the bomb

$$\text{HPA} = \text{tr} \{X(t_{r+}) Q_r + X_f Q_f\}$$

where

Q_r = propagation weighting matrix for release errors

Q_f = propagation weighting matrix for the forced response

X_f = impact covariance response due to wind gusts.

tr = trace operator

The expression given above shows that, with this performance measure, performance analysis of a weapon delivery process reduced to standard linear covariance analysis.

To directly minimize HPA, therefore, the performance index should be

$$J_2 = \text{HPA} + \int_{t_0}^{t_r} \text{tr} \{u' R u\} dt$$

Note that this is a performance index with the terminal cost, penalizing errors at the nominal release time t_r . This means that the optimal controller will be time varying even if the system dynamics are stationary. This makes for expensive analysis. If stationary dynamics are adequate, modifying the performance index such that it yields a stationary controller is desirable. A steady-state version of J_2 does just that:

$$J_3 = \text{HPA} + \text{tr} \{R U\}$$

where

$$U = E \{u u'\}$$

An important distinction exists between the optimization problems based on J_2 and J_3 and the optimization problem based on the earlier index J_1 . Solutions of the J_1 problem depend on the type of sight in the aircraft -- whether it is fixed, or drift stabilized, or pitch stabilized, etc. Solutions of the J_2 , J_3 problems, on the other hand, completely bypass the sighting system. They depend only on the basic constraint configuration, i.e., on the signals available for measurement and on the control points available for manipulation.

OVERALL ORGANIZATION OF ADAPS

The various subroutines implementing the above model provide the capacity to analyze weapon delivery as a general linear time-varying, stochastic process or to analyze it as a much simplified process that is stationary during each of its phases. The one extreme offers fidelity to the physical situation, while the other offers low computing costs and the possibility of many analysis iterations. By using the program organization shown in Figure 5, both extremes (as well as the many possibilities in between) are readily attainable. In this organization, the individual subroutines are accessible from a main program with which they share common memory. They communicate with each other within the groups indicated. Optional inputs are provided to cover the various special possibilities discussed above. A detailed description of the overall organization of ADAPS is presented in the Section II of Volume II.

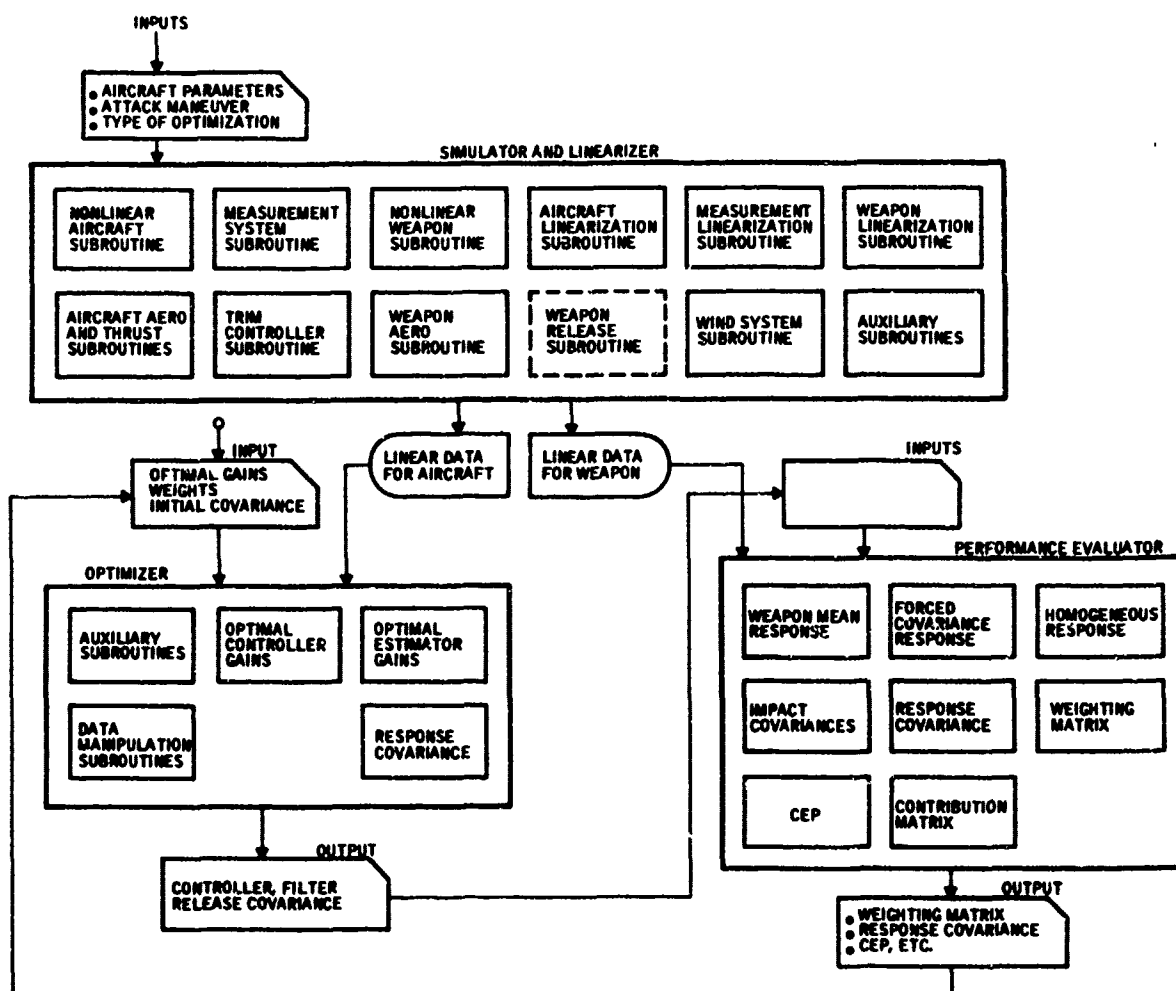


Figure 5. Overall Organization of Armament Delivery Analysis Programming System (ADAPS)

A typical analysis proceeds as follows:

- I - Linear Data Generation

1. Read input data for attack maneuver, read nonlinear aircraft aerodynamics.
2. Trim aircraft, and fly it to obtain nominal trajectory up to nominal release altitude.
3. Linearize the aircraft equations of motion numerically at specified time points during flight. Write on tape.
4. Read input data for nonlinear weapon aerodynamics.
5. Using the release conditions, generate free-fall trajectory by the nonlinear weapon model.
6. Linearize the weapon equations of motion numerically at specified time points along the free-fall trajectory, write on tape.

- II - Optimization

1. Generate the propagation weighting matrix using linear weapon data.
2. Input control points, measurement points, measurement variances.
3. Choose the type of optimization, and obtain controller gains, estimator gains, total system covariance at release.

- III - Performance Evaluation

1. Propagate the release covariance to impact using performance evaluator.
2. Compute impact covariance matrix, CEP performance measure and the variance contribution matrix.

This defines one complete cycle of the use of ADAPS. Each part can be used independently of the others, for different needs. The main program itself is largely at the discretion of the user, to be organized as best suits a particular analysis problem.

SECTION III

DEVELOPMENT OF A NONLINEAR DYNAMICAL MODEL FOR RIGID-BODY MOTIONS

The ADAPS is a six-degree-of-freedom optimal delivery control and aircraft-weapon simulation programming system. It is based on the THRUST program developed in Honeywell [12].

The equations of motion in ADAPS are referenced to a flat nonrotating earth. The forces and moments acting on the vehicle and the weapons are generated by gravity, aerodynamic effects, and thrust. The aerodynamic coefficients are input in tabular form as functions of Mach number, angle of attack, sideslip angle, etc. The aerodynamic force and moment subroutines allow the description of the vehicle and weapon characteristics over a wide range of flight conditions.

ADAPS has three running phases: (I) modeling and linearization phase; (II) controller optimization phase; and (III) performance evaluation phase. Briefly, phase I consists of generating a prescribed steady trajectory of an aircraft weapon system and its variational equations starting from a given initial condition to a weapon release point, then continuing to generate six-degree-of-freedom free-fall trajectories of a weapon and its variational equations until a prescribed target altitude is reached. The coefficients of the variational equations are obtained by a simple numerical differentiation process.

In the following, analyses pertaining to phase I of ADAPS operation are given.

DEVELOPMENT OF THE DIFFERENTIAL EQUATIONS OF MOTION

For completeness, this subsection presents the derivation of the equation of motion of an airplane and a weapon [13, 14, 15, 16, 17]. These equations of motion are implemented in subroutine DYNK. Since they are unaffected by the interchangeable subroutines describing alternate airframe and weapon aerodynamics, they are applicable to both aircraft and weapon. In the following, aircraft or weapon will be referred to as a body or a rigid body.

Reference Frames

The coordinates necessary to specify the six degrees of freedom of a rigid body are defined by means of two right-handed reference frames, the x_e, y_e, z_e frame, or earth-fixed frame, and the x, y, z frame, or moving frame or body frame. They are defined as follows:

- Earth-Fixed Frame —

0 = origin, fixed at the target

x_e -axis is horizontal, in the vertical plane containing the initial velocity vector of the mass center (downrange)

y_e -axis is crossrange to the right

z_e -axis is vertically downwards

- Moving Frame —

0 = origin at the center of gravity of body

x -axis is parallel to the longitudinal axis of the body

y -axis is perpendicular to the plane of symmetry (for a weapon which has more than one plane of symmetry choose the one most nearly parallel to the aircraft plane of symmetry before release)

z -axis is perpendicular to xy plane and positive down viewed by the pilot (before weapon release in the case of the weapon)

Earth-fixed and moving frame definitions for airplane and weapon are illustrated in Figure 6.

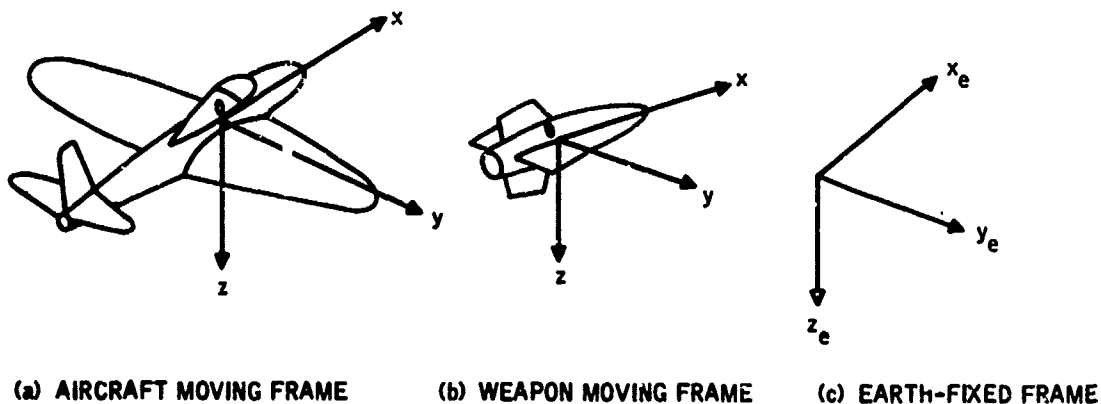


Figure 6. Earth-Fixed and Moving Coordinate Frames

It should be noted that the orientation of earth-fixed frame differs in accordance with its use [17]. The earth-fixed frame generally used in bombing and range tables is obtained by rotating the fixed frame described here by 90 degrees counterclockwise about the x-axis.

The differential equations of motion consist of:

The dynamical laws of motion

The kinematical relationships between the reference frames

The Dynamics of Motion

Two vector equations define the motion of a rigid body completely. They are [13, 16, 17] relative to the earth-fixed frame.

$$\vec{F} = m \frac{d\vec{v}_O}{dt} \quad (3.1)$$

$$\vec{T} = \frac{d\vec{h}}{dt} \quad (3.2)$$

where

$\vec{F} = \Sigma \vec{F}_i$ resultant external force acting upon the body

\vec{v}_O = velocity of mass center relative to inertial frame

$m = \Sigma \delta m$ total mass of the body

$\vec{T} = \Sigma \vec{T}_i$ resultant external torque about mass center

\vec{h} = angular momentum of the body about mass center

For a rigid body, the angular momentum about mass center is defined as

$$\vec{h} = \Sigma \vec{r} \times \vec{v} \delta m \quad (3.3)$$

with

$$\vec{v} = \vec{v}_O + \vec{\omega} \times \vec{r} \quad (3.4)$$

where

\vec{v} = velocity of the mass element δm relative to earth-fixed frame

\vec{v}_O = velocity of center of mass relative to earth-fixed frame

$\vec{\omega}$ = angular velocity of the body relative to earth-fixed frame

\vec{r} = position vector from c.g. to the mass element δm

Substituting (3.4) into (3.3) and using body-coordinates one obtains

$$\vec{h} = \vec{\omega} \Sigma(x^2 + y^2 + z^2)\delta m - \Sigma \vec{r}(px+qy+rz)\delta m$$

in matrix notation further simplification yields

$$\begin{bmatrix} h_x \\ h_y \\ h_z \end{bmatrix} = J \begin{bmatrix} p \\ q \\ r \end{bmatrix}$$

where J is the moment of inertia matrix given by

$$J = \begin{pmatrix} I_{xx} & -I_{xy} & -I_{xz} \\ -I_{xy} & I_{yy} & -I_{yz} \\ -I_{xz} & -I_{yz} & I_{zz} \end{pmatrix} \quad (3.5)$$

In order to suppress the derivatives of moment of inertia elements, the equations of motion given by (3.1) and (3.2) are expressed in body axes which rotate with the body.

Thus (3.1) and (3.2) expressed in rotating frame of reference become

$$\vec{F} = m \left(\frac{\delta \vec{v}}{\delta t} \right) + m(\vec{\omega} \times \vec{v}_O) \quad (3.6)$$

$$\vec{T} = \frac{\delta \vec{h}}{\delta t} + \vec{\omega} \times \vec{h} \quad (3.7)$$

where by definition

$$\frac{\delta \vec{v}}{\delta t} \triangleq \vec{i} \frac{dv_x}{dt} + \vec{j} \frac{dv_y}{dt} + \vec{k} \frac{dv_z}{dt} \quad (3.7)$$

Referring to Equation (3.7), let

$$\vec{\eta} = \vec{\omega} \times \vec{v}_O = \vec{i}(qw-rv) + \vec{j}(ru-pw) + \vec{k}(pv-qu) \quad (3.8)$$

In matrix notation (3.8) becomes

$$\eta = \begin{pmatrix} 0 & -r & q \\ r & 0 & -p \\ -q & p & 0 \end{pmatrix} \begin{pmatrix} u \\ v \\ w \end{pmatrix} \quad (3.9)$$

Now making use of (3.9) equations of motion (3.6) and (3.7) can be expressed

$$\begin{pmatrix} F_x \\ F_y \\ F_z \end{pmatrix} = m \begin{pmatrix} \dot{u} \\ \dot{v} \\ \dot{w} \end{pmatrix} + m \begin{pmatrix} 0 & -r & q \\ r & 0 & -p \\ -q & p & 0 \end{pmatrix} \begin{pmatrix} u \\ v \\ w \end{pmatrix} \quad (3.10)$$

and

$$\begin{pmatrix} M_x \\ M_y \\ M_z \end{pmatrix} = J \begin{pmatrix} \dot{p} \\ \dot{q} \\ \dot{r} \end{pmatrix} + \begin{pmatrix} 0 & -r & q \\ r & 0 & -p \\ -q & p & 0 \end{pmatrix} J \begin{pmatrix} p \\ q \\ r \end{pmatrix} \quad (3.11)$$

These six differential equations, called the Euler equations of motion, completely describe the dynamics of the rigid body.

The Kinematics of Motion

To describe the position and orientation of the body as a function of time, earth-fixed frame of reference is introduced as defined earlier. To find the differential equations of the coordinates of mass center relative to the fixed-frame (i.e., differential equations of the flight path), it is necessary to develop the time evolution of the transformation matrix $\Omega(t)$ which transforms a vector from the body coordinates to the earth-fixed coordinates, that is

$$v_e = \Omega v \quad (3.12)$$

Thus, if $\dot{x}_e, \dot{y}_e, \dot{z}_e$ are the velocity components of mass center in the earth-fixed reference system, and if (u, v, w) are the velocity components of mass center in the body frame it follows that

$$\begin{pmatrix} \dot{x}_e \\ \dot{y}_e \\ \dot{z}_e \end{pmatrix} = \Omega \begin{pmatrix} u \\ v \\ w \end{pmatrix} \quad (3.13)$$

Among the various angular coordinates that can be used to express the direction cosines (i.e., the elements of Ω matrix), a system of Eulerian angles is commonly used. Because of their trigonometrical form, however, Eulerian angles cause a singularity in the differential equations connecting the angular velocity with the Eulerian angles [17]. This singularity gives rise to a considerable truncation error in the integration process. To avoid this, the components of a normalized quaternion (versor, Euler symmetrical parameters) are used as angular coordinates. For completeness, discussions on both the usage of Eulerian angles and quaternions as angular coordinates are given in the following two subsections, respectively. Quaternions are implemented in the subroutine DYNK for nonlinear simulation. The Eulerian angles are used for the perturbation model.

The Eulerian Angles as Angular Coordinates -- In the following, the elements of the transformation matrix Ω are expressed in terms of the so-called Eulerian angles. In general, one can carry out the transformation from a given cartesian coordinate system to another by means of three successive rotations performed in a specific sequence. The Eulerian angles are then defined as the three successive angles of rotations. Unfortunately, there is no unanimity in the literature about the definition of the Eulerian angles. The convention of [17, 18], and [16] will be adopted here. The body is imagined first to be oriented so that its axes are parallel to earth-fixed axes. This system will be denoted by (x_1, y_1, z_1) . The sequence will be started by rotating the initial system of axes (x_1, y_1, z_1) by an angle ψ clockwise about the z_1 axis, and the resultant coordinate system will be labeled the x_2, y_2, z_2 axes. In the second stage the intermediate axes x_2, y_2, z_2 are rotated about the y_2 axis clockwise by an angle θ to produce another intermediate set x_3, y_3, z_3 . Finally the x_3, y_3, z_3 axes are rotated clockwise by an angle ϕ about the x_3 axis to produce the desired x, y, z body system of axes. Figure 7 illustrates the various stages of the sequence. The Eulerian angles θ, ψ, ϕ thus completely specify the orientation of the (x, y, z) body system relative to the (x_e, y_e, z_e) earth-fixed system.

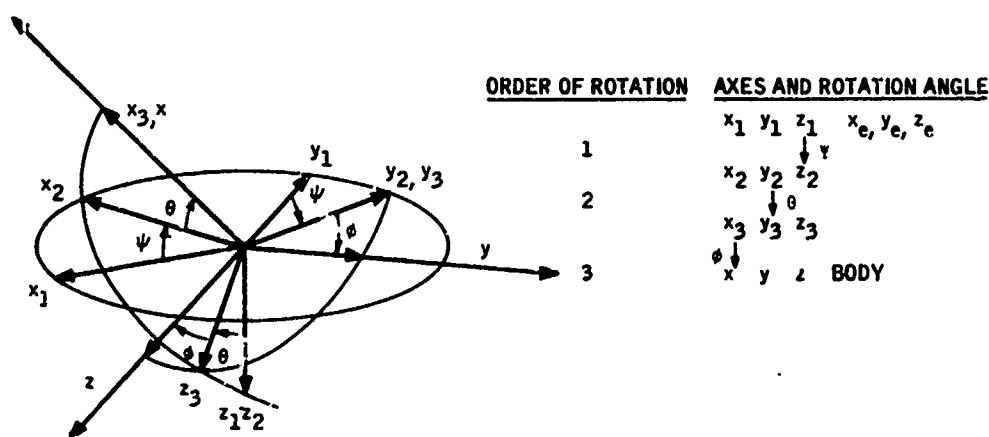


Figure 7. Body Orientation and Euler Angles

The elements of the complete transformation E can be obtained by writing the matrix as the triple product of the separate rotations. Let E_1, E_2, E_3 be transformations describing the rotations ψ, θ , and ϕ , respectively. The complete transformation E from earth-to-body system is given by

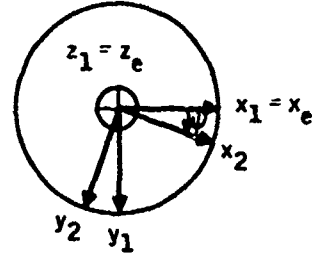
$$\begin{pmatrix} x \\ y \\ z \end{pmatrix} = E \begin{pmatrix} x_e \\ y_e \\ z_e \end{pmatrix} \quad (3.13a)$$

where

$$E = E_3 E_2 E_1$$

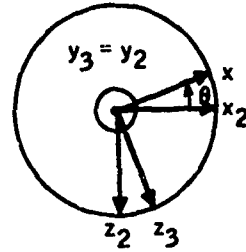
Clearly, rotation about z_1 axis by the angle ψ is given by

$$E_1 = \begin{bmatrix} \cos \psi & \sin \psi & 0 \\ -\sin \psi & \cos \psi & 0 \\ 0 & 0 & 1 \end{bmatrix}$$



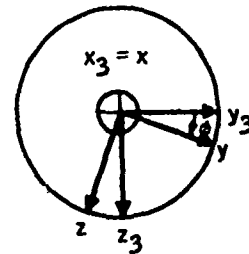
Similarly rotation about y_2 axis by the angle θ is given by

$$E_2 = \begin{bmatrix} \cos \theta & 0 & -\sin \theta \\ 0 & 1 & 0 \\ \sin \theta & 0 & \cos \theta \end{bmatrix}$$



Also rotation about x_3 axis by the angle ϕ is given by

$$E_3 = \begin{bmatrix} 1 & 0 & 0 \\ 0 & \cos \phi & \sin \phi \\ 0 & -\sin \phi & \cos \phi \end{bmatrix}$$



The product matrix E then follows as

$$E = \begin{bmatrix} \cos \theta \cos \psi & \cos \theta \sin \psi & -\sin \theta \\ -\cos \phi \sin \psi + \sin \phi \sin \theta \cos \psi & \cos \phi \cos \psi + \sin \phi \sin \theta \sin \psi & \sin \phi \cos \theta \\ \sin \phi \sin \psi + \cos \phi \sin \theta \cos \psi & -\sin \phi \cos \psi + \cos \phi \sin \theta \sin \psi & \cos \phi \cos \theta \end{bmatrix} \quad (3.14)$$

Since E is an orthogonal matrix, the inverse transformation from body coordinates to earth-fixed axes is then given by

$$\Omega = E^{-1} = E' \quad (3.15)$$

Equations (3.13) together with (3.14) and (3.15) constitute the flight-path equations of a rigid body in terms of body-axis velocity components which in turn are found by solving Equations (3.10) and (3.11). We develop in the following the differential equations of the Euler angles which when integrated enable one to evaluate the direction cosine matrix Ω as a function of time.

Let $\vec{\eta}$ be an arbitrary fixed vector. Let η_e and η be its component representation in the earth-fixed and body frames respectively.

Then one can write

$$\eta = E \eta_e \quad (3.16)$$

Differentiating (3.16) w. r. t time and noting that

$$\frac{d\eta_e}{dt} = 0$$

yields

$$\dot{\eta} = \dot{E} \eta_e \quad (3.17)$$

using (3.16) in (3.17) yields

$$\dot{\eta} = \dot{E} E' \eta \quad (3.18)$$

where

$$\eta = \text{col} \left(\frac{d\eta_x}{dt}, \frac{d\eta_y}{dt}, \frac{d\eta_z}{dt} \right)$$

On the other hand, the time derivative $\dot{\vec{\eta}}$ w. r. t. rotating frame of reference is given by

$$\frac{d\vec{\eta}}{dt} = \frac{\delta \vec{\eta}}{\delta t} + \vec{\omega} \times \vec{\eta} = 0 \quad (3.19)$$

where

$$\frac{\delta \vec{\eta}}{\delta t} \triangleq \vec{i} \frac{d\eta_x}{dt} + \vec{j} \frac{d\eta_y}{dt} + \vec{k} \frac{d\eta_z}{dt} \quad (3.19a)$$

In matrix notation (3.19) and 3.19a) become

$$\dot{\eta} = -W \eta \quad (3.20)$$

where

$$W = \begin{bmatrix} 0 & -r & q \\ r & 0 & -p \\ -q & p & 0 \end{bmatrix} \quad (3.21)$$

Comparing (3.18) and (3.20) yields

$$\dot{E}E' = -W \quad (3.22)$$

or

$$\dot{E} = -WE \quad (3.23)$$

The differential equation of angular coordinates θ , ψ , ϕ are obtained from the proper elements of equation (3.22):

$$\begin{pmatrix} \dot{\theta} \\ \dot{\phi} \\ \dot{\psi} \end{pmatrix} = \begin{pmatrix} 0 & \cos \phi & -\sin \phi \\ 1 & \sin \phi \tan \theta & \cos \phi \tan \theta \\ 0 & \sin \phi \sec \theta & \cos \phi \sec \theta \end{pmatrix} \begin{pmatrix} p \\ q \\ r \end{pmatrix} \quad (3.24)$$

The Quaternions Used as Angular Coordinates -- In this subsection a brief description of the properties of quaternions and their usage as angular coordinates is presented. Then the differential equations of the elements of a quaternion are developed [17, 19, 20, 21].

A quaternion may be thought of as a generalized complex number. It is defined as

$$q = q_0 + [iq_1 + jq_2 + kq_3] \quad (3.25)$$

where q_0 , q_1 , q_2 , q_3 are real numbers and i , j , k are basis elements satisfying the relations

$$\begin{aligned} i^2 &= j^2 = k^2 = -1 \\ (ij)k &= i(jk) = -1 \end{aligned} \quad (3.26)$$

An immediate consequence of (3.26) (since, for example, $k^{-1} = -k$) is

$$ij = -ji = k, \quad jk = -kj = i, \quad ki = -ik = j \quad (3.26a)$$

When $q_0 = 0$, the quaternion is said to be a pure quaternion. By definition then, a vector is a pure quaternion and, consequently, the bracketed term in (3.25) is called the vector part of q . Defining four angles α , β , γ , and φ in the following way, one obtains polar representation of a quaternion [17]

$$q = (q_0 + iq_1 + jq_2 + kq_3) = \sqrt{N(q)} \left[\cos \frac{\varphi}{2} + \sin \frac{\varphi}{2} (i \cos \alpha + j \cos \beta + k \cos \gamma) \right] \quad (3.27)$$

The conjugate of q is defined as

$$\bar{q} = q_0 - iq_1 - jq_2 - kq_3 \quad (3.28)$$

It may be verified that

$$q\bar{q} = \bar{q}q = N(q) \quad (3.29)$$

An equivalent definition expresses the quaternion as a 4×4 matrix of a special type

$$q \leftrightarrow Q = \begin{bmatrix} q_0 & q_1 & q_2 & q_3 \\ -q_1 & q_0 & -q_3 & q_2 \\ -q_2 & q_3 & q_0 & -q_1 \\ -q_3 & -q_2 & q_1 & q_0 \end{bmatrix} \quad (3.30)$$

where q_0, q_1, q_2, q_3 are the components of a quaternion given in (3.25). In matrix form the conjugate, \bar{q} , of the quaternion q becomes Q' , the transpose of Q .

$$\bar{q} \leftrightarrow Q' \quad (3.31)$$

The product $r = qp$ of two quaternions represents an operation on p that rotates p by an amount $\varphi/2$ and stretches its magnitude by $\sqrt{N(q)}$. Let

$$\begin{aligned} r &= r_0 + ir_1 + jr_2 + kr_3 \\ q &= q_0 + [iq_1 + jq_2 + kq_3] \\ p &= p_0 + ip_1 + jp_2 + kp_3 \end{aligned} \quad (3.32)$$

Using (3.26) and (3.26a) the product $r = qp$ can be expressed as

$$\begin{aligned}
r_0 &= (q_0 p_0 - q_1 p_1 - q_2 p_2 - q_3 p_3) \\
r_1 &= (q_1 p_0 + q_0 p_1 - q_3 p_2 + q_2 p_3) \\
r_2 &= (q_2 p_0 + q_3 p_1 + q_0 p_2 - q_1 p_3) \\
r_3 &= (q_3 p_0 - q_2 p_1 + q_1 p_2 + q_0 p_3)
\end{aligned} \tag{3.33}$$

The same result can also be obtained by considering the matrix equivalent of $r = qp$,

$$R = QP \tag{3.34}$$

and equating elements of the first row to find r_0, r_1, r_2, r_3

Clearly (3.33) can be written as

$$r = P'q \tag{3.35}$$

where r and q now are 4×1 column vectors. Equation (3.33) can also be written as

$$r = \tilde{Q}p \tag{3.36}$$

where p is the 4×1 vector representation of the quaternion and \tilde{Q} is a 4×4 matrix obtained from Q by interchanging the first row and the first column of Q .

Besides rotating and stretching four-dimensional vectors, quaternions also effect rotations and stretchings of the three-dimensional space, and it is this property that makes quaternions useful for the description of rigid rotations. To demonstrate this, let x be a pure quaternion (i.e., a vector) described by

$$x = ix_1 + jx_2 + kx_3 \tag{3.37}$$

Let λ be a unit quaternion (that is, $\lambda\bar{\lambda} = 1$) described by

$$\lambda = \lambda_0 + i\lambda_1 + j\lambda_2 + k\lambda_3 \tag{3.38}$$

and $\bar{\lambda}$ be the conjugate of λ .

Now consider the quaternion y defined by the triple product

$$y = \lambda x \bar{\lambda} \tag{3.39}$$

By actually performing the indicated multiplications with the rules given in (3.26) and (3.26a), or writing (3.39) with the aid of (3.35) and (3.36) as

$$\eta = \lambda x + \tilde{\Lambda} x \quad (3.39a)$$

$$y = (\lambda x) \tilde{\Lambda} = \eta \tilde{\Lambda} \quad (3.39b)$$

and substituting (3.39a) into (3.39b) upon returning from four to three dimensions for y one obtains the equation

$$y = \Omega x \quad (3.40)$$

where

$$\Omega = \begin{bmatrix} 2(\lambda_0^2 + \lambda_1^2) - 1 & 2(\lambda_1 \lambda_2 - \lambda_0 \lambda_3) & 2(\lambda_1 \lambda_3 + \lambda_0 \lambda_2) \\ 2(\lambda_1 \lambda_2 + \lambda_0 \lambda_3) & 2(\lambda_0^2 + \lambda_2^2) - 1 & 2(\lambda_2 \lambda_3 - \lambda_0 \lambda_1) \\ 2(\lambda_1 \lambda_3 - \lambda_0 \lambda_2) & 2(\lambda_2 \lambda_3 + \lambda_0 \lambda_1) & 2(\lambda_0^2 + \lambda_3^2) - 1 \end{bmatrix} \quad (3.41)$$

It can readily be shown that (3.39) preserves the norm, that is

$$x\bar{x} = y\bar{y} \quad (3.42)$$

On the basis of (3.40) and (3.42) one concludes that (3.39) defines a rotation of x . This demonstrates that quaternions can be used as angular coordinates. Now, the differential equations of the elements of a quaternion will be developed.

Let $\vec{\xi}$ and $\vec{\eta}$ be fixed-vectors attached to earth-fixed frame and rotating body frame respectively as shown in Figure 8.

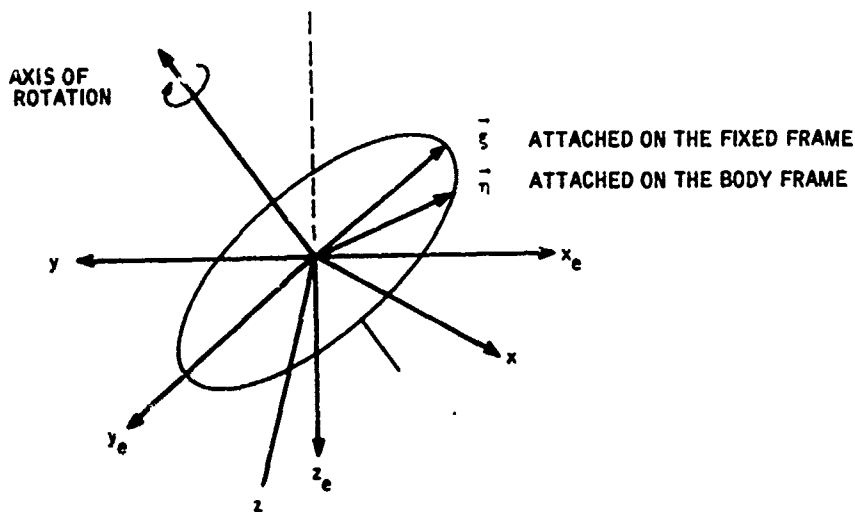


Figure 8. Relations between Fixed and Rotating Frames

Consider transformation defined by (see Equation 3.39)

$$\eta = \lambda \xi \bar{\lambda} \quad (3.43)$$

To keep track of reference frames, rewrite Equation (3.43) in the body frame as:

$$\eta_b = \lambda \xi_b \bar{\lambda} \quad (3.43a)$$

where the subscript b implies the corresponding vectors expressed in body frame (x, y, x) . Let us further assume that the two vector systems coincide when $\lambda = 1$.

That is

$$\eta_b = \xi_e \quad (3.44)$$

where the subscript e implies the corresponding vector expressed in the earth-fixed frame. Since η moves with the body frame, (3.44) holds for all values of λ .

Substituting (3.44) into (3.43a) yields

$$\xi_e = \lambda \xi_b \bar{\lambda} \quad (3.45)$$

or

$$\xi_b = \bar{\lambda} \xi_e \lambda \quad (3.45a)$$

This relates in quaternion notation the components of the vector $\vec{\xi}$ in the two coordinate frames. In matrix notation it becomes

$$Y = \Lambda' Y_e \Lambda \quad (3.46)$$

where Y is the matrix representation of the quaternion ξ .

Differentiating this and noting that Y_e is a fixed quaternion matrix yields

$$\dot{Y} = \dot{\Lambda}' Y_e \Lambda + \Lambda' Y_e \dot{\Lambda} \quad (3.47)$$

but from (3.46)

$$Y_e = \Lambda Y \Lambda' \quad (3.48)$$

Substituting this into (3.47) and simplifying yields

$$\dot{Y} = \dot{\Lambda}' \Lambda Y + Y \Lambda' \dot{\Lambda}$$

Noting that y is a pure quaternion so that [see Equation (3.30)], $Y' = -Y$ results in

$$\dot{Y} = \dot{\Lambda}' \Lambda Y - (\dot{\Lambda}' \Lambda Y)' \quad (3.49)$$

Now, differentiation of a vector in a rotating frame in vector notation gives Equation (3.19):

$$\dot{\vec{\xi}} = \vec{\omega} \times \vec{\xi} \quad (3.50)$$

which can be shown to have the quaternion representation

$$\dot{Y} = \left(-\frac{1}{2}\right) [WY - (WY)'] \quad (3.51)$$

where W is the quaternion matrix of the angular velocity vector of the rotating frame presented in the rotating frame, that is

$$\vec{\omega} = \vec{i}p + \vec{j}q + \vec{k}r \quad (3.52)$$

Comparing (3.49) and (3.51) gives

$$\dot{\Lambda}' \Lambda = -\frac{1}{2} W$$

or

$$\dot{\Lambda}' = \left(-\frac{1}{2}\right) W \Lambda' \quad (3.53)$$

In the manner of Equation (3.34), after performing the multiplication the first column of this equation constitutes the differential equations of the components of the quaternion λ , which are given by [see Equation (3.30)]

$$\begin{pmatrix} \dot{\lambda}_0 \\ \dot{\lambda}_1 \\ \dot{\lambda}_2 \\ \dot{\lambda}_3 \end{pmatrix} = \left(-\frac{1}{2}\right) \begin{bmatrix} 0 & p & +q & r \\ -p & 0 & -r & q \\ -q & r & 0 & -p \\ -r & -q & p & 0 \end{bmatrix} \begin{pmatrix} \lambda_0 \\ \lambda_1 \\ \lambda_2 \\ \lambda_3 \end{pmatrix} \quad (3.54)$$

To integrate this set of equations, an initial value of λ must be specified.

Initialization of the Angular Coordinates -- By comparing corresponding elements of matrices (3.14) and (3.41), the components of the vector can be related to Euler angles [21] as follows

$$\begin{aligned}
 \lambda_0 &= \cos \frac{\psi}{2} \cos \frac{\theta}{2} \cos \frac{\phi}{2} + \sin \frac{\psi}{2} \sin \frac{\theta}{2} \sin \frac{\phi}{2} \\
 \lambda_1 &= \cos \frac{\psi}{2} \cos \frac{\theta}{2} \sin \frac{\phi}{2} - \sin \frac{\psi}{2} \sin \frac{\theta}{2} \cos \frac{\phi}{2} \\
 \lambda_2 &= \cos \frac{\psi}{2} \sin \frac{\theta}{2} \cos \frac{\phi}{2} + \sin \frac{\psi}{2} \cos \frac{\theta}{2} \sin \frac{\phi}{2} \\
 \lambda_3 &= -\cos \frac{\psi}{2} \sin \frac{\theta}{2} \sin \frac{\phi}{2} + \sin \frac{\psi}{2} \cos \frac{\theta}{2} \cos \frac{\phi}{2}
 \end{aligned}
 \tag{3.55}$$

This set of equations can be used to obtain initial values of the versor (unit vector) components. An alternate way of obtaining the versor components from the Euler angles is to compute the initial cosine matrix and use the following easily verified relations:

$$\lambda_0^2 = \frac{1 + \text{tr} E}{4}$$

where tr is the trace operator, and

$$\begin{pmatrix} 0 & -\lambda_3 & \lambda_2 \\ \lambda_3 & 0 & -\lambda_1 \\ -\lambda_2 & \lambda_1 & 0 \end{pmatrix} = \frac{E' - E}{4\lambda_0}
 \tag{3.56}$$

provided that $\lambda_0 \neq 0$. Since for certain initial conditions (i.e., $\theta = \pi$, $\psi = 0$, $\phi = 0$) this condition is violated, Equation (3.55) is complemented in ADAPS instead of (3.56)

Gravity Components in the Body Axes

The inertial components of gravity are resolved into the required body components by using the direction cosine matrix.

$$\begin{pmatrix} g_x \\ g_y \\ g_z \end{pmatrix} = E \begin{pmatrix} 0 \\ 0 \\ g \end{pmatrix}_e
 \tag{3.58}$$

which picks the third column of E given in (3.14), that is

$$\begin{pmatrix} g_x \\ g_y \\ g_z \end{pmatrix} = g \begin{pmatrix} -\sin \theta \\ \cos \theta \sin \phi \\ \cos \theta \cos \phi \end{pmatrix} \quad (3.59)$$

This finishes the analysis of the equations of motion.

Summary of the Analysis

In the development of the equations of motion, the aerodynamic forces are taken to be through the aircraft mass center and the moments are about the body axes. The accelerations on the aircraft are computed by combining the aerodynamic forces and the forces from the engine. All cross products of inertia are included to allow for a nonsymmetrical body.

- Accelerations due to Aero and Thrust Forces in Body Coordinates

$$\begin{bmatrix} a_x \\ a_y \\ a_z \end{bmatrix} = \frac{1}{m} \begin{bmatrix} X + X_T \\ Y \\ Z + Z_T \end{bmatrix} \quad (3.60)$$

- Total Moments in Body Coordinates

$$\begin{bmatrix} M_x \\ M_y \\ M_z \end{bmatrix} = \begin{bmatrix} L + L_T \\ M + M_T \\ N + N_T \end{bmatrix} \quad (3.61)$$

- Differential Equations of Body Translation Velocities in Body Coordinates -

$$\begin{bmatrix} \dot{u} \\ \dot{v} \\ \dot{w} \end{bmatrix} = \begin{bmatrix} a_x \\ a_y \\ a_z \end{bmatrix} + g \begin{bmatrix} -\sin \theta \\ \cos \theta \sin \phi \\ \cos \theta \cos \phi \end{bmatrix} + \begin{bmatrix} 0 & r & -q \\ -r & 0 & p \\ q & -p & 0 \end{bmatrix} \begin{bmatrix} u \\ v \\ w \end{bmatrix} \quad (3.62)$$

with prescribed initial conditions

$$\begin{bmatrix} \bar{u}(0) \\ \bar{v}(0) \\ \bar{w}(0) \end{bmatrix} = \begin{bmatrix} u_0 \\ v_0 \\ w_0 \end{bmatrix}$$

- Differential Equations of Body Angular Velocities in Body Coordinates -

$$\begin{pmatrix} \dot{p} \\ \dot{q} \\ \dot{r} \end{pmatrix} = J^{-1} \left\{ \begin{bmatrix} M_x \\ M_y \\ M_z \end{bmatrix} - \begin{bmatrix} 0 & -r & q \\ r & 0 & -p \\ -q & p & 0 \end{bmatrix} J \begin{bmatrix} p \\ q \\ r \end{bmatrix} \right\} \quad (3.63)$$

where

$$J = \begin{bmatrix} I_{xx} & -I_{xy} & -I_{xz} \\ -I_{xy} & I_{yy} & -I_{yz} \\ -I_{xz} & -I_{yz} & I_{zz} \end{bmatrix} \quad (3.64)$$

is a symmetric matrix; or

$$\begin{pmatrix} \dot{p} \\ \dot{q} \\ \dot{r} \end{pmatrix} = \begin{bmatrix} d_{11} & d_{12} & d_{13} \\ d_{21} & d_{22} & d_{23} \\ d_{31} & d_{32} & d_{33} \end{bmatrix} \begin{bmatrix} f_1 \\ f_2 \\ f_3 \end{bmatrix} \quad (3.65)$$

where the coefficient matrix D is J^{-1} and symmetric and

$$\begin{bmatrix} f_1 \\ f_2 \\ f_3 \end{bmatrix} = \begin{bmatrix} M_x \\ M_y \\ M_z \end{bmatrix} + \begin{bmatrix} [(I_y - I_z)q]r - I_{yz}(r^2 - q^2) + (I_{zx}q - I_{xy}r)p \\ [(I_z - I_x)p]r - I_{zx}(p^2 - r^2) + (I_{xy}r - I_{yz}p)q \\ [(I_x - I_y)p]q - I_{xy}(q^2 - p^2) + (I_{yz}p - I_{zx}q)r \end{bmatrix} \quad (3.66)$$

and

$$\begin{aligned}
 d_{11} &= \left(1 - \frac{I_{yz}^2}{I_y I_z} \right) / (I_x K) \\
 d_{12} &= \left(I_{xy} + \frac{I_{yz} I_{zx}}{I_z} \right) / (I_y I_x K) \\
 d_{13} &= \left(I_{xz} + \frac{I_{xy} I_{yz}}{I_y} \right) / (I_z I_x K) \\
 d_{21} &= \left(I_{xy} + \frac{I_{yz} I_{zx}}{I_z} \right) / (I_x I_y K) \\
 d_{22} &= \left(1 - \frac{I_{zx}^2}{I_x I_y} \right) / (I_y K) \\
 d_{23} &= \left(I_{yz} + \frac{I_{zx} I_{xy}}{I_x} \right) / (I_z I_y K) \\
 d_{31} &= \left(I_{zx} + \frac{I_{xy} I_{yz}}{I_y} \right) / (I_x I_z K) \\
 d_{32} &= \left(I_{yz} + \frac{I_{zx} I_{xy}}{I_x} \right) / (I_y I_z K) \\
 d_{33} &= \left(1 - \frac{I_{xy}^2}{I_x I_y} \right) / (I_z K)
 \end{aligned} \tag{3.67}$$

$$K = 1 - \frac{I_{xy}^2}{I_x I_y} - \frac{I_{yz}^2}{I_y I_z} - \frac{I_{zx}^2}{I_z I_x} - 2 \frac{I_{xy} I_{yz} I_{zx}}{I_x I_y I_z}$$

with prescribed initial conditions

$$\begin{bmatrix} p(0) \\ q(0) \\ r(0) \end{bmatrix} = \begin{bmatrix} p_0 \\ q_0 \\ r_0 \end{bmatrix}$$

- Differential Equations of the Angular Coordinates (i. e., Quaternions) -

$$\begin{bmatrix} \dot{\lambda}_0 \\ \dot{\lambda}_1 \\ \dot{\lambda}_2 \\ \dot{\lambda}_3 \end{bmatrix} = 1/2 \begin{bmatrix} -\lambda_1 & -\lambda_2 & -\lambda_3 \\ \lambda_0 & -\lambda_3 & \lambda_2 \\ \lambda_3 & \lambda_0 & -\lambda_1 \\ -\lambda_2 & \lambda_1 & \lambda_0 \end{bmatrix} \begin{bmatrix} p \\ q \\ r \end{bmatrix} \quad (3.68)$$

with initial conditions (expressed in terms of the initial Euler angles ψ_0, θ_0, ϕ_0)

$$\begin{bmatrix} \lambda_0(0) \\ \lambda_1(0) \\ \lambda_2(0) \\ \lambda_3(0) \end{bmatrix} = \begin{bmatrix} \cos \frac{\psi_0}{2} \cos \frac{\theta_0}{2} \cos \frac{\phi_0}{2} + \sin \frac{\psi_0}{2} \sin \frac{\theta_0}{2} \sin \frac{\phi_0}{2} \\ \cos \frac{\psi_0}{2} \cos \frac{\theta_0}{2} \sin \frac{\phi_0}{2} - \sin \frac{\psi_0}{2} \sin \frac{\theta_0}{2} \cos \frac{\phi_0}{2} \\ \cos \frac{\psi_0}{2} \sin \frac{\theta_0}{2} \cos \frac{\phi_0}{2} + \sin \frac{\psi_0}{2} \cos \frac{\theta_0}{2} \sin \frac{\phi_0}{2} \\ -\cos \frac{\psi_0}{2} \sin \frac{\theta_0}{2} \sin \frac{\phi_0}{2} + \sin \frac{\psi_0}{2} \cos \frac{\theta_0}{2} \cos \frac{\phi_0}{2} \end{bmatrix} \quad (3.69)$$

- Earth to Body Transformation Matrix in Terms of Quaternions -

$$E = \begin{bmatrix} \lambda_0^2 + \lambda_1^2 - \lambda_2^2 - \lambda_3^2 & 2(\lambda_1\lambda_2 + \lambda_0\lambda_3) & 2(\lambda_1\lambda_3 - \lambda_0\lambda_2) \\ 2(\lambda_1\lambda_2 - \lambda_0\lambda_3) & \lambda_0^2 + \lambda_2^2 - \lambda_3^2 - \lambda_1^2 & 2(\lambda_2\lambda_3 + \lambda_0\lambda_1) \\ 2(\lambda_1\lambda_3 + \lambda_0\lambda_2) & 2(\lambda_2\lambda_3 - \lambda_0\lambda_1) & \lambda_0^2 + \lambda_3^2 - \lambda_1^2 - \lambda_2^2 \end{bmatrix} \quad (3.70)$$

- The Euler Angles -

$$\begin{aligned} \theta &= -\sin^{-1}(e_{13}) \\ \phi &= \tan^{-1}(e_{23}/e_{33}) \\ \psi &= \tan^{-1}(e_{12}/e_{11}) \end{aligned} \quad (3.71)$$

- The Differential Equations of Body Mass Center in the Earth-Fixed Coordinates (i. e., Flight Path) -

$$\begin{bmatrix} \dot{x}_e \\ \dot{y}_e \\ \dot{z}_e \end{bmatrix} = E' \begin{bmatrix} u \\ v \\ w \end{bmatrix} \quad (3.72)$$

with prescribed initial conditions

$$\begin{bmatrix} x_e(0) \\ y_e(0) \\ z_e(0) \end{bmatrix}$$

DEVELOPMENT OF INTEGRATION ALGORITHM FOR THE EQUATIONS OF MOTION

The method of integrating the differential equations of motion in ADAPS is the open quadrature process (i. e., Adams formula) [22]. It is given by

$$x_k = x_{k-1} + h(1 + \frac{1}{2} \nabla) \dot{x}_{k-1} \quad (3.73)$$

where

$$h = t_k - t_{k-1} \quad (3.74)$$

$$\dot{x} = f(x, t) \quad (3.75)$$

and

∇ = backward difference operator

Truncation error associated with the process is of the order of h^3 and is given by

$$E = a_2 h^3 x^{(3)}(\xi), \quad t_{k-2} < \xi < t_k \quad (3.76)$$

This integration process can be written as

$$x_k = x_{k-1} + \frac{h}{2} (3\dot{x}_{k-1} - \dot{x}_{k-2}) \quad \begin{array}{ccc} | & | & | \\ t_{k-2} & t_{k-1} & t_k \end{array} \quad (3.77)$$

To start the solution, the derivatives at two time points are needed. The solution can be started by using

$$x_k = x_{k-1} + h\dot{x}_{k-1} \quad (3.78)$$

with

$$E = \frac{h^2}{2} \ddot{x}(\xi) \quad t_{k-1} < \xi < t_k \quad (3.79)$$

In ADAPS, the initial values, \dot{x}_1 , are set to zero for simplicity. For small h the error caused by this simplification is small.

SECTION IV

DEVELOPMENT OF TOTAL FORCE AND MOMENT SYSTEM FOR RIGID BODIES MOVING IN UNSTEADY AIRMASS

The methods by which the aerodynamic and thrust forces and moments are introduced into the six-degree-of-freedom trajectory program are presented in this section. Aerodynamic forces and moments for aircraft are treated first. The computer program which implements the aerodynamical model of aircraft is called subroutine AERK. The aerodynamic of bombs are treated next. The corresponding subroutine is called subroutine WAERK. Then a model for the thrust forces and moments is developed. The program which implements this model is called subroutine THRUSK. Finally, the effects of moving air mass on the aerodynamics of rigid bodies are treated to take into account the mean winds and stochastic wind gusts. The program which implements the wind model is called subroutine WINDK.

AERODYNAMIC FORCES AND MOMENTS FOR AIRCRAFT

The aerodynamic forces and moments are computed by making use of extensive aerodynamic data tables. The primary objective of the function lookup subroutine (FLOOK), presented in Volume II is to provide for a complete accounting of the various contributions to the aerodynamic forces and moments regardless of the flight conditions or the body (i. e., aircraft, weapon) being considered. The technique used is an n-dimensional table lookup and linear interpolation. This method has the advantage of accurately describing even the most nonlinear variations with a minimum of preparation effort. However, the amount of storage space and computing time increases rapidly with the number of dimensions of the tables.

The Functional Form of the Aerodynamic Forces and Moments

The major variables that affect the aerodynamic characteristics of a body are: Mach number, M ; dynamic pressure, \bar{q} ; angle of attack, α ; angle of sideslip, β ; total linear velocity, angular velocity, and control surface deflections. Two typical functional-dependence relations can be written as

$$F = F(x_1, \dot{x}_1, x_2, \dot{x}_2, \delta, \dot{\delta}, h, M) \quad (4.1)$$

$$= F(V, \alpha, \beta, \dot{V}, \dot{\alpha}, \dot{\beta}, x_2, \dot{x}_2, \delta, \dot{\delta}, h, M) \quad (4.2)$$

where

- x_1 = linear velocity state vector
- x_2 = angular velocity state vector
- δ = control surface deflection vector
- h = altitude
- M = Mach number
- V = total velocity
- α = angle of attack
- β = sideslip angle

The decomposition of (4.1) or (4.2) into functional relationships with fewer number of arguments is needed for practical reasons. Unfortunately, there is no standard form for this decomposition, and it is dependent on the available data. Usually airframe and weapon manufacturers provide empirical or estimated relations in the form of curves or data tables.

Usage of Aerodynamic Data

Aerodynamic characteristics strongly depend upon the orientation of the relative wind or velocity vector with respect to body, so the angle of attack, α , and sideslip angle, β , which define the orientation with respect to the air mass are used often, as indicated in equation (4.2). In general, the aerodynamic data is classified into two groups; static data and dynamic data. Static data implies that, during the wind tunnel testing, the body is at rest with respect to the relative wind. The dynamic data implies that body oscillates or rotates with respect to the relative wind.

The aerodynamic data are usually given in the "wind-tunnel stability axes" defined as follows [15]:

Origin: center of mass (cg)

- x_s : in the direction of motion along the projection of V upon the body reference plane.
- y_s : same as body axes, positive right
- z_s : perpendicular to $x_s y_s$ plane forming right-hand triad

The wind tunnel stability axes system is illustrated in Figure 9. Clearly the body axes system and stability axes systems are related to each other by

$$\begin{pmatrix} x_s \\ y_s \\ z_s \end{pmatrix} = E_s \begin{pmatrix} x \\ y \\ z \end{pmatrix} \quad (4.3)$$

where

$$E_s = \begin{pmatrix} \cos \alpha & 0 & \sin \alpha \\ 0 & 1 & 0 \\ -\sin \alpha & 0 & \cos \alpha \end{pmatrix}$$

The resolution of the total aerodynamic force in the xz plane is shown in Figure 10 where lift, L, and drag, D, are forces normal and parallel, respectively, to the projection of V in the xz plane. Lift and drag are defined to be positive as illustrated.

Aerodynamic forces and moments are expressed in terms of the basic aerodynamic coefficients in the wind tunnel stability axes with origin located at an arbitrary reference point. The aerodynamic force and moment coefficients are defined by the following relations:

$$f_{sa} = \begin{pmatrix} X_s \\ Y_s \\ Z_s \end{pmatrix} = \begin{pmatrix} -D \\ Y \\ -L \end{pmatrix} = \begin{bmatrix} -(\bar{q}S) & 0 & 0 \\ 0 & (\bar{q}S) & 0 \\ 0 & 0 & -(\bar{q}S) \end{bmatrix} \begin{bmatrix} \Sigma C_D \\ \Sigma C_Y \\ \Sigma C_L \end{bmatrix} \quad (4.4)$$

$$m_{sca} = \begin{pmatrix} L_{sc} \\ M_{sc} \\ N_{sc} \end{pmatrix} = \begin{bmatrix} (\bar{q}S)b & 0 & 0 \\ 0 & (\bar{q}S)\bar{c} & 0 \\ 0 & 0 & (\bar{q}S)b \end{bmatrix} \begin{bmatrix} \Sigma C_{lsc} \\ \Sigma C_{msc} \\ \Sigma C_{nsc} \end{bmatrix} \quad (4.5)$$

where

- \bar{q} = dynamic pressure (lb/ft²)
- S = wing area (ft²)
- b = wing span (ft)
- \bar{c} = wing mean aerodynamic chord (ft)

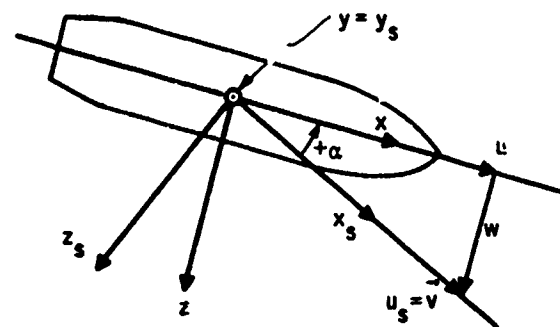


Figure 9. Body and Wind Tunnel Stability Axes Systems

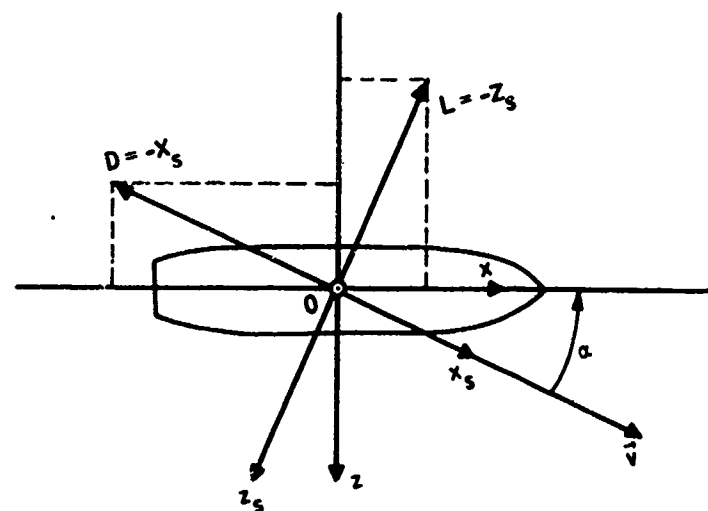


Figure 10. Aerodynamic Force Angular Resolution

It is assumed that the moment reference center 0_{ca} is located by $\vec{\Delta r}_{ca}$ from the cg of the aircraft as shown in Figure 11.

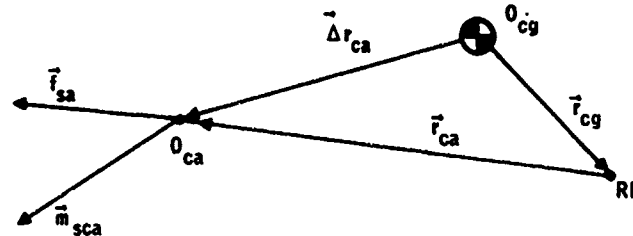


Figure 11. Moment Reference Center With Respect to Mass Center

The total aerodynamic forces at the cg in body axes are then given by

$$\vec{f}_a = E'_s \vec{f}_{sa} = E'_s \begin{bmatrix} X_s \\ Y_s \\ Z_s \end{bmatrix} \quad (4.6)$$

Similarly the total aerodynamic moments at the cg about the wind tunnel stability axes are given by

$$\vec{M}_{sa} = \vec{M}_{sca} + (\vec{\Delta r}_{ca})_s \times \vec{f}_{sa} \quad (4.7)$$

Or in matrix notation, and in body axes

$$\vec{M}_a = E'_s \vec{M}_{sca} + \Delta R_{ca} \vec{f}_a \quad (4.8)$$

where, in terms of a reference point RP on the body (see Figure 11),

$$\vec{\Delta r}_{ca} = \vec{r}_{cg} + \vec{r}_{ca} \quad (4.9)$$

and

$\vec{\Delta r}_{ca}$ = position vector from 0_{cg} to 0_{ca}

\vec{r}_{cg} = position vector from 0_{cg} to RP

\vec{r}_{ca} = position vector from RP to 0_{ca}

and, with coordinates expressed in body axes,

$$\Delta R_{ca} = \begin{bmatrix} 0 & -\Delta z_{ca} & \Delta y_{ca} \\ \Delta z_{ca} & 0 & -\Delta x_{ca} \\ -\Delta y_{ca} & \Delta x_{ca} & 0 \end{bmatrix} \quad (4.10)$$

Substituting (4.5) and (4.9) into (4.8) yields the moment components in body axes at the cg.

$$\begin{bmatrix} L \\ M \\ N \end{bmatrix} = E'_s \begin{bmatrix} L_{sc} \\ M_{sc} \\ N_{sc} \end{bmatrix}_s + \begin{bmatrix} 0 & -\Delta z_{ca} & \Delta y_{ca} \\ \Delta z_{ca} & 0 & -\Delta x_{ca} \\ -\Delta y_{ca} & \Delta x_{ca} & 0 \end{bmatrix} \begin{bmatrix} X \\ Y \\ Z \end{bmatrix} \quad (4.11)$$

Total Aerodynamic Coefficient Model for Aircraft

In the formulae given below the superscript "o" indicates degrees, the subscript "a" denotes quantities with respect to the air-mass, and subscript "w" stands for wings with respect to the air mass ($\alpha_w = \alpha_a + i_w$). This notion will be useful in treating a moving air mass as discussed later. The aerodynamic force coefficients in the wind tunnel stability axes are assumed to be in the following form [36]:

$$\begin{bmatrix} \Sigma C_D \\ \Sigma C_Y \\ \Sigma C_L \end{bmatrix}_s = \begin{bmatrix} C_D(Pow M_a, C_L) + C_D(\delta_{sb}, C_L, M_a) \\ 0 \\ C_L(M_a, h, \alpha_w^o) \end{bmatrix} \\ + \begin{bmatrix} 0 & 0 \\ 0 & C_{y_\beta}(\alpha_w^o, h, M_a) \\ 0 & 0 \end{bmatrix} \begin{pmatrix} \alpha_w^o \\ \beta_a^o \end{pmatrix} + \begin{bmatrix} 0 & 0 \\ 0 & 0 \\ -C_{L_\alpha}(h, M_a) & 0 \end{bmatrix} \begin{pmatrix} \frac{\bar{c}}{2u_s} & 0 \\ 0 & \frac{b}{2u_s} \end{pmatrix} \begin{pmatrix} \dot{\alpha}_a \\ \dot{\beta}_a \end{pmatrix} \\ + \begin{bmatrix} 0 & 0 & 0 \\ C_{y_p}(h, \alpha_w^o, M_a) & 0 & C_{y_r}(\alpha_w^o, h, M_a) \\ 0 & -C_{L_q}(h, M_a) & 0 \end{bmatrix} \begin{bmatrix} \frac{b}{2u_s} & 0 & 0 \\ 0 & \frac{\bar{c}}{2u_s} & 0 \\ 0 & 0 & \frac{b}{2u_s} \end{bmatrix} \begin{bmatrix} p_{sa} \\ q_{sa} \\ r_{sa} \end{bmatrix} +$$

$$\begin{aligned}
& + \begin{bmatrix} C_{D_{\delta a}}(h, M_a) & C_{D_{\delta s}}(h, \alpha_w^0, M_a) & 0 \\ C_{y_{\delta a}}(M_a) & 0 & C_{y_{\delta r}}(h, M_a) \\ C_{L_{\delta a}}(h, M_a) & C_{L_{\delta s}}(h, \alpha_w^0, M_a) & 0 \end{bmatrix} \begin{bmatrix} \delta_a^0 \\ \delta_s^0 \\ \delta_r^0 \end{bmatrix} \\
& + \begin{bmatrix} C_{D_{\delta sp}}(h, M_a) & 0 & C_{D_{\delta lg}}(\alpha_w^0) \\ C_{y_{\delta sp}}(M_a) & 0 & 0 \\ C_{L_{\delta sp}}(h, M_a) & C_{L_{\delta sb}}(\alpha_w^0, M_a) & C_{L_{\delta lg}}(\alpha_w^0) \end{bmatrix} \begin{bmatrix} \delta_{sp}^0 \\ \delta_{sb}^0 \\ \delta_{lg}^0 \end{bmatrix}
\end{aligned}$$

Similarly the aerodynamic moment coefficients in the stability axes are assumed to be in the form of

$$\begin{aligned}
& \begin{bmatrix} \Sigma C_{1sc} \\ \Sigma C_{msc} \\ \Sigma C_{nsc} \end{bmatrix} = \begin{bmatrix} 0 \\ C_{msc}(M_a, h, \alpha_w^0) \\ 0 \end{bmatrix} \\
& + \begin{bmatrix} 0 & C_{1_\beta}(\alpha_w^0, h, M_a) \\ 0 & 0 \\ 0 & C_{n_\beta}(\alpha_w^0, h, M_a) \end{bmatrix} \begin{pmatrix} \alpha_w^0 \\ \beta_w^0 \end{pmatrix} + \begin{bmatrix} 0 & 0 \\ C_{m_{\dot{\alpha}}}(\alpha_w^0, h, M_a) & 0 \\ 0 & 0 \end{bmatrix} \begin{bmatrix} \frac{\bar{c}}{2u_s} & 0 \\ 0 & \frac{b}{2u_s} \end{bmatrix} \begin{pmatrix} \dot{\alpha}_a \\ \dot{\beta}_a \end{pmatrix} \\
& + \begin{bmatrix} C_{1_p}(\alpha_w^0, h, M_a) & 0 & C_{1_r}(\alpha_w^0, h, M_a) \\ 0 & C_{m_q}(h, M_a) & 0 \\ C_{n_p}(h, \alpha_w^0, M_a) & 0 & C_{n_r}(M_a, h, \alpha_w^0) \end{bmatrix} \begin{bmatrix} \frac{b}{2u_s} & 0 & 0 \\ 0 & \frac{\bar{c}}{2u_s} & 0 \\ 0 & 0 & \frac{b}{2u_s} \end{bmatrix} \begin{bmatrix} p_a \\ q_a \\ r_a \end{bmatrix} \\
& + \begin{bmatrix} C_{1_{\delta a}}(\alpha_w^0, h, M_a) & 0 & C_{1_{\delta r}}(\alpha_w^0, h, M_a) \\ C_{m_{\delta a}}(\alpha_w^0, h, M_a) & C_{m_{\delta s}}(h, \alpha_w^0, M_a) & 0 \\ C_{n_{\delta a}}(\alpha_w^0, h, M_a) & 0 & C_{n_{\delta r}}(h, M_a) \end{bmatrix} \begin{bmatrix} \delta_a^0 \\ \delta_s^0 \\ \delta_r^0 \end{bmatrix} +
\end{aligned}$$

$$+ \begin{bmatrix} C_{l_{\delta}}(\alpha_w^o, h, M_a) & 0 & 0 \\ C_{m_{\delta}^{sp}}(\alpha_w^o, h, M_a) & C_{m_{\delta}^{sb}}(M_a, \alpha_w^o) & C_{m_{\delta}^{lg}}(\alpha_w^o) \\ C_{n_{\delta}^{sp}}(\alpha_w^o, M_a) & 0 & 0 \end{bmatrix} \begin{bmatrix} \delta^o_{sp} \\ \delta^o_{sb} \\ \delta^o_{lg} \end{bmatrix}$$

AERODYNAMIC FORCE AND MOMENT MODEL FOR BOMB

A complete aerodynamic model for a slowly spinning, four-finned bomb is given in [17], where the aerodynamic parameters are assumed to be linear functions of spin, cross-spin and accidental configurational asymmetry but nonlinear functions of yaw orientation and roll orientation. Then the effects of roll orientation on the aerodynamic forces and moments are obtained by a Fourier series expansion of roll angle (the angle between the [plane of yaw] and a reference fin). The model based on [17] (i.e., Cohen's model) requires approximately 20 aerodynamic tables (i.e., tests), and these tables are not readily available.

In ADAPS, a simplified aerodynamic bomb model is developed. It utilizes generally available bomb aerodynamic data. The effect of roll orientation is ignored. [The cross-velocity frame and cross-spin frame are the same as defined in [17].]

Simplified Aerodynamic Model for Bomb

The reference axes used in the bomb aerodynamic model are illustrated in Figure 12.

0 = origin, at the [center of gravity] of bomb

The weapon body axes are defined as follows:

x-axis is along the bomb body, positive forward

y-axis is horizontal positive right

z-axis is perpendicular to the xy plane, positive down.

The cross-velocity axes are defined as follows:

x_1 is the same as the body x-axis

z_1 is in the direction of cross-velocity \vec{v}_{ca} ($V_{ca}^2 = v^2 + w^2$)

y_1 is perpendicular to the $x_1 z_1$ plane forming a right-handed system.

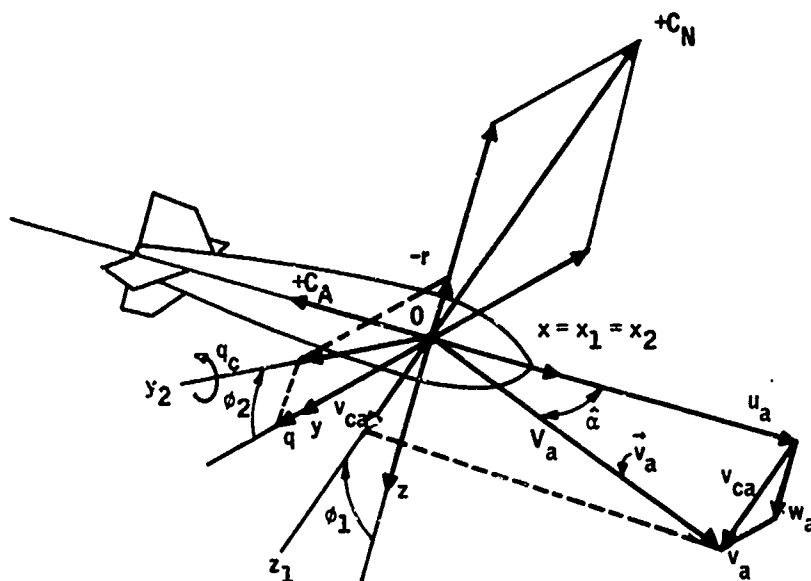


Figure 12. Definition of Stability-Like Axes for Bomb

The cross-spin axes are defined as follows:

x_2 is the same as the body-axis

y_2 is in the direction of cross-spin, $\bar{q}_c (q_c^2 = q^2 + r^2)$

z_2 is perpendicular to $x_2 y_2$, the plane forming a right-handed system.

The aerodynamic forces and moments in body axes are given as

$$\begin{pmatrix} X \\ Y \\ Z \end{pmatrix} = \bar{q}S \begin{pmatrix} \Sigma C_x \\ \Sigma C_y \\ \Sigma C_z \end{pmatrix}$$

$$\begin{pmatrix} L \\ M \\ N \end{pmatrix} = \bar{q}Sd \begin{pmatrix} \Sigma C_l \\ \Sigma C_m \\ \Sigma C_n \end{pmatrix}$$

where

$$\bar{q} = 1/2 \rho V_a^2, \text{dynamic pressure, lb/ft}^2$$

$$S = \text{cross-sectional area of the bomb} = \pi \frac{d^2}{4}, \text{ft}^2$$

$$d = \text{diameter of the bomb, ft}$$

and $(\Sigma C_x, \Sigma C_y, \Sigma C_z) = \text{aerodynamic force coefficients in body axes system}$

$(\Sigma C_l, \Sigma C_m, \Sigma C_n) = \text{aerodynamic moment coefficients in body axes system}$

The nondimensional aerodynamic data are given in the cross-velocity frame. They are:

$C_A(\hat{\alpha}, M) = \text{axial force coefficient, along x-axis, positive aft}$

$C_N(\hat{\alpha}, M) = \text{normal force coefficient perpendicular to the plane of yaw}$

$C_{N\delta}(\hat{\alpha}, M) = \text{coefficient of normal force due to canted fin shielding}$

$C_m(\hat{\alpha}, M) = \text{restoring moment coefficient, about } y_1\text{-axis}$

$C_{m\delta}(\hat{\alpha}, M) = \text{restoring moment coefficient, due to canted fin shielding about } y_1\text{-axis}$

$C_{mq}(\hat{\alpha}, M) = \text{damping moment coefficient about } y_2\text{-axis}$

The data for the moment coefficients are referenced to the center of gravity [26, 29].

The transformation matrices from the cross-velocity frame to body frame, and from the cross-spin frame to body frame are given respectively as

$$\xi = E_1 \xi_1 \quad \eta = E_2 \eta$$

where

$$E_1 = \begin{bmatrix} 1 & 0 & 0 \\ 0 & \cos \phi_1 & \sin \phi_1 \\ 0 & -\sin \phi_1 & \cos \phi_1 \end{bmatrix}, \quad E_2 = \begin{bmatrix} 1 & 0 & 0 \\ 0 & \cos \phi_2 & \sin \phi_2 \\ 0 & -\sin \phi_2 & \cos \phi_2 \end{bmatrix}$$

and

$$\phi_1 = \tan^{-1} \frac{v_a}{w_a} \text{ and } \phi_2 = \tan^{-1} \frac{-r}{q}, \text{deg}$$

The aerodynamic coefficients along the body axes are given by

$$\begin{pmatrix} \Sigma C_x \\ \Sigma C_y \\ \Sigma C_z \end{pmatrix} = E_1 \begin{pmatrix} -C_A(M) \\ 0 \\ -C_N(\hat{\alpha}, M) \quad -C_{N_\delta}(\hat{\alpha}, M) \hat{\delta} \end{pmatrix}$$

$$\begin{pmatrix} \Sigma C_1 \\ \Sigma C_m \\ \Sigma C_n \end{pmatrix} = E_1 \begin{pmatrix} 0 \\ C_m(\hat{\alpha}, M) + C_{m_\delta}(\hat{\alpha}, M) \hat{\delta} \\ 0 \end{pmatrix} + E_2 \begin{pmatrix} 0 \\ C_{m_q}(\hat{\alpha}, M) \left(\frac{d}{2V_a} \right) q_c \\ 0 \end{pmatrix}$$

where

$$\hat{\alpha} = \tan^{-1} \frac{v_{ca}}{u_a}, \text{ magnitude of yaw (deg)}$$

$$v_{ca} = \sqrt{v_z^2 + w_a^2}, \text{ cross-velocity (ft/sec)}$$

$$V_a = \sqrt{u_a^2 + v_a^2 + w_a^2}, \text{ total velocity (ft/sec)}$$

$$\delta = \sqrt{\delta_z^2 + \delta_y^2}, \text{ magnitude of fin cant angle (deg)}$$

$$q_c = \sqrt{q^2 + r^2}, \text{ cross-spin (deg/sec)}$$

DEVELOPMENT OF A MODEL FOR THRUST FORCES AND MOMENTS

In general, the total thrust forces and moments acting on a rigid body depend upon the positions and orientations of the thrust producers with respect to the body axes and the magnitudes of the thrusts (geometry). There are also dynamics associated with the thrust variables since they are produced and oriented by engines and actuators.

To provide an analysis tool by which the effects of various control points and methods can be investigated, both aspects are considered in the development of a thrust model in ADAPS.

In the following, a geometric model for the effective thrust acting on a rigid body is developed first. Then the dynamics of thrust producers are treated. In the development, the effects of angular momentum of rotating thrust producers are neglected.

A Geometrical Model of Thrust Producers

In the following, first the description of a geometrical model for thrust producers is given. Then the total force and moment contributions of thrust producers are developed in the form of

$$f_T = B_T (x_d) y_T \quad (4.12)$$

$$m_T = \hat{B}_T (x_d) y_T \quad (4.13)$$

where

f_T = total thrust force vector along body axes

m_T = total thrust moment vector along body axes

B_T = thrust force coefficient matrix of size $3 \times v$

\hat{B}_T = thrust moment coefficient matrix of size $3 \times v$

x_d = state vector of thrust orientation actuator positions

y_T = effective thrust output magnitude vector

v = number of thrust points in the thrust-producing system

Figure 13 shows the geometry of a single thrust producer.

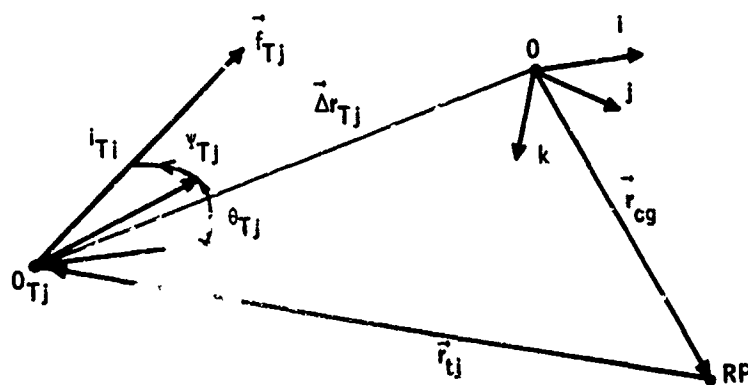


Figure 13. Geometry of a Thrust Producer

In this model, the nozzle of the j^{th} thrust producer is located by vector $\vec{\Delta r}_{Tj}$ from the cg of body. It is assumed that the orientation of the nozzle axis is described by (θ_{Tj}, ψ_{Tj}) , the elevation and azimuth angles from body to nozzle axes. The position vector $\vec{\Delta r}_{Tj}$ is assumed to vary as the position of the cg varies. In this model it is assumed that the movement of the mass center is confined to the xz plane. The position vectors \vec{r}_{cg} and \vec{r}_{Tj} from a body-fixed reference point RP are used to specify $\vec{\Delta r}_{Tj}$. Denoting the thrust vectors by \vec{f}_{Tj} , the total forces and moment due to thrust producers become

$$\vec{f}_T = \sum_{j=1}^v \vec{f}_{Tj} \quad (4.14)$$

$$\vec{m}_T = \sum_{j=1}^v \vec{\Delta r}_{Tj} \times \vec{f}_{Tj} \quad (4.15)$$

where

$$\vec{\Delta r}_{Tj} = \vec{r}_{c.g.} + \vec{r}_{Tj} \quad j = 1, 2, \dots, v \quad (4.16)$$

and

$$\vec{\Delta r}_{Tj} = \text{position vector from } 0 \text{ to } 0_{Tj}$$

$$\vec{r}_{c.g.} = \text{position vector from } 0 \text{ to RP}$$

$$\vec{r}_{Tj} = \text{position vector from RP to } 0_{Tj}$$

as shown in Figure 13.

In matrix notation

$$f_T = \sum_{j=1}^v f_{Tj} \quad (4.17)$$

and

$$m_T = \sum_{j=1}^v \Delta R_{Tj} f_{Tj} \quad (4.18)$$

where

$$\Delta R_{Tj} = \begin{bmatrix} 0 & -\Delta z_{Tj} & \Delta y_{Tj} \\ \Delta z_{Tj} & 0 & -\Delta x_{Tj} \\ -\Delta y_{Tj} & \Delta x_{Tj} & 0 \end{bmatrix} \quad (4.19)$$

and

$$\Delta r_{Tj} = \begin{pmatrix} \Delta x_{Tj} \\ \Delta y_{Tj} \\ \Delta z_{Tj} \end{pmatrix} = \begin{pmatrix} x_{c.g.} \\ 0 \\ z_{c.g.} \end{pmatrix} + \begin{pmatrix} x_{Tj} \\ y_{Tj} \\ z_{Tj} \end{pmatrix} \quad (4.20)$$

Let T_j be the effective thrust magnitude of the j th thruster. Then, in terms of the elevation and azimuth angles, θ_{Tj} and ψ_{Tj} of the nozzle axis from the body axis, the components of thrust forces f_{Tj} along body axes can be expressed as

$$f_{Tj} = b_j T_j \quad j = 1, 2, \dots, v \quad (4.21)$$

where

$$b_j = \begin{pmatrix} b_{1j} \\ b_{2j} \\ b_{3j} \end{pmatrix} = \begin{bmatrix} \cos \psi_{Tj} \cos \theta_{Tj} \\ \sin \psi_{Tj} \\ -\cos \psi_{Tj} \sin \theta_{Tj} \end{bmatrix} \quad (4.22)$$

Making use of (4.21) and (4.22) yields

$$f_T = B_T y_T \quad (4.23)$$

where

$$B_T = [b_1 | b_2 | \dots | b_v] \text{ and } y_T = \begin{pmatrix} T_1 \\ T_2 \\ \vdots \\ T_v \end{pmatrix} \quad (4.24)$$

Similarly, using (4.21) in (4.18) yields

$$m_T = \hat{B}_T u_T \quad (4.25)$$

where

$$\hat{B}_T = [\hat{b}_1 | \hat{b}_2 | \dots | \hat{b}_v] \quad (4.26)$$

with

$$\hat{b}_j = \Delta R_{Tj} b_j \text{ and} \quad (4.27)$$

$$\hat{b}_j = \begin{bmatrix} \hat{b}_{1j} \\ \hat{b}_{2j} \\ \hat{b}_{3j} \end{bmatrix} = \begin{bmatrix} (\Delta y_{Tj})(b_{3j}) - (\Delta z_{Tj})(b_{2j}) \\ (\Delta z_{Tj})(b_{1j}) - (\Delta x_{Tj})(b_{3j}) \\ (\Delta x_{Tj})(b_{2j}) - (\Delta y_{Tj})(b_{1j}) \end{bmatrix} \quad (4.28)$$

Equations (4.23) and (4.25) constitute the geometry of the thrust producers. In the following, the dynamics of thrust producers and thrust orientation actuators are treated briefly.

Dynamical Model for Thrust Magnitudes

It is assumed that the magnitude dynamics of each thrust producer can be represented by a first-order transfer function. This is shown in Figure 14.

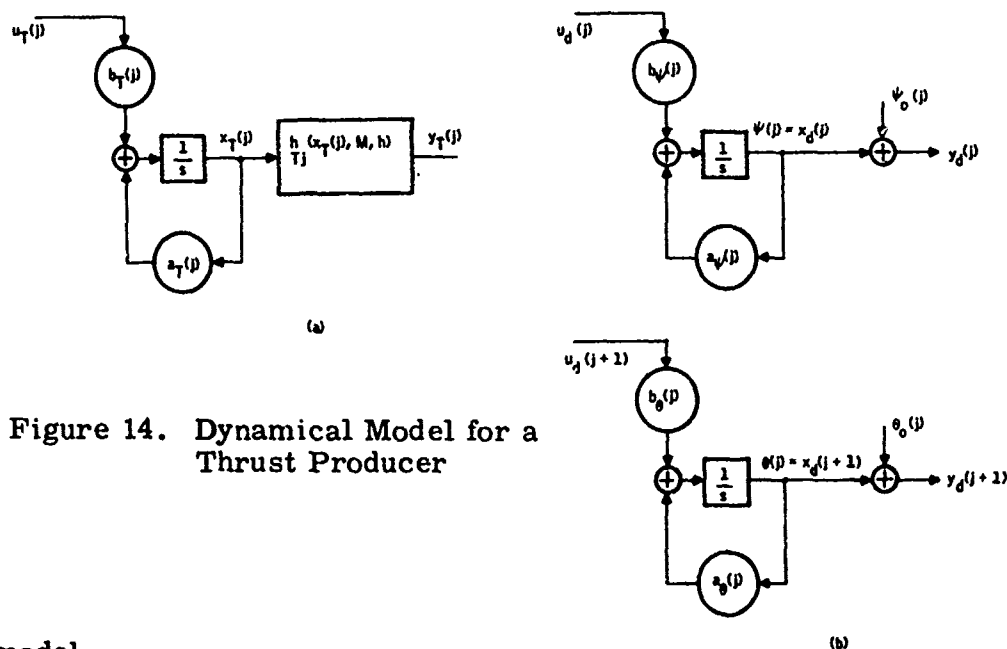


Figure 14. Dynamical Model for a Thrust Producer

In this model

- $x_T(j)$ = the magnitude state of the j^{th} thrust producer in percent
- $y_T(j)$ = effective thrust output of the j^{th} thrust producer acting on the rigid body in lbs
- $h_T(j)$ = nonlinear output function
- $u_T(j)$ = throttle input to j^{th} thrust producer in percent
- $a_T(j), b_T(j)$ = transition and input coefficients of the producer

The output function for the two main thrust producers (i. e., engines) is assumed to be in the following form [36]:

$$y_T(j) = [(1+e_1M)(1+e_0h)]y_0 + \left\{ (1+e_2M)(1+e_0h)(c)[x_T(j)-\xi_T(j)] \right\}, j = 1, 2$$

In this equation e_0 , e_1 and e_2 are Mach-number- and altitude-dependent coefficients of the effective thrust, y_0 is thrust bias, c is the thrust output coefficient, and $\xi_T(j)$ is a function of $x_T(j)$. These coefficients are piece wise-constant functions of $x_T(j)$, and typical values for F-4 engines are given in Table I.

Dynamical Model for Thrust Orientation Actuators

The thrust orientation state of each thrust producer is described by the azimuth and elevation angles of the nozzle axis as defined in Figure 13.

$$x_d(j) = \begin{bmatrix} \psi(j) \\ \theta(j) \end{bmatrix} \quad (4.29)$$

Table I. Effective Thrust Output Coefficients, $j = 1, 2$

Coefficient	$0 \leq x_T \leq 50$	$50 \leq x_T \leq 100$
y_0	700	9650
c	179	137
ξ_T	0	50
e_1	0	-0.2342
e_2	-0.25150	0.32846
e_0	$-(0.25)10^{-4}$	$-(0.25)10^{-4}$

It is assumed that first-order dynamics is associated with thrust orientation actuators. Thus for each thrust producer (see Figure 14b)

$$\dot{x}_d = A_d x_d + B_d u_d \quad (4.30)$$

$$y_d = y_{do} + x_d \quad (4.31)$$

where

$$y_{do} = \text{orientation bias} = \begin{pmatrix} \psi_b \\ \theta_b \end{pmatrix} \quad (4.32)$$

Implementation of the thrust orientation dynamics is outside the scope of the present program. However, in ADAPS, the thrust model includes equation (4.31) through which thrust orientation dynamics can be inserted into the overall program.

EFFECT OF MOVING AIR MASS ON THE AERODYNAMICS OF A RIGID BODY

The aerodynamic force and moment system developed above is with respect to the air mass (i. e., atmosphere). It is known that the air mass through which a rigid body flies or falls is in a motion which is variable both in time and in space (Figure 15). In this subsection the influence of this motion on the rigid-body aerodynamics is presented.

Modeling for the Influence of Unsteady Air Mass

Meteorological observations indicate that the velocity field of air mass (i. e., winds) in the lower atmosphere consists of two distinct components, a low-frequency component with energies concentrated in 0.01-cycle/hour range and a high-frequency component with energies in the 70-cycle/hour range. The former is called the "mean wind", and the latter is referred to as atmospheric turbulence or simply as "wind gust".

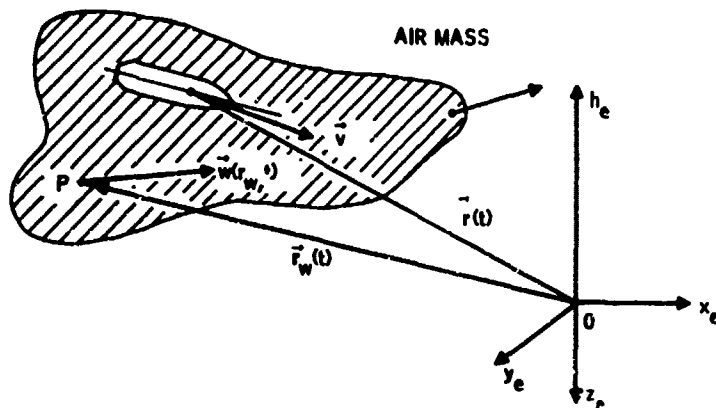


Figure 15. Rigid Body in an Unsteady Air Mass

In the earth axes, the velocity field of the air mass can therefore be decomposed into

$$\vec{w}_e = \vec{\bar{w}}_e + \vec{\tilde{w}}_e \quad (4.33)$$

where, in matrix notation,

\vec{w}_e = velocity field vector

$\vec{\bar{w}}_e$ = mean velocity field vector

$\vec{\tilde{w}}_e$ = gust velocity field vector

and all are, in general, position- and time-dependent.

The influence of motion of the air mass on rigid-body aerodynamics is taken into account with various degrees of accuracy by considering a rigid body as a point, line, surface or volume. When a rigid body is considered as a point in the air mass, then the relative motion appears as the difference

$$\vec{v}_a = \vec{v} - \vec{w} \quad (4.34)$$

where \vec{w} is the velocity field vector in body axes. In this case, the aerodynamic effect of the motion of air mass is accounted for by the use of the equivalent (i. e., producing the same aerodynamic effects) velocity \vec{v}_a , angle of attack α_a and angle of sideslip β_a .

It should be noted that the equivalent linear velocities are to be used only for developing the aerodynamic forces and moments. Elsewhere in the dynamical equations the inertial velocities are used.

If a rigid body is assumed to have one or more dimensions in space, then the space distribution of the velocity field on the assumed rigid-body model must be taken into account. At this point, various approximations are made to simplify the modeling problem. One such approximation is given in [30] where the space distribution of the velocity field is lumped at the various stations on the body. The resulting equivalent velocities are used for computing aerodynamic forces and moments. In [30], the penetration effects of the wind gusts are also considered. The treatment with such depth produces a relatively complex model for the air-mass velocities; it is recommended for cases where the body velocities with respect to ground are relatively low and the body-bending modes are significant.

In ADAPS, a simpler model can be used because of relatively high aircraft and weapon velocities and rigid-body model. It is assumed that the velocity field is linearly distributed about the cg of a rigid body. The overall influence of the motion of air mass is accounted for by \vec{v}_a and its space gradient matrix $\frac{\partial \vec{v}_a}{\partial x}$ evaluated at the cg of a rigid body. It can be shown [16, 31] that the effects of space gradients can be conveniently taken into account by use of the equivalent angular velocity vector defined by

$$\vec{\omega}_a = \vec{\omega} + \vec{\omega}_w \quad (4.35)$$

where $\vec{\omega}_w$ is the synthetic angular velocity vector corresponding to the gradient effects of the moving air mass.

In the following, a simplified model for the equivalent linear and angular velocities is presented.

Modeling for the Equivalent Linear and Angular Velocities

First the modeling for the mean wind is presented. Then modeling for the turbulence (i. e., gust) is treated.

Mean Wind Model -- As shown in Figure 16, the mean wind is described by its magnitude and its orientation in the earth-fixed axes as follows:

$$\vec{w} = \begin{bmatrix} \bar{V} \\ \bar{\psi} \\ \bar{\theta} \end{bmatrix} \quad (4.36)$$

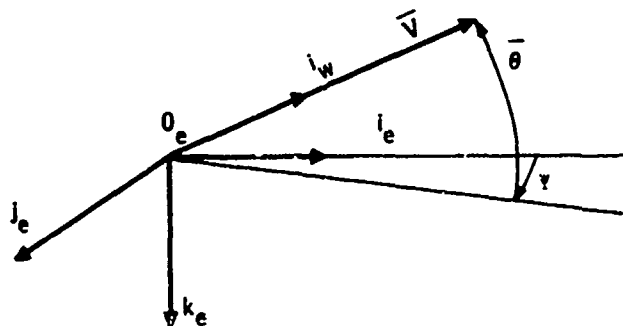


Figure 16. Description of the Mean Wind

where

\bar{V} = magnitude of the mean velocity vector relative to the origin of the earth-fixed axes

$\bar{\psi}$ = azimuth angle of the mean velocity vector with respect to earth axes

$\bar{\theta}$ = elevation angle of the mean velocity vector with respect to earth axes

The transformation matrix from the mean wind axes to the earth-fixed axes becomes

$$\bar{E}' = \begin{bmatrix} \cos \bar{\theta} \cos \bar{\psi} & -\sin \bar{\psi} & \sin \bar{\theta} \cos \bar{\psi} \\ \cos \bar{\theta} \sin \bar{\psi} & \cos \bar{\psi} & \sin \bar{\theta} \sin \bar{\psi} \\ -\sin \bar{\theta} & 0 & \cos \bar{\theta} \end{bmatrix} \quad (4.37)$$

Thus the components of the mean velocity vector along the earth-fixed axes becomes

$$\bar{w}_e = \bar{E}' \begin{bmatrix} \bar{V}_w \\ 0 \\ 0 \end{bmatrix} \quad (4.38)$$

or

$$\bar{w}_e = \begin{pmatrix} \cos \bar{\theta} \cos \bar{\psi} \\ \cos \bar{\theta} \sin \bar{\psi} \\ -\sin \bar{\theta} \end{pmatrix} \bar{V} \quad (4.39)$$

Then along the body axes the mean wind has the following components:

$$\bar{w} = E \bar{w}_e \quad (4.40)$$

where E is the transformation matrix from earth to body axes as defined by equation (3.14) in Section III.

The magnitude \bar{V} of the mean wind is assumed to be altitude-dependent according to the following simplified functional relationship

$$\bar{V}(h) = \bar{V}_0 \left(\frac{h}{h_0} \right)^e \quad (4.41)$$

where

- h = the altitude of interest
- h_o = a reference altitude at which the mean wind speed is known
- \bar{V}_o = the mean wind speed at reference altitude h_o
- e = an empirical exponent which expresses the thermal stability conditions of the atmosphere and the degree of roughness of the surface beneath

For slightly unstable air, typical values of e range from 0.12 for smooth surfaces (such as deserts) to 0.38 for very rough terrain. In ADAPS, a constant value of 0.25 is used, representing average conditions. Equations (4.39), (4.40) and (4.41) constitute the mean-wind model used in ADAPS.

Gust (Turbulence) Model -- The gust model used in ADAPS is the form attributed to Dryden with the coefficients specified in Ref. 31. In this form, it is assumed that gust velocities are locally isotropic (i. e., locally invariant with respect to position and orientation) and that time variations are statistically equivalent to distance variations in traversing the gust field.

The translational gust velocity vector is defined as

$$\tilde{w} = \begin{pmatrix} u_g \\ v_g \\ w_g \end{pmatrix} \quad (4.42)$$

The power spectral densities for the translational gust velocity components are given by

$$\Phi_w(\Omega) = \begin{pmatrix} \phi_{ug}(\Omega) \\ \phi_{vg}(\Omega) \\ \phi_{wg}(\Omega) \end{pmatrix} = \begin{bmatrix} \sigma_u^2 \left(\frac{2L_u}{\pi} \right) & \frac{1}{[1+(L_u\Omega)^2]} \\ \sigma_v^2 \left(\frac{L_v}{\pi} \right) & \frac{[1+3(L_v\Omega)^2]}{[1+(L_v\Omega)^2]^2} \\ \sigma_w^2 \left(\frac{L_w}{\pi} \right) & \frac{[1+3(L_w\Omega)^2]}{[1+(L_w\Omega)^2]^2} \end{bmatrix} \quad (4.43)$$

where

$$\Omega = \frac{2\pi}{\lambda} = \text{spatial frequency, (rad/ft)} \quad (4.44)$$

$$\lambda = \text{wavelength, (ft)}$$

$$L_i = \text{scales (ft)}$$

$$\sigma_i = \text{the root mean-square gust velocities (ft/sec)}$$

$$i = u, v, w$$

The mean-square gust velocities and the scales are related to each other through the following set of equations:

$$\frac{\sigma_u^2}{L_u} = \frac{\sigma_v^2}{L_v} = \frac{\sigma_w^2}{L_w} \quad (4.45)$$

The quantities appearing above have the following altitude dependence:

$$100 < h < 1750 \text{ ft}$$

$$L_w = h$$

$$L_u = L_v = 145.0 h^{1/3} \quad (4.46)$$

$$h > 1750 \text{ ft}$$

$$L_w = L_u = L_v = 1750 \text{ ft}$$

$$\sigma_w = 5.25 - \log_{10} \left(\frac{h}{10,000} \right)^{1.25}$$

For $0 < h < 100$, the value of $h = 100$ is used in the above equations.

The gradient effects of gust velocities are considered as explained earlier by defining angular gust velocities as follows:

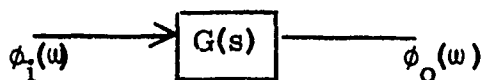
$$\underline{\omega} = \begin{pmatrix} p_g \\ q_g \\ r_g \end{pmatrix} = \begin{pmatrix} -\frac{\partial w_g}{\partial y} \\ +\frac{\partial w_g}{\partial x} \\ -\frac{\partial v_g}{\partial x} \end{pmatrix} \quad (4.47)$$

The spectra for the angular gust velocity vector ω_w are given by

$$\underline{\phi}_w(\Omega) = \begin{bmatrix} \phi_{p_g}(\Omega) \\ \phi_{q_g}(\Omega) \\ \phi_{r_g}(\Omega) \end{bmatrix} = \begin{bmatrix} \left(\frac{\sigma_w^2}{L_w} \right) \frac{(0.8) \left(\frac{\pi L_w}{4b} \right)^{1/3}}{\left[1 + \left(\frac{4b}{\pi} \Omega \right)^2 \right]} \\ \frac{\Omega^2}{\left[1 + \left(\frac{4b}{\pi} \Omega \right)^2 \right]} \phi_{w_g}(\Omega) \\ \frac{\Omega^2}{1 + \left(\frac{3b}{\pi} \Omega \right)^2} \phi_{v_g}(\Omega) \end{bmatrix} \quad (4.48)$$

where b = wing span, (ft)

Random velocities with above spectra are obtained by passing a gaussian random "white" noise through a linear system with a proper transfer function $G(s)$



It is known that

$$\phi_o(\omega) = |G(j\omega)|^2 \phi_i(\omega) \quad (4.49)$$

where the bars denote the magnitude of the complex variable.

The power spectral densities given above are ratios of polynomials in ω^2 where ω is the temporal frequency given by

$$\omega = V_a \Omega \text{ rad/sec} \quad (4.50)$$

can be spectrally factored out. This process yields the proper transfer functions as follows:

$$\begin{bmatrix} G_{ug}(s) \\ G_{vg}(s) \\ G_{wg}(s) \end{bmatrix} = \begin{bmatrix} \sigma_u \sqrt{\frac{2L_u}{\pi V_a}} \frac{1}{[1 + (\frac{L_u}{V_a})s]} \\ \sigma_v \sqrt{\frac{L_v}{\pi V_a}} \frac{[1 + (\frac{\sqrt{3}L_v}{V_a})s]}{[1 + (\frac{L_v}{V_a})s]^2} \\ \sigma_w \sqrt{\frac{L_w}{\pi V_a}} \frac{[1 + (\frac{\sqrt{3}L_w}{V_a})s]}{[1 + (\frac{L_w}{V_a})s]^2} \end{bmatrix} \quad (4.51)$$

$$\begin{bmatrix} G_{pg}(s) \\ G_{qg}(s) \\ G_{rg}(s) \end{bmatrix} = \begin{bmatrix} \left(\sigma_w \sqrt{\frac{1}{L_w V_a}} \right) \left(\sqrt{(0.8) \left(\frac{\pi L_w}{4b} \right)^{1/3}} \right) \frac{1}{[1 + (\frac{4b}{\pi V_a})s]} \\ \left(\frac{1}{V_a} \right) \frac{s}{[1 + (\frac{4b}{\pi V_a})s]} G_{wg}(s) \\ - \left(\frac{1}{V_a} \right) \frac{s}{[1 + (\frac{3b}{\pi V_a})s]} G_{vg}(s) \end{bmatrix} \quad (4.52)$$

The outputs of these six filters are combined as shown in the following to obtain equivalent translational and angular velocities to be used in the aerodynamics model

$$\begin{pmatrix} u_a \\ v_a \\ w_a \end{pmatrix} = \begin{pmatrix} u \\ v \\ w \end{pmatrix} - \begin{bmatrix} \bar{u} \\ \bar{v} \\ \bar{w} \end{bmatrix} + \begin{pmatrix} u_g \\ v_g \\ w_g \end{pmatrix} \quad (4.53)$$

$$\begin{pmatrix} p_a \\ q_a \\ r_a \end{pmatrix} = \begin{pmatrix} p \\ q \\ r \end{pmatrix} + \begin{pmatrix} p_g \\ q_g \\ r_g \end{pmatrix} \quad (4.54)$$

Figure 17 shows the structure of the equivalent linear and angular gust velocity generator model, Figure 18 shows its state representation, and Table II gives the filter coefficients.

The pole locations of roll, pitch and yaw gust filters for aircraft are inversely proportional to wing span, b . The corresponding term for a weapon would be its diameter. When weapon diameter is used in place of wing span, the magnitudes of poles of roll pitch, and yaw filters become excessively large. Numerical integration (i. e., non-real-time simulation) of these extremely fast dynamics requires very small integration step size. For small weapons, the space gradient effects of wind gust (i. e., roll, pitch and yaw filters) are small. For this reason, these filters are omitted in the simulation of weapons in ADAPS.

Steady-State Output Variances of the Dryden Gust Filter -- In the following, only side gust filter covariance analysis is presented. Others follow the same pattern.

The transfer function for the side gust is given as [see equation (4.51)]

$$G_{vg}(s) = \sigma_v \sqrt{\frac{L_v}{\pi V_a}} \frac{\left[1 + \left(\frac{\sqrt{3} L_v}{V_a} \right) s \right]}{\left[1 + \left(\frac{L_v}{V_a} \right) s \right]^2} \quad (4.51a)$$

This can be written as:

$$G_{vg}(s) = k \left[\frac{s+b}{(s+a)^2} \right] \quad (4.55)$$

or

$$= k \left[\frac{1}{s+a} + \frac{b-a}{(s+a)^2} \right] \quad (4.56)$$

$$\text{where } a = \frac{V_a}{L_v}, \quad b = \frac{a}{\sqrt{3}}, \quad k = \sigma_v \sqrt{\frac{3a}{\pi}} \quad (4.57)$$

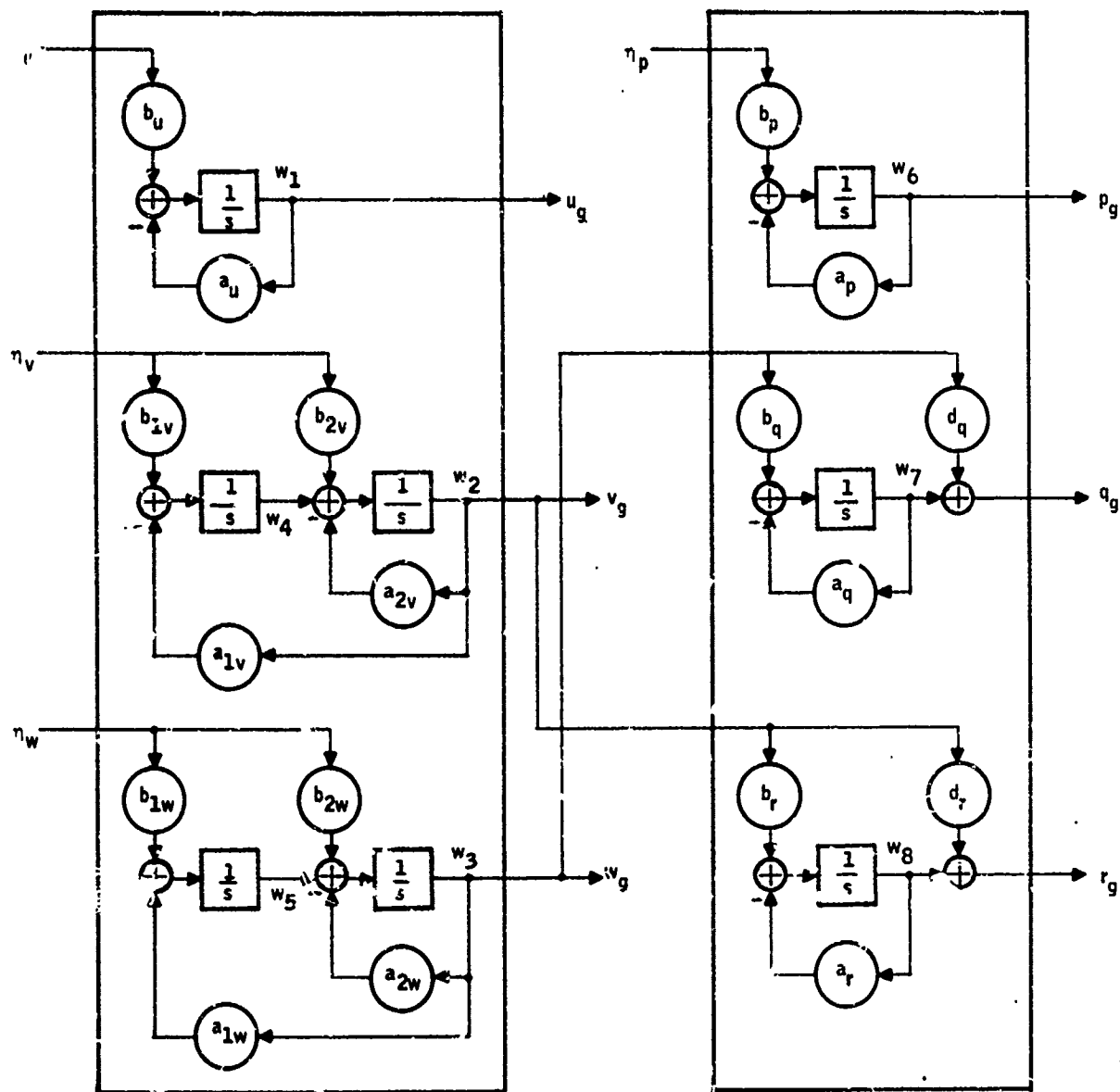


Figure 17. Structure of the Equivalent Linear and Angular Velocity Gust Generator (Dryden Model)

$$\begin{aligned}
 \dot{w} &= F_w w + G_w \eta \\
 y_w &= H_w w
 \end{aligned}$$

$$\begin{bmatrix} \dot{w}_1 \\ \dot{w}_2 \\ \dot{w}_3 \\ \dot{w}_4 \\ \dot{w}_5 \\ \hline \dot{w}_6 \\ \dot{w}_7 \\ \dot{w}_8 \end{bmatrix} = \begin{bmatrix} -a_u & 0 & 0 & 0 & 0 & 0 & 0 & 0 \\ 0 & -a_{2v} & 0 & 1.0 & 0 & 0 & 0 & 0 \\ 0 & 0 & -a_{2w} & 0 & 1.0 & 0 & 0 & 0 \\ 0 & -a_{1v} & 0 & 0 & 0 & 0 & 0 & 0 \\ 0 & 0 & -a_{1w} & 0 & 0 & 0 & 0 & 0 \\ \hline 0 & 0 & 0 & 0 & 0 & -a_p & 0 & 0 \\ 0 & 0 & b_q & 0 & 0 & -a_q & 0 & 0 \\ 0 & b_r & 0 & 0 & 0 & 0 & 0 & -a_t \end{bmatrix} \begin{bmatrix} w_1 \\ w_2 \\ w_3 \\ w_4 \\ w_5 \\ \hline w_6 \\ w_7 \\ w_8 \end{bmatrix} + \begin{bmatrix} b_u & 0 & 0 & 0 & 0 & 0 & 0 & 0 \\ 0 & b_{2v} & 0 & b_{2w} & 0 & 0 & 0 & 0 \\ 0 & 0 & b_{1v} & 0 & b_{1w} & 0 & 0 & 0 \\ \hline 0 & 0 & 0 & 0 & 0 & 0 & b_p & 0 \\ 0 & 0 & 0 & 0 & 0 & 0 & 0 & 0 \end{bmatrix} \begin{bmatrix} \eta_u \\ \eta_v \\ \eta_w \\ \hline \eta_p \end{bmatrix}$$

$$\begin{bmatrix} u_g \\ v_g \\ w_g \\ \hline p_g \\ q_g \\ r_g \end{bmatrix} = \begin{bmatrix} 1.0 & 0 & 0 & 0 & 0 & 0 & 0 & 0 \\ 0 & 1.0 & 0 & 0 & 0 & 0 & 0 & 0 \\ 0 & 0 & 1.0 & 0 & 0 & 0 & 0 & 0 \\ \hline 0 & 0 & 0 & d_r & 0 & 1.0 & 0 & 0 \\ 0 & 0 & d_q & 0 & 0 & 0 & 1.0 & 0 \\ 0 & d_r & 0 & 0 & 0 & 0 & 0 & 1.0 \end{bmatrix} \begin{bmatrix} w_1 \\ w_2 \\ w_3 \\ w_4 \\ w_5 \\ w_6 \\ w_7 \\ w_8 \end{bmatrix}$$

Figure 18. State Equation of the Gust Generator

Table II. Wind-Filter Coefficients

Linear Velocity Coefficients			Angular Velocity Coefficients		
u_g	v_g	w_g	p_g	q_g	r_g
$a_u = \frac{Va}{L_u}$	$a_v = \frac{Va}{L_v}$	$a_w = \frac{Va}{L_w}$	$a_p = \frac{\pi Va}{4b}$	$a_q = \frac{\pi Va}{4b}$	$a_r = \frac{\pi Va}{3b}$
$b_u = \sigma_u \sqrt{\frac{2}{\pi}} a_u$	$b_{2v} = \sigma_v \sqrt{\frac{3}{\pi}} a_v$	$b_{2w} = \sigma_w \sqrt{\frac{3}{\pi}} a_w$	$b_p = \sigma_w \sqrt{\frac{1}{L_w V}} (0.8) \left(\frac{\pi L_w}{\tau} \right)^{1/3} (a_p)$	$d_q = \frac{a_q}{Va}$	$d_r = \frac{a_r}{Va}$
	$b_{1v} = \frac{a_v b_{2v}}{\sqrt{3}}$	$b_{1w} = \frac{a_w b_{2w}}{\sqrt{3}}$		$b_q = a_q d_q$	$b_r = a_r d_r$
	$a_{1v} = a_v^2$	$a_{1w} = a_w^2$			
	$a_{2v} = 2a_v$	$a_{2w} = 2a_w$			

The Jordan-state diagram for (4.56) is given in Figure 19.

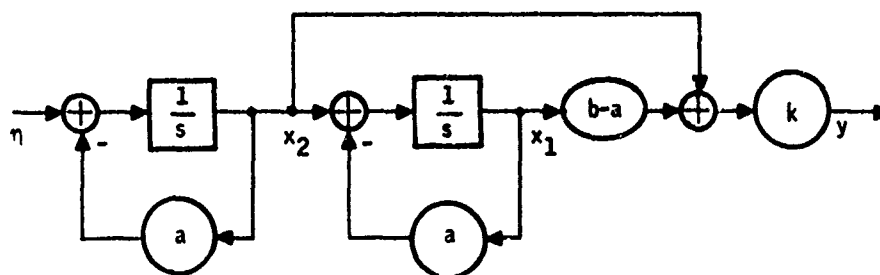


Figure 19. State Diagram for Side Gust Filter

The state equation is given by

$$\begin{aligned}\dot{\mathbf{x}} &= \mathbf{A}\mathbf{x} + \mathbf{b}\eta \\ y &= \mathbf{C}\mathbf{x}\end{aligned}\tag{4.58}$$

where

$$\mathbf{A} = \begin{bmatrix} -a & 1 \\ 0 & -a \end{bmatrix}, \quad \mathbf{b} = \begin{bmatrix} 0 \\ 1 \end{bmatrix}, \quad \mathbf{C} = k \begin{bmatrix} (b-a) \\ 1 \end{bmatrix}\tag{4.59}$$

With a unity input covariance, the steady-state output covariance is obtained from

$$\dot{\mathbf{X}} = \mathbf{A}\mathbf{X} + \mathbf{X}\mathbf{A}' + \mathbf{b}\mathbf{W}\mathbf{b}' = 0\tag{4.60}$$

$$\mathbf{Y} = \mathbf{C}'\mathbf{X}\mathbf{C}\tag{4.61}$$

where

$$\mathbf{X} = \begin{bmatrix} x_{11} & x_{12} \\ x_{12} & x_{22} \end{bmatrix} \quad \text{and} \quad \mathbf{b}\mathbf{W}\mathbf{b}' = \begin{bmatrix} 0 & 0 \\ 0 & 1 \end{bmatrix}\tag{4.62}$$

From (4.60) the following solution is obtained

$$x_{22} = \frac{1}{2a}, \quad x_{12} = \frac{1}{4a^2}, \quad x_{11} = \frac{1}{4a^3}\tag{4.63}$$

Substituting these into (4.61) yields

$$\mathbf{Y} = \frac{k^2}{4a} \left[1 + \left(\frac{b}{a} \right)^2 \right]\tag{4.64}$$

Finally using (4.57) in (4.64) results in

$$y = \frac{\sigma_v^2}{\pi} \quad (4.65)$$

This shows that in order to obtain variance σ_v^2 at the output, the input noise η must have a variance

$$\sigma_\eta^2 = \pi \quad (4.66)$$

instead of unity, or the gain element k in transfer function (4.51a) should be

$$k = \sigma_v \sqrt{\frac{L_v}{V}} \quad (4.67)$$

with a unity input covariance.

Subroutine WINDK computes the coefficients of the gust filter having the Dryden spectrum and the components of the mean wind along the body axes as a function of altitude.

SECTION V

DEVELOPMENT OF MEASUREMENT SYSTEM MODEL

Sensors on board an aircraft can be divided into two groups: instruments for the automatic control of vehicle motion and instruments for the avionics (i.e., fire control navigation, etc.).

In general, the readings (i.e., observations) of sensors on board an aircraft depend upon where and how the sensors are mounted with respect to the body axes of the aircraft (geometry). There may also be dynamics associated with sensors.

To provide an analysis tool by which the effects of various measurement points and methods can be investigated, both aspects are considered in the development of a measurement model in ADAPS.

In the following, a geometric model for the overall measurement system is developed first (i.e., observation equations). Then the dynamics of sensors are treated. Throughout this development it is assumed that the body on which instruments are mounted is rigid. Aeroelastic effects for the measurements and controls are beyond the scope of the present program.

DEVELOPMENT OF A GEOMETRIC MODEL FOR MEASUREMENTS

The basic vector quantities which may be measured are:

- Control surface deflection vector:

$$\mathbf{x}_0 = \text{col}(\delta_a, \delta_s, \delta_r, \delta_{sp}) \text{ (deg)}$$

- Linear acceleration and velocity vectors:

$$\dot{\mathbf{x}}_1 = \text{col}(\ddot{u}, \ddot{v}, \ddot{w}) \text{ (ft/sec}^2\text{)}$$

$$\mathbf{x}_1 = \text{col}(u, v, w) \text{ (ft/sec)}$$

- Angular acceleration and velocity vectors:

$$\dot{\mathbf{x}}_2 = \text{col}(\dot{p}, \dot{q}, \dot{r}) \text{ (rad/sec}^2\text{)}$$

$$\mathbf{x}_2 = \text{col}(p, q, r) \text{ (rad/sec)}$$

- Angular position vector
(i.e., body attitude with respect to earth-fixed axes)

$$\mathbf{x}_3 = \text{col}(\theta, \psi, \phi)$$

- Translational position vector

$$x_4 = \text{col}(x_e, y_e, z_e) \text{ (ft)}$$

As is shown in the subsequent subsections and illustrated in Figure 20, instruments sense, in general, the nonlinear combinations of these quantities. This is referred to as the geometry of the measurements or in state space terminology, the observation relations.

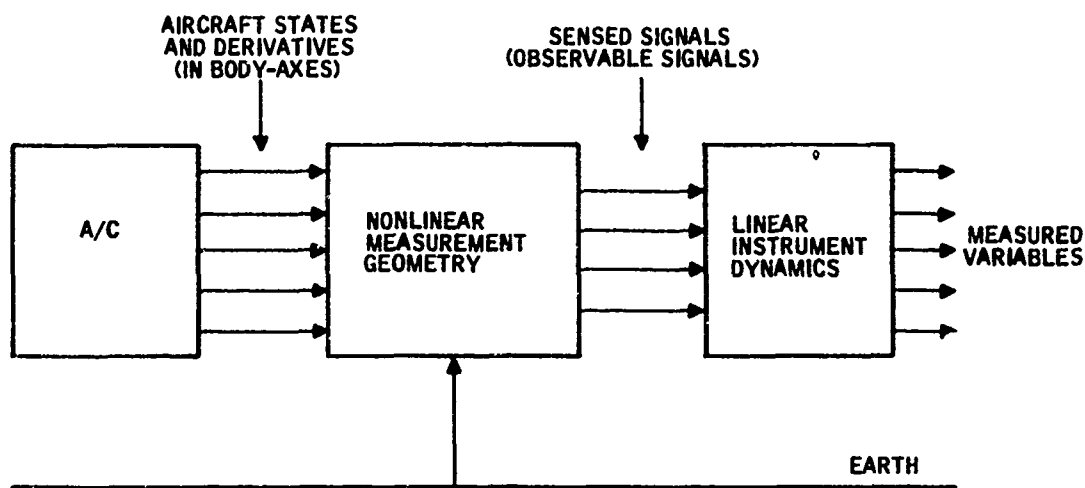


Figure 20. General Structure of Perfect-Measurement Model

In the following, first the geometry of the measurements for the automatic control of vehicles motion are given. Subsequently, a geometric model for air data measurements is presented for completeness. Then a simple geometric model for fire control measurements (i.e., radar measurements) is developed.

Geometry of Control Measurements

Attitude Measurements -- The geometric model of very simple forms of free gyros (i.e., vertical and directional gyros) are given in [15]. In many advanced vehicles, however, more complex attitude and direction-sensing instrumentation is used. Models for those which are used in fire control system are treated later.

The relation between the attitude state x_3 and the sensed (i. e., measurable) attitude y_{3S} is given by

$$y_{3S} = h_{x_3}(x_3, E_\Omega) = E_\Omega x_3 \quad (5.1)$$

where E_Ω is a fixed transformation matrix which takes into account the nonalignments effects of the gyro axes and is normally equal to an identity matrix.

Velocity and Acceleration Measurements --

Linear-Velocity Measurements -- The geometric model of linear-velocity measurements is given in Figure 21. In this model, it is assumed that the origin, 0_v , of the instrument axes system is located by a vector $\Delta \vec{r}_v$ from the origin, 0 , of the body axes. It is further assumed that, ψ_v , θ_v and ϕ_v are fixed Euler angles from body to instrument axes, and E_v is the corresponding transformation matrix as described in Section III.

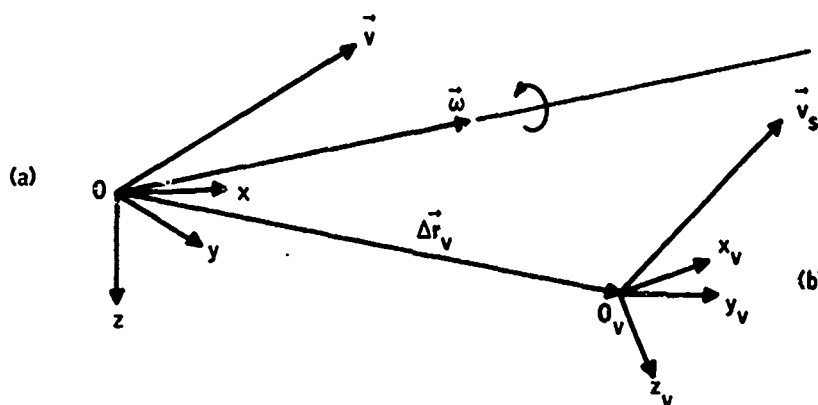


Figure 21. Axes Systems for Linear Velocity and Acceleration Measurements: (a) Body Axes, (b) Instrument Axis

The linear (i. e., translational) velocity of the point 0_v in body axes is given [16] by

$$\vec{v}_{SB} = \vec{v} + \vec{\omega} \times \Delta \vec{r}_v \quad (5.2)$$

where

\vec{v} = linear velocity of cg with respect to earth axes in body-axes system

$\vec{\omega}$ = angular velocity of body with respect to earth axes in body-axes system

$\Delta \vec{r}_v$ = position vector from 0 to 0_v in body-axes system

As described in Section III, the matrix equivalent of (5.2) is

$$v_{SB} = v + W \Delta r_v \quad (5.3)$$

where

$$v_{SB} = \begin{bmatrix} u_{SB} \\ v_{SB} \\ w_{SB} \end{bmatrix}, \quad W = \begin{bmatrix} 0 & -r & q \\ r & 0 & -p \\ -q & p & 0 \end{bmatrix}, \quad \Delta r_v = \begin{bmatrix} \Delta x_v \\ \Delta y_v \\ \Delta z_v \end{bmatrix} \quad (5.4)$$

Transforming (5.3) from body to instrument axes system yields the measurable velocity components along the instrument axes

$$v_s = E_v [v + W \Delta r_v] \quad (5.5)$$

Equation (5.5) constitutes the geometric model of the linear velocity observations. It is noted that the measurable velocity vector is a linear combination of the linear and angular velocities in body axes; E_v and Δr_v are the velocity observation parameters.

In state vector notation (5.5) becomes:

$$y_{1s} = h_{x_1}(x_1, x_2, \Delta r_v, E_v) \quad (5.6)$$

where

$$h_{x_1} = E_v \{x_1 + [W(x_2)] \Delta r_v\} \quad (5.7)$$

and $W(x_2)$ is defined by (5.4).

Linear-Acceleration Measurements -- The accelerometers are assumed to be located and oriented in much the same way as the velocity instruments. In the following the geometric relations which express the accelerometer observations in terms of the vehicle body axes acceleration are developed similar to previous section.

Differentiating (5.2) in a rotating frame of reference (i.e., body axes) yields the following equation:

$$\dot{\vec{v}}_s = \frac{\delta}{\delta t} [\vec{v} + \vec{\omega} \times \Delta \vec{r}_a] + \vec{\omega} \times [\vec{v} + \vec{\omega} \times \Delta \vec{r}_a] \quad (5.8)$$

Noting that Δr_a is constant, one obtains

$$\dot{\vec{v}}_s = \frac{\delta \vec{v}}{\delta t} + \frac{\delta \vec{\omega}}{\delta t} \times \Delta \vec{r}_a + \vec{\omega} \times \vec{v} + \vec{\omega} \times (\vec{\omega} \times \Delta \vec{r}_a) \quad (5.9)$$

where

- \vec{v}_s = acceleration of point 0_a where accelerometer is located expressed in body axes
 \vec{v} = acceleration of mass center, 0, expressed in body axes
 $\Delta \vec{r}_a$ = position vector from 0 to 0_a , expressed in body axes

The matrix equivalent of (5.9) is:

$$\dot{v}_s = \dot{v} + W v + (\dot{W} + W^2) \Delta r_a \quad (5.10)$$

Now let ψ_a , θ_a , and ϕ_a be the fixed Euler angles from body to accelerometer axes, and E_a be the corresponding transformation matrix, then the observable acceleration components along the accelerometer axes are given by

$$a_s = E_a [(a + \dot{W} \Delta r_a) + (Wv + W^2 \Delta r_a)] \quad (5.11)$$

Equation (5.11) constitutes the geometric model of the linear accelerometer observations. It is noted that the observable acceleration vector, a_s , is linearly dependent to body axes accelerations, but also contains nonlinear combinations of the velocities. E_a and Δr_a are the acceleration observation parameters.

In state vector notation (5.11) becomes

$$\dot{y}_{1s} = h_{x_1} (\dot{x}_1, \dot{x}_2, x_1, x_2, \Delta r_a, E_a) \quad (5.12)$$

where

$$h_{x_1} = E_a \left\{ \dot{x}_1 + [W(\dot{x}_2)] \Delta r_a + W(x_2)x_1 + [W(x_2)]^2 \Delta r_a \right\} \quad (5.13)$$

Angular-Velocity and Acceleration Measurements -- Here it is tacitly assumed that the axes of the instruments which measure the angular velocity and acceleration with respect to nonrotating earth are fixed with respect to the body axes. It should be noted that, in radar-based measurements which are treated later, the radar axes system on which rate sensors are mounted moves with respect to the body.

Let E_ω and $E_{\dot{\omega}}$ be fixed transformation matrices from body to angular rate and angular accelerometer axes respectively. Then the observed angular rates and accelerations are given by

$$\begin{aligned}
 \omega_s &= E_\omega \omega \\
 \dot{\omega}_s &= E_{\dot{\omega}} \dot{\omega}
 \end{aligned}$$

Here E_ω and $E_{\dot{\omega}}$ are the observation parameters. In state notations these equations become

$$\begin{aligned} y_{2s} &= h_w(x_2) \\ \dot{y}_{2s} &= h_{\dot{w}}(\dot{x}_2) \end{aligned} \quad (5.14)$$

where

$$\begin{aligned} h_w &= [E_w] x_2 \\ h_{\dot{w}} &= [E_{\dot{w}}] \dot{x}_2 \end{aligned} \quad (5.15)$$

Air Data Measurements

Three measurements are made on the air data: (1) static pressure (2) total pressure and (3) total temperature. These measurements are used by the air data computer to obtain, among other things, the altitude, altitude rate, mach number and airspeed.

In the following, the geometry of the air data measurements are developed via the physics of the variables which are observed.

Static Pressure Measurement -- The observed static pressure is a non-linear function of the altitude. The static pressure-altitude relation is derived from the barometric equation which may be expressed in the following form [38]:

$$d \log_e p_s = - \frac{g W_m}{RT} dh \quad (5.16)$$

and

$$T = T_o + t \quad (5.16a)$$

where

- h = altitude
- g = acceleration of gravity
- W_m = molecular weight of air
- R = gas constant
- T = absolute temperature (Kelvin)
- t = temperature (centigrade)
- T_o = constant

Approximately, one can write from (5.16)

$$p_s = p_b e^{\frac{k_1}{T} h} \quad (5.17)$$

or in state space notation

$$p_s = p_b e^{\frac{k_1}{T} c' x_4} \quad (5.18)$$

where

$$c = \text{col}(0 \ 0 \ 1)$$

and p_b , k_1 are the observation parameters.

Total Pressure Measurement -- The observed total pressure is connected to the static pressure and the speed of air with respect to body, through the following relationship:

$$p_T = p_s \left[1 + \frac{\gamma-1}{2} \frac{V_a^2}{a^2} \right]^{\frac{\gamma}{\gamma-1}} \quad (5.19)$$

where $\gamma = 1.4$

and V_a = airspeed with respect to body

a = speed of sound

At this point, it is convenient to introduce the Mach number parameter defined by

$$M = \frac{V_a}{a} \quad (5.20)$$

Temperature observations are functions of this parameter.

The speed of sound is related to the temperature as follows:

$$a = \sqrt{k_o} \sqrt{T_o + t} \quad (5.21)$$

$$\text{where } k_o = \gamma \frac{p_{s0}}{p_o T_o} \quad (5.22)$$

Now combining (5.21) with 5.19) and noting that

$$V_a = V - W \quad (5.23)$$

One can write in terms of states, the following observation equation:

$$p_T = p_S \left[1 + \left(\frac{.2}{k_o t + k_1} \right) (x_{1a})' (x_{1a}) \right] \quad (3.5) \quad (5.24)$$

where

$$\begin{aligned} x_{1a} &= (x_1 - x_{1w}) \\ k_1 &= k_o T_o \end{aligned} \quad (5.25)$$

Total Temperature Measurement -- The total temperature is related to the static temperature t , by [38]

$$t_s = (1 - .2M^2) (1 - .004M^2)t \quad (5.26)$$

and is observed by a resistive sensor obeying the Callendar-Van Dusen equation

$$R_T = g(t_s) \quad (5.27)$$

where the function g is a second-degree polynomial in t_s . Thus in (5.24) the parameter t (i. e., temperature) is indirectly observed and this observation is described by (5.26) and (5.27).

In summary, the air data observation vector is connected to the states as

$$\begin{aligned} p_{ss} &= h_{ps}(x_4, p_b, t) \\ p_{Ts} &= h_{pT}(x_1, x_{1w}, p_{ss}, t) \\ R_{Ts} &= h_{TT}(x_1, x_{1w}, t) \end{aligned} \quad (5.28)$$

where

$$\begin{pmatrix} h_{ps} \\ h_{pT} \\ h_{T'T} \end{pmatrix} = \begin{bmatrix} p_b \frac{k_1}{e(T_o+t)} c' x_4 \\ (h_{ps}) \left[1 + 2 \frac{(x_1 - x_{1w})' (x_1 - x_{1w})}{k_o (T_o+t)} \right]^{3.5} \\ g(t_s) \end{bmatrix} \quad (5.29)$$

Fire Control Measurements

Description of Fire Control Measurement Model -- Fire control measurements involve body-mounted sensors also. From the readings of these sensors, the target's relative position and velocity with respect to aircraft are derived [39].

The radar measurement model considered here, is illustrated in Figure 22. In this model the relative position of target is defined by the vector

$$y_{RP} = \begin{bmatrix} R_R \\ \psi_R \\ \theta_R \end{bmatrix} \quad (5.30)$$

where

R_R = magnitude of the position vector of target relative to point O_R on aircraft

ψ_R = azimuth angle of position vector with respect to body axes

θ_R = elevation angle of position vector with respect to body axes

It is assumed that the relative position vector y_{RP} as defined above is observed using a radar device which is located by a vector Δr_R from the origin, O , of the body axes. The radar axes are assumed to be oriented by synchros so that the antenna (i. e., i_R vector) always points to the target. It is further assumed that the angular velocities q_R and r_R of radar axes with respect to earth are observed by antenna-mounted rate gyros, and the rate of change of R_R is observed by doppler shift. This describes the fire control measurement model used in ADAPS. In the following, the geometry of the radar-based measurements are developed parallel to the previous subsections.

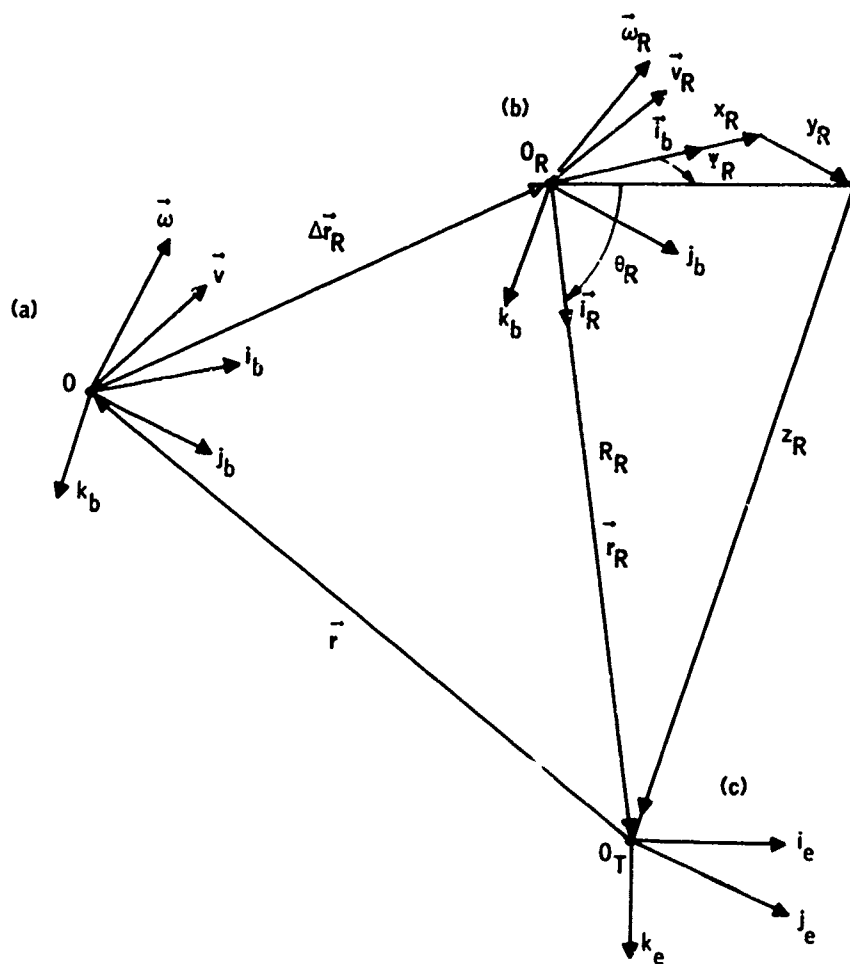


Figure 22. Radar Measurement Geometry: (a) Body Axes, (b) Radar Axes, (c) Earth Axes

Geometry of Fire Control Measurements --

Position Measurements -- From Figure 22, the position vector \vec{r} of c. g. is given by

$$\vec{r} = -(\Delta r_R + \vec{r}_R) \quad (5.31)$$

where:

$$\begin{aligned} \vec{r} &= \text{position vector from } 0_T \text{ to } 0 \\ \Delta r_R &= \text{position vector from } 0 \text{ to } 0_R \\ \vec{r}_R &= \text{position vector from } 0_R \text{ to } 0_T \end{aligned}$$

From (5.31) one obtains \vec{r}_R in body axes and in matrix notation as

$$r_R = \begin{pmatrix} x_R \\ y_R \\ z_R \end{pmatrix} = - [E(\theta, \psi, \phi)r + \Delta r_R] \quad (5.32)$$

In state space notation (5.32) becomes

$$r_R = - [E(x_3)]x_4 + \Delta r_R \quad (5.33)$$

On the other hand y_{RP} as defined in (5.30) can be expressed in terms of cartesian components of (5.32) as

$$y_{RP} = h_{RP}(x_3, x_4, \Delta r_R) \quad (5.34)$$

where

$$h_{RP} = \begin{bmatrix} \sqrt{x_R^2 + y_R^2 + z_R^2} \\ \tan^{-1} \frac{y_R}{x_R} \\ \tan^{-1} \frac{z_R}{\sqrt{x_R^2 + y_R^2}} \end{bmatrix} \quad (5.35)$$

Thus (5.33), (5.34) and (5.35) constitute the position observation equations, with Δr_R position observation parameter.

Velocity Measurements -- Differentiating \vec{r}_R in rotating radar frame one obtains

$$\frac{d\vec{r}_R}{dt} = \frac{\delta \vec{r}_R}{\delta t} + \vec{\omega}_R \times \vec{r}_R \quad (5.36)$$

Since

$$\frac{d\vec{r}_R}{dt} = -\vec{v}_R \quad (5.37)$$

where \vec{v}_R is the linear velocity of O_R with respect to earth-fixed frame origin O_T . One obtains from (5.36) and (5.37):

$$-\vec{v}_R = \frac{\delta \vec{r}_R}{\delta t} + \vec{\omega}_R \times \vec{r}_R \quad (5.38)$$

In matrix notation

$$-v_R = \frac{\delta r_R}{\delta t} + W_R r_R \quad (5.39)$$

where

$$r_R = \begin{pmatrix} R \\ 0 \\ 0 \end{pmatrix}, \quad \frac{\delta r_R}{\delta t} = \begin{pmatrix} \dot{R} \\ 0 \\ 0 \end{pmatrix}, \quad W_R = \begin{bmatrix} 0 & -r_R & q_R \\ r_R & 0 & -p_R \\ -q_R & p_R & 0 \end{bmatrix} \quad (5.40)$$

Using (5.40) in (5.39) yields

$$v_R = \begin{bmatrix} -\dot{R} \\ -R r_r \\ R q_r \end{bmatrix} \quad (5.41)$$

It is noted that R , \dot{R} , and angular rates q_R and r_R of radar axes with respect to earth axes are the observed quantities.

Now, the linear velocity of O_R can be expressed in terms of the velocity of cg in body coordinates:

$$\vec{v}_{RB} = \vec{v} + \vec{\omega} \times \Delta \vec{r}_R \quad (5.42)$$

Let $E_R = E_R(\theta_R, \psi_R)$ be the transformation matrix from body axes to radar axes. (E_R is obtained from equation (3.14) of Section III, by letting $\theta = \theta_R$, $\psi = \psi_R$ and $\phi = 0$).

Then in matrix notation the linear velocity of O_R in radar axes becomes

$$v_R = [E_R(\theta_R, \psi_R)] [v + \Delta r_R] \quad (5.43)$$

where v_R is given by (5.41).

Defining the velocity observations by

$$y_{RV} \triangleq \begin{bmatrix} \dot{R} \\ r_R \\ q_r \end{bmatrix} \quad (5.44)$$

one can write using (5.41)

$$y_{RV} = D(R) v_r \quad (5.45)$$

where

$$D(R) = \begin{bmatrix} -1 & 0 & 0 \\ 0 & -\frac{1}{R} & 0 \\ 0 & 0 & \frac{1}{R} \end{bmatrix} \quad (5.46)$$

Finally substituting (5.43) into (5.45) yields the observation equations in the form

$$y_{RV} = h_{RV}(x_1, x_2, y_{RP}, \Delta r_R) \quad (5.47)$$

where

$$h_{RV} = D(R) [E_R(\theta_R, \psi_R)] [x_1 + W(x_2) \Delta r_R] \quad (5.48)$$

This finishes the treatment of the observation equations of the measurement system considered in ADAPS.

In the subsection that follows, the development of a model for the dynamics of sensors which read the above observations is briefly presented.

DEVELOPMENT OF A DYNAMICAL MODEL FOR SENSORS

Almost invariably, the dynamics associated with each measured-scalar signal is of second order. Therefore, the overall system order increases very rapidly when the number of measured signals increases. To overcome this difficulty, the sensor dynamics with poles lying outside of the significance circle of radius R_s on the complex plane as shown in Figure 23 are ignored in the dynamical representation of the overall system. However, their positions are checked after the optimal gain loop is closed, because of the sensitivity of high-frequency open-loop poles to feedback.

Figure 24 is the block diagram of the i^{th} sensor dynamics.

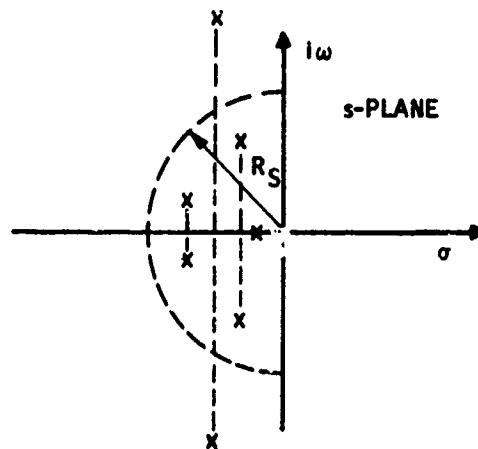


Figure 23. Dynamical Significance Radius

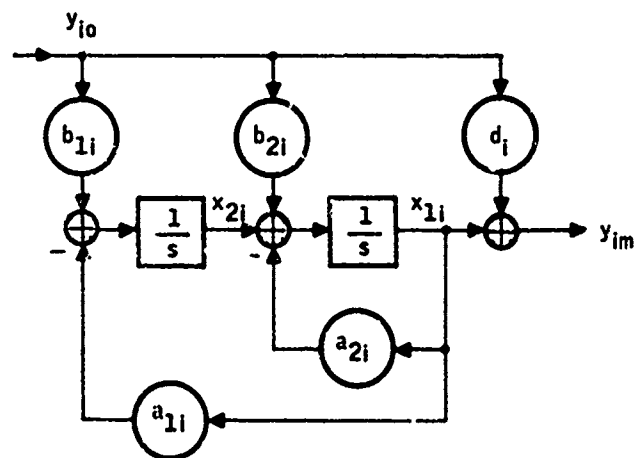


Figure 24. Measurement Dynamics of i^{th} Scalar Signal

In this diagram, y_{io} and y_{im} correspond to the i^{th} scalar observable and measured signals respectively; x_{1i} and x_{2i} are the state components of the i^{th} sensor.

The dynamics of each sensor are identified by five coefficients, a_{1i} , a_{2i} , b_{1i} , b_{2i} , and d_i , where i is the sensor index. These coefficients correspond to the output-frobenius implementation of the sensor transfer function. For those cases in which the transfer coefficients (i.e., d_i) are zero, this representation provides output as the first component of sensor state. This finishes the development of a dynamical model for sensors.

Figure 25 shows in detail the kinematics and dynamics of measurements.

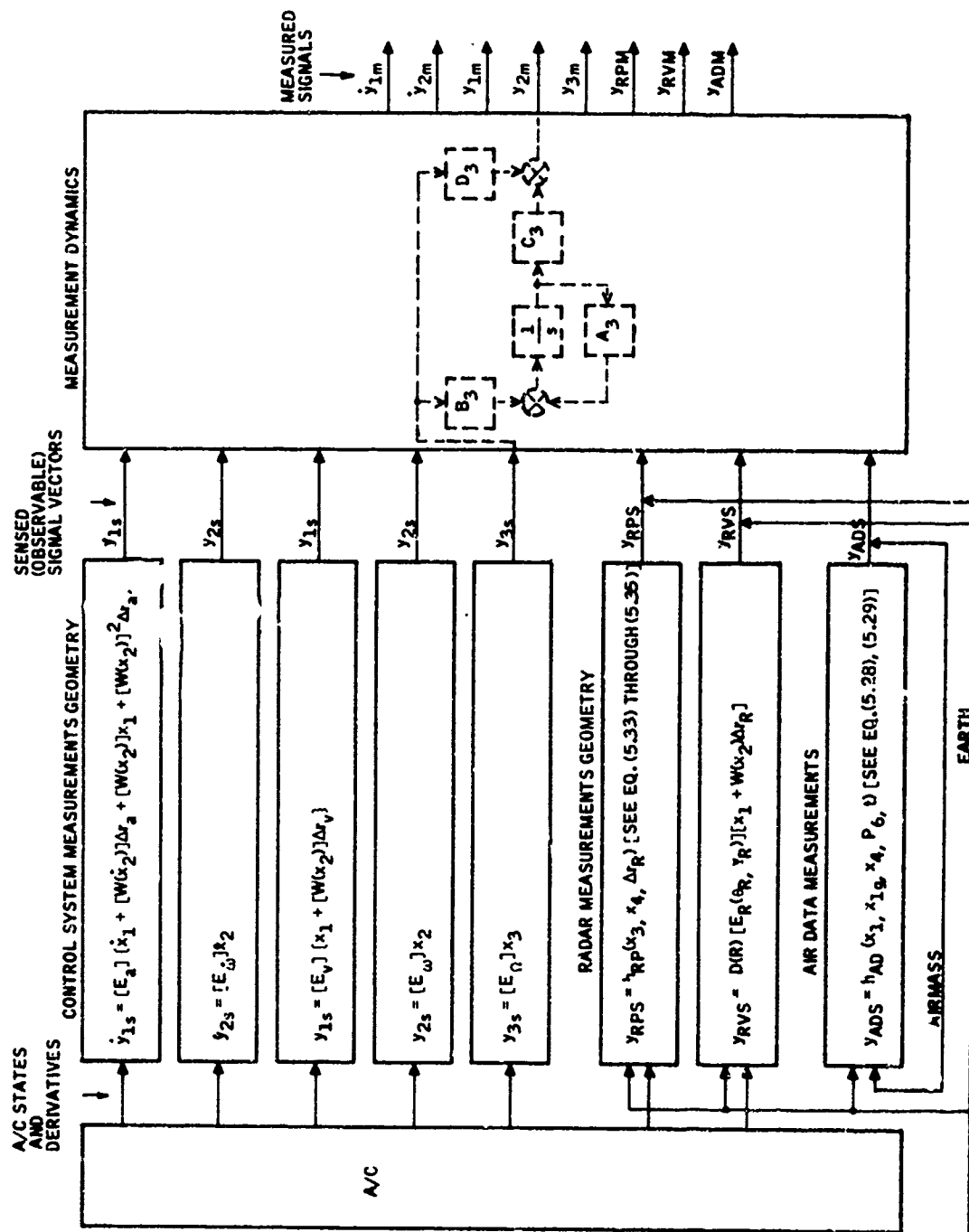


Figure 25. General Measurement Model

SECTION VI

LINEARIZATION OF THE WEAPON DELIVERY PROCESS

The weapon delivery process is a nonlinear stochastic phenomenon. To analyze the nonlinear equations, practically, they are linearized about the nominal path. The nominal path considered here corresponds to a dive-toss maneuver and consists of essentially three phases: (a) dive, (b) pull-up, and (c) free-fall, as shown in Figure 26.

The development of a model for the release transient phase is outside the scope of this work. This part of the nominal trajectory is taken into account in a simplified manner, by introducing an independent, additive, stochastic error on the initial condition for the free-fall trajectory.

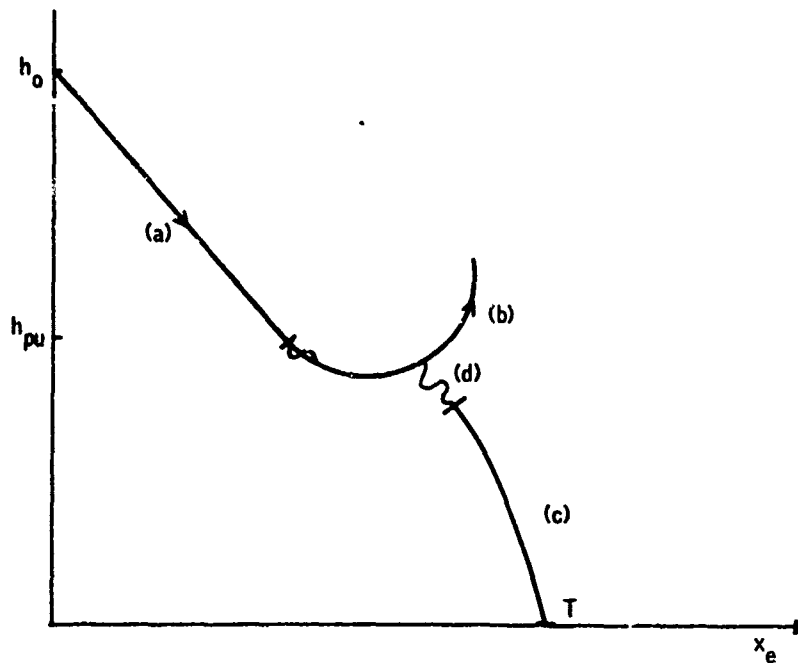


Figure 26. Nominal Trajectory for Dive-Toss Maneuver:
(a) Dive Phase, (b) Pull-up Phase, (c) Free-Fall Phase, (d) Release Transient Phase

LINEARIZATION PROCESS

It is assumed that the dive and pull-up maneuvers are carried out with a fixed thrust level, and by controlling the elevator deflection. The missing states and parameters along the paths (a) and (b) are obtained either by solving a set of trim equations developed for the case at hand or by a soft flight-path controller. The trajectory (c) is developed by integrating the six degree-of-freedom free-fall equations of an iron bomb

The linearization process along the paths (a) and (b) yields the state transition and the input matrix pair (F,G) of the aircraft, which are used to design an optimal weapon delivery controller. The linearization along the path (c) yields the sensitivity matrices which are used in translating the dispersion errors at bomb release to the impact of the bomb on the target as well as errors which occur during the free-fall.

The numerical development of the ideal nominal trajectory is illustrated in Figure 27 for the algebraic trimming. The process starts at $t = t_0$ with altitude h_0 and range x_0 . First a trimming is performed as outlined in Section VII; then a linearization is performed. This sequence continues with every ΔT seconds along the dive path until the pull-up altitude, h_{pu} , is reached. Similar steps are carried out along the pull-up trajectory, until the release time, t_r , is reached. Subsequently, integration of the six degree-of-freedom equations of motion of the bomb is carried out N steps with $\Delta t = \Delta T/N$ time interval. Then a linearization is performed at $t = t_r + \Delta T$. The process is continued until the impact plane is reached.

The equations which describe the general motion of a rigid body are given in Section III. Many problems of rigid-body motion involve only small disturbances (i. e., perturbations) from steady or quasi-steady flight conditions. In the following, the assumption of small disturbances from reference flight conditions is used to reduce the equations from nonlinear to linear form.

DEVELOPMENT OF THE PERTURBATION EQUATIONS

In the state vector notation, the general equations of motion of a rigid body, as developed in Section III, is described by a nonlinear vector differential equation of the form

$$\dot{x} = f[x(t), u] \quad (6.1)$$

where f is real, continuous and has continuous first order partial derivatives with respect to x_i , $i = 1, 2, \dots, n$; and u_j , $j = 1, 2, \dots, r$; in a region of (x, u) space which contains the solution curve $(x(t), u)$ with $t_0 \leq t < t_f$.

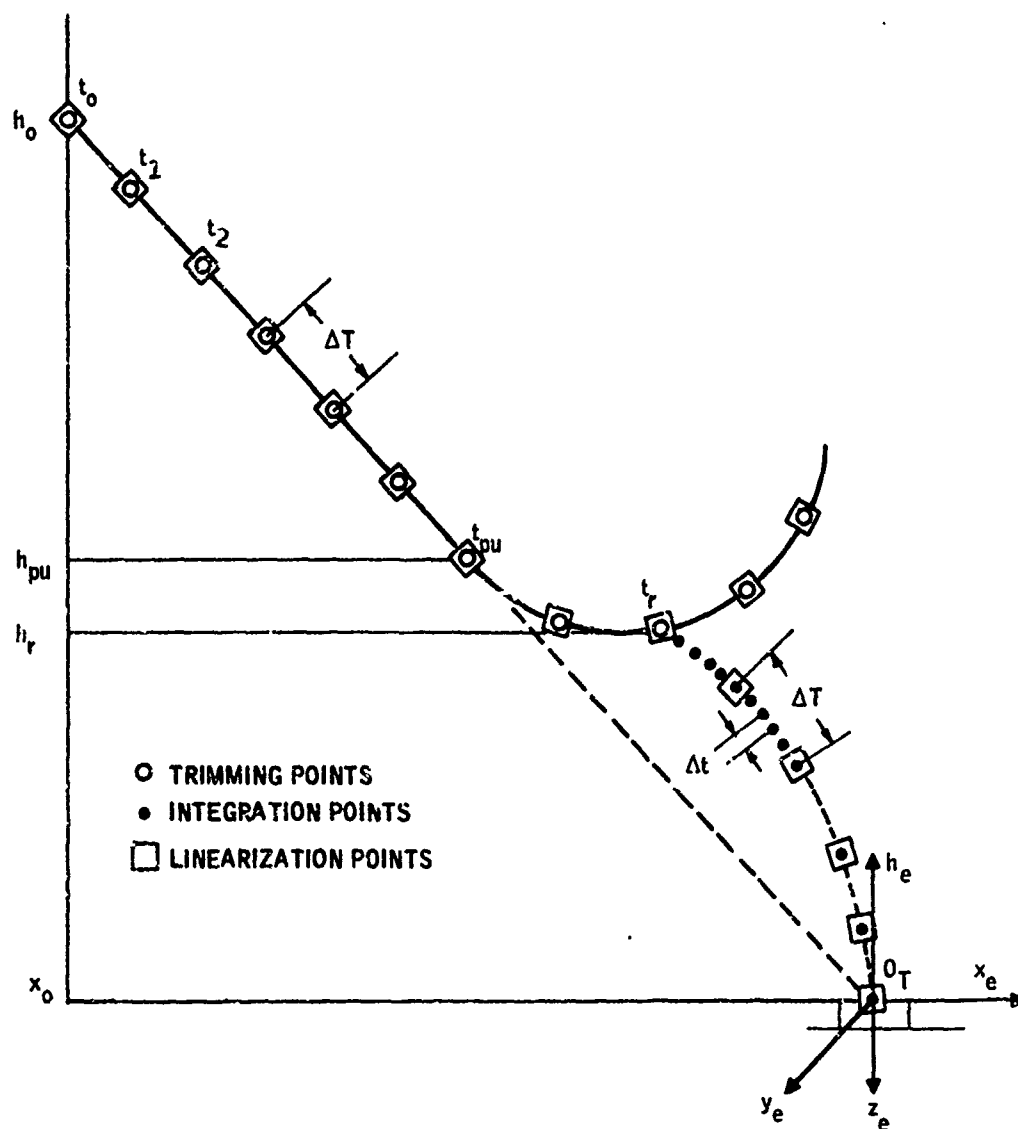


Figure 27. Development of Nominal Trajectories and Linearized Equations of Motion for an Aircraft Weapon Pair for a Dive-Toss Maneuver in xz Plane

Let (\bar{x}, \bar{u}) and (\tilde{x}, \tilde{u}) be two neighboring pair of solution curves satisfying (6.1). Define

$$\xi = \tilde{x} - \bar{x}$$

and

$$\eta = \tilde{u} - \bar{u}$$

(6.2)

Also let the matrices with columns

$$\left(\frac{\partial f}{\partial x_i} \right) \bigg|_{(\bar{x}(t), \bar{u})}, \quad i = 1, \dots, n,$$

and

$$\left(\frac{\partial f}{\partial u_j} \right) \bigg|_{(\bar{x}(t), \bar{u})}, \quad j = 1, \dots, r$$

be denoted by $F_x(\bar{x}(t), \bar{u})$, $F_u(\bar{x}(t), \bar{u})$, respectively. Then from (6.2) it follows that [40]

$$\frac{d\xi}{dt} = f(\xi + \bar{x}(t), \eta + \bar{u}) - f(\bar{x}(t), \bar{u}) \quad (6.3)$$

or

$$\frac{d\xi}{dt} = F_x(\bar{x}, \bar{u})\xi + F_u(\bar{x}, \bar{u})\eta + o(|\xi|) + o(|\eta|) \quad (6.4)$$

where $o(\epsilon)$ is a vector such that

$$\lim_{\epsilon \rightarrow 0} \frac{o(\epsilon)}{\epsilon} = 0 \quad (6.5)$$

When the last two terms in (6.4) are omitted, there occurs the linear system

$$\frac{dy}{dt} = F_x(\bar{x}(t), \bar{u})y + F_u(\bar{x}(t), \bar{u})v \quad (6.6)$$

with

$$y(t_0) = \tilde{x}(t_0) - \bar{x}(t_0) \quad (6.7)$$

which is called the first variation of (6.1) with respect to the solution $(\bar{x}(t), \bar{u})$. It is also called the variational equation of (6.1). The first variation determines the dependence of solutions on the initial conditions and parameters. It also determines in some cases the nature of the stability of the solutions (\bar{x}, \bar{u}) of (6.1).

In engineering practice, the procedure described above is called the linearization process, and the variational equation (6.6), is called the linearized equation of motion. Also the solution (\bar{x}, \bar{u}) is referred to as the nominal solution or the reference trajectory. It follows from (6.6) and the definitions of F_x and F_u that, in order to carry out the linearization:

- (a) the solution (\bar{x}, \bar{u}) must be specified on an interval $t_0 \leq t \leq t_f$, and
- (b) the first partials of $f(t, x, u)$ with respect to x_i and u_j must be developed.

In the following, first the development of the nominal solution (\bar{x}, \bar{u}) is given then the development of first partials is presented. At this point a few words on the notation for small disturbances (i. e., perturbations) are in order.

Usually, perturbations of velocity and orientation variables are designated by the lower case symbols for these quantities, i. e.,

$$\begin{pmatrix} u \\ v \\ w \end{pmatrix}, \begin{pmatrix} p \\ q \\ r \end{pmatrix}, \begin{pmatrix} \phi \\ \theta \\ \psi \end{pmatrix}, \begin{pmatrix} x_e \\ y_e \\ z_e \end{pmatrix}$$

Upper case symbols are used with a subscript zero to denote the reference values of these variables. Thus

$$\begin{pmatrix} U_0 \\ V_0 \\ W_0 \end{pmatrix}, \begin{pmatrix} P_0 \\ Q_0 \\ R_0 \end{pmatrix}, \begin{pmatrix} \phi_0 \\ \theta_0 \\ \psi_0 \end{pmatrix}, \begin{pmatrix} X_{e0} \\ Y_{e0} \\ Z_{e0} \end{pmatrix}$$

are reference values for linear and angular velocity components, orientation angles, and positions. Incremental changes in aerodynamic force and moment components are denoted by the pertinent symbol with a prefix Δ , e. g., ΔX , ΔZ , ΔM , etc.

DEVELOPMENT OF THE NOMINAL SOLUTION

The way the nominal solution (\bar{x}, \bar{u}) is developed depends upon whether or not the parameter vector \bar{u} is controlled or uncontrolled. The term "controlled" here implies the description of \bar{u} over a time interval such that the solution (\bar{x}, \bar{u}) behaves as specified. Uncontrolled \bar{u} on the other hand implies generally, disturbance parameters effecting the evolution of the solution.

The nominal solutions (i. e., reference trajectories) are developed by means of a set of specified reference-flight conditions. Reference-flight conditions are divided into two groups: free reference-flight conditions and controlled reference-flight conditions.

Free reference-flight conditions constitute the specification of an initial value of the state, $x(t_0) = x_0$ and the specification of the free parameter u over an interval $t_0 \leq t \leq t_f$. The nominal solution in this case is developed by integrating (6.1) over the specified time interval.

A nominal motion of an iron bomb, released from an aircraft falling freely under the influence of the gravity and winds is an example of this case.

The set of controlled reference-flight conditions consists of steady flight conditions, quasisteady flight conditions, straight flight conditions, and symmetric flight conditions [15]:

- Steady Flight Conditions imply a motion with zero linear and angular accelerations. That is

$$\frac{d}{dt} \begin{pmatrix} u \\ v \\ w \end{pmatrix} = 0, \text{ and } \frac{d}{dt} \begin{pmatrix} p \\ q \\ r \end{pmatrix} = 0 \quad (6.8)$$

Steady sideslip, level turns, and helical turns are examples to this kind of motion.

- Quasisteady Flight Conditions imply a motion with some nonzero linear and/or angular accelerations. A steady pitching motion (i. e., steep dive) which is described by the quasisteady flight conditions

$$\frac{d}{dt} \begin{pmatrix} u \\ v \\ w \end{pmatrix} = \begin{pmatrix} \dot{u} \\ 0 \\ \dot{w} \end{pmatrix}, \quad \frac{d}{dt} \begin{pmatrix} p \\ q \\ r \end{pmatrix} = 0 \quad (6.9)$$

is an example to this case.

- Straight Flight Conditions imply a motion with zero angular velocity components. That is

$$\begin{pmatrix} p \\ q \\ r \end{pmatrix} = 0 \quad (6.10)$$

Steady sideslips and dives or climbs without longitudinal acceleration are examples of this kind of motion.

- Symmetric Flight Conditions imply a motion in which the body plane of symmetry (i. e., xz plane), remains fixed in space throughout the flight. That is the asymmetric variables are all zero:

$$\begin{pmatrix} p \\ q \\ r \end{pmatrix} = \begin{pmatrix} 0 \\ q \\ 0 \end{pmatrix}, \quad \begin{pmatrix} u \\ v \\ w \end{pmatrix} = \begin{pmatrix} u \\ 0 \\ w \end{pmatrix}, \quad \begin{pmatrix} \theta \\ \psi \\ \phi \end{pmatrix} = \begin{pmatrix} \theta \\ 0 \\ 0 \end{pmatrix} \quad (6.11)$$

Wings level dives, climbs, and pull-ups with no sideslips are examples of this kind of motion.

The set of mathematical consequences associated with all specified reference flight conditions is used to construct the nominal trajectory.

At this point it should be noted that some of the reference flight conditions are on the derivatives of the state variables rather than on the state variables themselves.

The process of finding the values of involved state variables and inputs so that the conditions as specified by the equations given above are satisfied is called "trimming". (The process of trimming for a particular set of flight conditions, i. e., dive and pull-up maneuver, is described in Section VII.)

DEVELOPMENT OF THE FIRST PARTIALS

Consider a general rigid-body motion characterized by

$$\dot{x} = f(x, u, w) \quad (6.12)$$

where

- x = state vector of the motion
- u = control vector of the motion
- w = disturbance inputs of the motion

Equation (6.12) can be decomposed into the following form by using the Equations (3.62), (3.63), (3.24) and (3.72) of Section III:

$$\dot{x}_1 = -W(x_2)x_1 + E(x_3)g_e + \frac{1}{m} f_a(x_1, x_2, x_3, \delta, w) + \frac{1}{m} B_T y_T \quad (6.13)$$

$$\dot{x}_2 = -J^{-1} W(x_2) J x_2 + J^{-1} m_a(x_1, x_2, x_3, \delta, w) + J^{-1} B_T y_T \quad (6.14)$$

$$\dot{x}_3 = G(x_3) x_2 \quad (6.15)$$

$$\dot{x}_4 = E'(x_3) x_1 \quad (6.16)$$

where the subvectors are defined as follows:

$$x_1 = \begin{pmatrix} u \\ v \\ w \end{pmatrix} \quad \text{linear velocity vector}$$

$$x_2 = \begin{pmatrix} p \\ q \\ r \end{pmatrix} \quad \text{angular velocity vector}$$

$$x_3 = \begin{pmatrix} \theta \\ \phi \\ \psi \end{pmatrix} \quad \text{angular position vector}$$

$$x_4 = \begin{pmatrix} x_e \\ y_e \\ z_e \end{pmatrix} \quad \text{translational position vector (flight path state)}$$

$$\delta = \begin{pmatrix} \delta_a \\ \delta_s \\ \delta_r \end{pmatrix} \quad \text{control surface deflection vector}$$

$$y_T \quad \text{effective thrust input}$$

$$w = \begin{pmatrix} u_w \\ v_w \\ w_w \end{pmatrix} \quad \text{wind velocity vector}$$

and finally f_a and m_a are the aerodynamic force and moment vectors, respectively, expressed in the body coordinates. These two vector functions, in general, do not have analytic form. Their values as functions of their arguments are supplied in the form of tables. In this work, the dependencies of f_a and m_a to the derivative of the state vectors as defined above are ignored.

If a quaternion is used to describe the angular position coordinates, then equations (6.13) through (6.16) basically remain the same except the angular position vector becomes

$$\tilde{x}_3 = \begin{pmatrix} \lambda_0 \\ \lambda_1 \\ \lambda_2 \\ \lambda_3 \end{pmatrix}$$

and the differential equation of angular position can be written as [see Section III, Equations (3.54) and (3.68)]

$$\dot{\tilde{x}}_3 = \tilde{G}(x_2) \tilde{x}_3 = \hat{G}(x_3) x_2 \quad (6.15a)$$

where $\tilde{G}(x_2)$ and $\hat{G}(x_3)$ are linear functions of x_2 and \tilde{x}_3 respectively. The state diagram of the nonlinear equations of motion is illustrated in Figure 28.

Equations (6.13) and (6.14) describe the evolution of the linear and angular velocity vectors, respectively. Equations (6.15) and (6.16) describe the evolution of the angular and translational position vectors, respectively. Two approaches are available for the development of partials of the right-hand sides of (6.13) through (6.16): (a) mixed (i.e., analytical and numerical) partial differentiation approach or (b) pure numerical partial differentiation approach. Depending upon what approach is used for obtaining the partials, linearization will be referred to as (a) mixed linearization, and (b) pure numerical linearization. Both approaches are presented in the following, but only the pure numerical linearization approach is utilized for the linearization in ADAPS.

Mixed Linearization Approach

It is intuitively obvious that mixed partial differentiation approach for the linearization is more accurate than that of pure numerical partial differentiation approach. However, as will be seen in the following development, it requires more programming effort and computer memory for its implementation. Observation of the right-hand sides of equations (6.13) through (6.16) reveals that the majority of the analytical terms are in the form of

$$f(x_i, x_j) = F(x_i) x_j \quad (6.17)$$

In the following the incremental change in $f(x_i, x_j)$ is developed for various values of i and j :

- Case 1: [see Equation (6.13)] Clearly, an incremental change in f about the nominal states (x_1, x_2) in terms of perturbations δx_1 and δx_2 is given by

$$\delta f(x_1, x_2) = \delta [W(x_2)x_1] = [W(x_2)]_0 \delta x_1 + [\delta W(x_2)]_1 x_1 \quad (6.18)$$

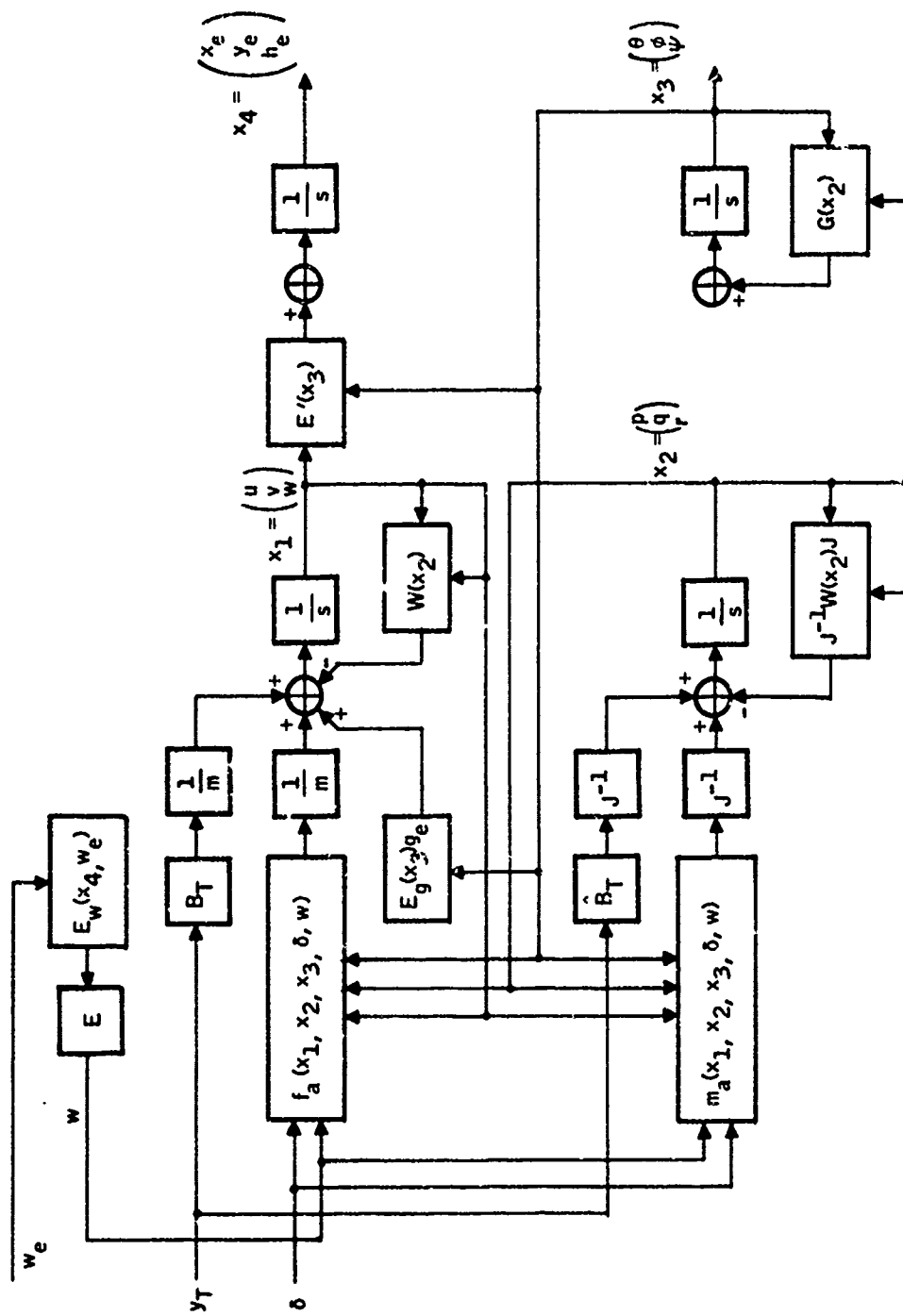


Figure 28. State Diagram of the Nonlinear Equations of Motion of a Rigid Body

On the other hand

$$\delta[W(x_2)] = \left. \frac{\partial W}{\partial p} \right|_0 \delta p + \left. \frac{\partial W}{\partial q} \right|_0 \delta q + \left. \frac{\partial W}{\partial r} \right|_0 \delta r \quad (6.19)$$

So that

$$\begin{aligned} \delta f(x_1, x_2) &= \delta[W(x_2)x_1] = [W(x_2)]_0 \delta x_1 + \\ &\quad \left(\left. \frac{\partial W}{\partial p} \right|_0 x_1 + \left. \frac{\partial W}{\partial q} \right|_0 x_1 + \left. \frac{\partial W}{\partial r} \right|_0 x_1 \right) \delta x_2 \end{aligned} \quad (6.20)$$

Since $W(x_2)$ is a linear function of x_2 , indicated partials are constant matrices. When the components of $W(x_2)$ are used in (6.20) in accordance with equation (3.21) of Section III, one obtains

$$\delta[W(x_2)x_1] = W(x_2)_0 \delta x_1 - W(x_1)_0 \delta x_2 \quad (6.21)$$

where

$$W(x_1) = \begin{bmatrix} 0 & -w & v \\ w & 0 & -u \\ -v & u & 0 \end{bmatrix}, \quad W(x_2) = \begin{bmatrix} 0 & -r & q \\ r & 0 & -p \\ -q & p & 0 \end{bmatrix} \quad (6.21a)$$

The same result can also be obtained from the vector notation representation of f by noting that

$$\vec{f} = \vec{w} \times \vec{v} = -\vec{v} \times \vec{w} \quad (6.22)$$

so that

$$\delta \vec{f} = \left. \vec{w} \right|_0 \times \delta \vec{v} - \left. \vec{v} \right|_0 \times \delta \vec{w} \quad (6.23)$$

Equation (6.21) is matrix representation of equation (6.23).

• Case 2:

$$f = [J^{-1}W(x_2)J]x_2 \quad (6.24)$$

Following the similar steps

$$\begin{aligned} \delta f(x_2, x_2) &= \delta [J^{-1} W(x_2) J x_2] = [J^{-1} W(x_2) J]_0 \delta x_2 \\ &+ \left(J^{-1} \frac{\partial W}{\partial p} J x_2 \mid J^{-1} \frac{\partial W}{\partial q} J x_2 \mid J^{-1} \frac{\partial W}{\partial r} J x_2 \right)_0 \delta x_2 \end{aligned} \quad (6.25)$$

• Case 3:

$$f(x_2, x_3) = [G(x_3)] x_2 \quad (6.26)$$

so that

$$\delta f(x_2, x_3) = [G(x_3)]_0 \delta x_2 + [\delta G(x_3)] x_2 \mid_0 \quad (6.27)$$

But

$$\delta(G(x_3)) = \frac{\partial G}{\partial \theta} \delta \theta + \frac{\partial G}{\partial \phi} \delta \phi + \frac{\partial G}{\partial \psi} \delta \psi \quad (6.28)$$

So that

$$\delta f(x_2, x_3) = [G(x_3)]_0 \delta x_2 + \left(\frac{\partial G}{\partial \theta} x_2 \mid \frac{\partial G}{\partial \phi} x_2 \mid \frac{\partial G}{\partial \psi} x_2 \right)_0 \delta x_3 \quad (6.29)$$

• Case 4:

$$f(x_1, x_3) = [E'(x_3)] x_1 \quad (6.30)$$

so that

$$\delta f(x_1, x_3) = [E'(x_3)]_0 \delta x_1 + \left(\frac{\partial E'}{\partial \theta} x_1 \mid \frac{\partial E'}{\partial \phi} x_1 \mid \frac{\partial E'}{\partial \psi} x_1 \right)_0 \delta x_3 \quad (6.31)$$

In summary, the linearization of the analytic terms in (6.13) through (6.16) yields the following set of equations:

$$\begin{aligned} \delta x_1 &= -[W(x_2)]_0 \delta x_1 - \left(\frac{\partial W}{\partial p} x_1 \mid \frac{\partial W}{\partial q} x_1 \mid \frac{\partial W}{\partial r} x_1 \right)_0 \delta x_2 + \left(\frac{\partial E}{\partial \theta} g_e \mid \frac{\partial E}{\partial \phi} g_e \mid \frac{\partial E}{\partial \psi} g_e \right)_0 \delta x_3 \\ &+ \frac{1}{m} B_T \delta y_T + \frac{1}{m} \Delta f_a(x_1, x_2, x_3, \delta, w) \end{aligned} \quad (6.32)$$

$$\delta \dot{x}_2 = - \left[J^{-1} W(x_2) J + \left(J^{-1} \frac{\partial W}{\partial p} J x_2 \mid J^{-1} \frac{\partial W}{\partial q} J x_2 \mid J^{-1} \frac{\partial W}{\partial r} J x_2 \right)_0 \right] \delta x_2 + J^{-1} \hat{B}_T \delta y_T + J^{-1} \Delta m_a(x_1, x_2, x_3, \delta, w) \quad (6.33)$$

$$\delta \dot{x}_3 = [G(x_3)]_0 \delta x_2 + \left(\frac{\partial G}{\partial \theta} x_2 \mid \frac{\partial G}{\partial \phi} x_2 \mid \frac{\partial G}{\partial \psi} x_2 \right)_0 \delta x_3 \quad (6.34)$$

$$\delta \dot{x}_4 = [E'(x_3)]_0 \delta x_1 + \left(\frac{\partial E'}{\partial \theta} x_1 \mid \frac{\partial E'}{\partial \phi} x_1 \mid \frac{\partial E'}{\partial \psi} x_1 \right)_0 \delta x_3 \quad (6.35)$$

where the matrices W , E , and G are defined by equations (3.21), (3.14) and (3.24) of Section III, respectively. The set of equations (6.32) through (6.35) can be written as

$$\begin{bmatrix} \delta \dot{x}_1 \\ \delta \dot{x}_2 \\ \delta \dot{x}_3 \\ \delta \dot{x}_4 \end{bmatrix} = \begin{bmatrix} -F_{11} & -F_{12} & F_{13} & 0 \\ 0 & -F_{22} & 0 & 0 \\ 0 & F_{23} & F_{33} & 0 \\ F_{41} & 0 & F_{43} & 0 \end{bmatrix} \begin{bmatrix} \delta x_1 \\ \delta x_2 \\ \delta x_3 \\ \delta x_4 \end{bmatrix} + \begin{bmatrix} \frac{1}{m} B_T \\ J^{-1} \hat{B}_T \Delta y_T \\ 0 \\ 0 \end{bmatrix} + \begin{bmatrix} \frac{1}{m} \Delta f_a(x_1, x_2, x_3, \delta, w) \\ J^{-1} \Delta m_a(x_1, x_2, x_3, \delta, w) \\ 0 \\ 0 \end{bmatrix} \quad (6.36)$$

This finishes the linearization of the analytical terms. What remains to be done to finish the problem is to compute Δf and Δm appearing in (6.36). Since these vector functions have tabular representations, one must resort to a numerical procedure to compute them in terms of the increments in their arguments. At this point there exist two methods of approach: (a) the equations of the force and moment vectors presented in Section IV can be utilized to further the analytical differentiation process/ this procedure finally yields to the stability derivatives of the aerodynamic force and moment system; or (b) direct numerical partial differentiation of f and m .

This brings us to the problem of numerical partial differentiation of vectors with several arguments. Since the size of a vector and its arguments are immaterial, the computational procedure presented in the section that follows for the pure numerical partial differentiation approach applies here as well.

Pure Numerical Linearization Approach

As can be seen from the equations (6.32) through (6.35), the mixed-linearization approach requires more effort in its computer implementation

and it does not completely eliminate the numerical differentiation process. For this reason, sacrifice is made in the accuracy of computations to grossly simplify the linearization process. In the following, a set of candidate numerical algorithms is presented and the one which is implemented in ADAPS is discussed.

Numerical Differentiation Algorithms -- Numerical differentiation algorithms can be developed either by (a) differentiating the Lagrange interpolating polynomial of a table function or (b) using the discrete approximation to the derivative operator.

By differentiating three-point Lagrangian interpolation formulas and evaluating the results at tabular points, the following derivative formula is obtained [41]:

$$f'_0 = \left(\frac{f_1 - f_{-1}}{2h} \right) - \frac{h^2}{6} f'''(\xi), \quad x_0 - h < \xi < x_0 + h \quad (6.37)$$

If it is known that $|f'''(x)| < M_3$ in the interval $(x_0 - h, x_0 + h)$ and if all given data were exact, the maximum possible error in the calculation of $f'(x_0)$ would be

$$|E_3|_{\max} = \frac{M_3 h^2}{6} \quad (6.38)$$

On the other hand, if each of the ordinates involved is in error by $\pm \epsilon$, then the magnitude of the corresponding error in the calculation of $f'(x_0)$ could be as large as

$$|R_3|_{\max} = \frac{\epsilon}{h} \quad (6.39)$$

whereas a reduction of the truncation error E_3 would generally require a decrease in h , a small value of h would lead to a large possible round-off error R_3 and, conversely, a reduction in $|R_3|_{\max}$ would generally correspond to an increase in $|E_3|_{\max}$.

A reasonable procedure consists in determining the interval h such that the predictable upper bounds on the two errors are about equal, if this is feasible. The optimum value of h and the corresponding maximum total error T^* are then found to be [41]

$$h^* = 1.8 \epsilon^{1/3} M_3^{-1/3}, \quad T^* = 1.1 \epsilon^{2/3} M_3^{1/3} \quad (6.40)$$

By using a discrete approximation to the derivative operator, the derivative of a function at discrete points can be expressed in terms of the differences of the function at tabular points. Let s be a differential operator, that is

$$sf(x) = f'(x) \quad (6.41)$$

If z is a shift operator defined by

$$zf(x) = f(x+h) \quad (6.42)$$

Then it can be shown by using Taylor series expansion that

$$z = e^{hs} \quad (6.43)$$

If Δ is a forward difference operator defined by $\Delta f(x) \triangleq f(x+h) - f(x)$, then one can write $z = (1+\Delta)$ and

$$s = \frac{\log z}{h} = \frac{\log(1+\Delta)}{h} = \frac{1}{h} \left(\Delta - \frac{1}{2} \Delta^2 + \dots \right) \quad (6.44)$$

In terms of backward differences, $z = (1-\nabla)^{-1}$

$$s = \frac{-\log(1-\nabla)}{h} = \frac{1}{h} \left(\nabla + \frac{1}{2} \nabla^2 + \dots \right) \quad (6.45)$$

If the expansion is truncated after the first term one obtains

$$\frac{d}{dx} \approx \frac{1}{h} (\Delta) \quad (6.46)$$

so that

$$\frac{d}{dx} f(x) = \frac{1}{h} \frac{f(x+h) - f(x)}{h} \quad (6.47)$$

Derivatives using more data points can be obtained from (6.44) or (6.45).

At this point a remark is made about algorithm selection. In aircraft or weapon linearization problems, the listed increments in the function arguments are much larger than that of increments that can occur about a nominal argument set due to small perturbations. Consider a table function

$$f = f(\mu)$$

where

$$\mu = \begin{bmatrix} h(x, u) \\ M(x, u) \\ \alpha(x, u) \end{bmatrix}$$

is the data argument set of the table function. Let

$$\Delta\mu = \begin{pmatrix} \Delta h \\ \Delta M \\ \Delta\alpha \end{pmatrix}$$

be the set of increments on which data is given. Then there is a perturbation $(\delta x, \delta u)$ such that

$$|\delta \mu| < |\Delta \mu| \leq |C_1| |\delta x| + |C_2| |\delta u| \quad (6.48)$$

This fact is illustrated in Figure 29.

On the other hand, for every $\begin{bmatrix} h \\ M \\ \alpha \end{bmatrix}$ in the i, j, k data cube, $f(h, M, \alpha)$ is represented by

$$\begin{aligned} f(h, M, \alpha) = & l_0 + l_1 \tilde{h} + l_2 \tilde{M} + l_3 \tilde{\alpha} \\ & + l_{12} \tilde{h} \tilde{M} + l_{23} \tilde{M} \tilde{\alpha} + l_{31} \tilde{\alpha} \tilde{h} \\ & + l_{123} \tilde{h} \tilde{M} \tilde{\alpha} \end{aligned} \quad (6.49)$$

where l 's are functions of data point indices i, j, k only, and $\tilde{h}, \tilde{M}, \tilde{\alpha}$ are linear functions of (h, M, α) . This representation follows from the multi-dimensional linear interpolation algorithm used in ADAPS for generating a value for a table function inside the interval of tabular points. It follows from (6.49) that the partials

$$\left(\frac{\partial f}{\partial h}, \frac{\partial f}{\partial M}, \frac{\partial f}{\partial \alpha} \right)_0$$

depend only upon (a) the data cube in which the nominal parameter vector is located, and (b) the value of the nominal parameter vector. It does not depend upon the size of the perturbations as long as the perturbation cube is

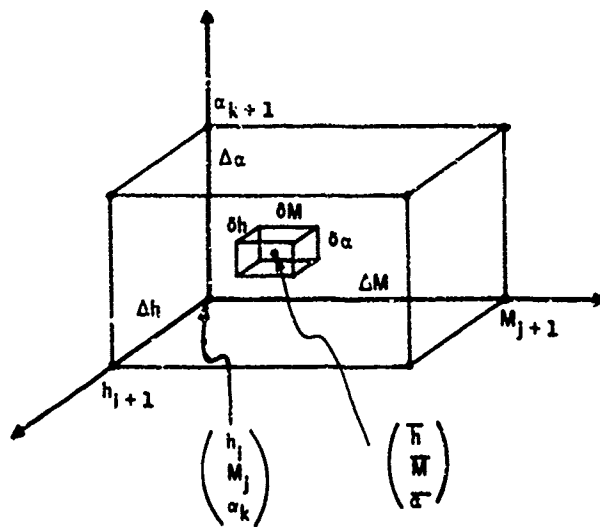


Figure 29. "Data Increment" and "Parameter Perturbation" Cubes

inside the data increment cube. Therefore, we may conclude that a two-point linear interpolation algorithm is used for representing a tabular function inside the data interval, and when small perturbations are assumed then, the use of elaborate differentiation algorithms is not justified for the table functions and partial differentiation algorithms given by

$$\left[\frac{f(\alpha + \delta\alpha) - f(\alpha)}{\delta\alpha} \right] \quad (6.50)$$

$$\left[\frac{f(\alpha) - f(\alpha - \delta\alpha)}{\delta\alpha} \right] \quad (6.51)$$

$$\left[\frac{f\left(\alpha + \frac{\delta\alpha}{2}\right) - f\left(\alpha - \frac{\delta\alpha}{2}\right)}{\delta\alpha} \right] \quad (6.52)$$

are all equivalent and moreover independent of the size of $\delta\alpha$ provided that $|\delta\alpha| < \Delta\alpha$.

For pure numerical linearization process, however, the use of the central differences given by equation (6.52) provide better accuracy in the linearization of analytic functions appearing in the equations of motion. For this reason (6.52) is utilized with a set of fixed perturbation increments, in ADAPS.

The analysis presented up to this point is implemented as the subroutine LINK. It is used to linearize numerically, the nonlinear state equations of motion.

TRANSFORMATION OF THE PERTURBATION STATES

A few words are in order here about the state component assignment to various physical quantities in the dynamics. The standard state component assignment for the nonlinear equations of motion has been defined to be

$$\begin{aligned} \mathbf{x} &= \text{col}(x_1, x_2, x_3 | x_4, x_5, x_6 | x_7, x_8, x_9 | x_{10}, x_{11}, x_{12}) \\ &= \text{col}(u, v, w | p, q, r | \theta, \phi, \psi | x_e, y_e, z_e) \end{aligned} \quad (6.53)$$

The resulting state perturbation equation of motion is illustrated in Figure 30.

When dealing with the linearized equations, the state components may be reordered with respect to longitudinal and lateral dynamics for convenience. The state component assignment for this case is defined as

$$\delta\mathbf{x} = \text{col}(\delta x_e, \delta h_e, \delta u, \delta \theta, \delta q, \delta w | \delta y, \delta \psi, \delta r, \delta v, \delta \phi, \delta p) \quad (6.54)$$

The resulting state perturbation equation of motion is illustrated in Figure 31.

	δu	δv	δw	δp	δq	δr	$\delta \theta$	$\delta \phi$	$\delta \psi$	δx_e	δy_e	δh_e	
$\delta \dot{u}$	X_u	0	X_w	0	X_q	0	X_θ	0	0			X_h	$\delta \dot{u}$
$\delta \dot{v}$	0	Y_v	0	Y_p	0	Y_r	0	Y_θ	0			0	$\delta \dot{v}$
$\delta \dot{w}$	Z_u	0	Z_w	0	Z_q	0	Z_θ	0	0			Z_h	$\delta \dot{w}$
$\delta \dot{p}$	0	L_v	0	L_p	0	L_r						0	$\delta \dot{p}$
$\delta \dot{q}$	M_u	0	M_w	0	M_q	0						M_h	$\delta \dot{q}$
$\delta \dot{r}$	0	N_v	0	N_p	0	N_r						0	$\delta \dot{r}$
$\delta \dot{\theta}$				0	1.0	0	0	0	0				$\delta \dot{\theta}$
$\delta \dot{\phi}$				1.0	0	ϕ_r	0	ϕ_θ	0				$\delta \dot{\phi}$
$\delta \dot{\psi}$				0	0	ψ_r	0	ψ_θ	0				$\delta \dot{\psi}$
$\delta \dot{x}_e$	X_{eu}	0	X_{ew}				$X_{e\theta}$	0	0				$\delta \dot{x}_e$
$\delta \dot{y}_e$	0	1.0	0				0	$Y_{e\theta}$	$Y_{e\psi}$				$\delta \dot{y}_e$
$\delta \dot{h}_e$	H_{eu}	0	H_{ew}				$H_{e\theta}$	0	0				$\delta \dot{h}_e$

(6.55)

δa	δs	δr	δ_{sp}		δu_g	δv_g	δw_g	δp_g	δq_g	δr_g
0	X_{cs}	0	0	$\delta \dot{a}$	X_{ug}	0	X_{wg}	0	X_{qg}	0
$Y_{\delta a}$	0	$Y_{\delta r}$	$Y_{\delta_{sp}}$	$\delta \dot{s}$	0	Y_{vg}	0	Y_{pg}	0	Y_{rg}
0	$Z_{\delta s}$	0	0	$\delta \dot{r}$	Z_{ug}	0	Z_{wg}	0	Z_{qg}	0
$L_{\delta a}$	0	$L_{\delta r}$	0	$\delta \dot{p}_g$	0	L_{vg}	0	L_{pg}	0	L_{rg}
$M_{\delta a}$	$M_{\delta s}$	0	$M_{\delta_{sp}}$	$\delta \dot{q}_g$	M_{ug}	0	M_{wg}	0	M_{qg}	0
$N_{\delta a}$	0	$N_{\delta r}$	$N_{\delta_{sp}}$	$\delta \dot{r}_g$	0	N_{vg}	0	N_{pg}	0	N_{rg}

Figure 30. Linearized State Equations of Airframe with Nominal State Component Assignment

Figure 31. Linearized State Equations of Airframe with Channeled State Component Assignment

The gust filter states (Section IV) are also grouped with respect to longitudinal and lateral excitations:

$$w = \text{col}(w_1, w_7, w_3, w_5 | w_8, w_2, w_4, w_6) \quad (6.57)$$

The resulting state equation of the full-gust filter is illustrated in Figure 32 and the state equation of the reduced gust filter (rolling gust terms omitted) is illustrated in Figure 33. These definitions, produce almost upper-block triangular transition matrices. They are obtained by permutational similarity transformations. This operation is referred to as "Shuffling" of the linear data and is carried out by Subroutine SHUFF.

Besides permutational similarity transformations, as explained above, there are transformations induced by the various selections of physical variables as state components. For instance, instead of selecting (v, v, w) as state components, one may choose (V, β, α) to describe the velocity vector.

Consider the state differential equation given by (6.12). Let ξ be a chosen state vector related to standard state vector x by a nonlinear relation:

$$\xi = g(x) \quad (6.58)$$

Then

$$\dot{\xi} = h(x, u) \quad (6.59)$$

where

$$h(x, u) = \left[\frac{\partial g(x)}{\partial x} \right] f(x, u) \quad (6.60)$$

Let us assume that x , ξ and $\dot{\xi}$ are evaluated for each nominal point using (6.12), (6.58) and (6.59). Then the partials

$$\left(\frac{\partial f}{\partial x} \right)_0, \left(\frac{\partial f}{\partial u} \right)_0, \left(\frac{\partial g}{\partial x} \right)_0, \left(\frac{\partial h}{\partial x} \right)_0, \text{ and } \left(\frac{\partial h}{\partial u} \right)_0 \text{ can be computed along the}$$

nominal trajectory during the linearization process with the standard state, as described previously.

Noting that

$$\delta \xi = \left(\frac{\partial g}{\partial x} \right)_0 \delta x \quad (6.61)$$

and

$$\dot{\delta \xi} = \left(\frac{\partial h}{\partial x} \right)_0 \delta x + \left(\frac{\partial h}{\partial u} \right)_0 \delta u \quad (6.62)$$

The state perturbation equations in terms of the new perturbation state vector become

$$\dot{\delta \xi} = F_{\xi} \delta \xi + G_{\xi} \delta u \quad (6.63)$$

where

$$F_{\xi} = \left(\frac{\partial h}{\partial x} \right)_0 \left(\frac{\partial g}{\partial x} \right)_0^{-1} \quad (6.64)$$

and

$$G_{\xi} = \left(\frac{\partial h}{\partial u} \right)_0 \quad (6.65)$$

By this procedure, the linear data can be generated for any arbitrary axes system.

$$\begin{array}{c}
 \begin{array}{c} \dot{w}_1 \\ \dot{w}_7 \\ \dot{w}_3 \\ \dot{w}_5 \end{array} \quad \begin{array}{c} w_1 \\ w_7 \\ w_3 \\ w_5 \end{array} \quad \begin{array}{c} w_7 \\ w_3 \\ w_5 \end{array} \quad \begin{array}{c} w_1 \\ w_7 \\ w_3 \\ w_5 \end{array} \quad \begin{array}{c} w_2 \\ w_6 \end{array} \quad \begin{array}{c} w_2 \\ w_6 \end{array} \quad \begin{array}{c} w_4 \\ w_4 \end{array} \\
 \left[\begin{array}{c|c|c|c|c|c|c|c} -a_u & 0 & 0 & 0 & 0 & & & \\ 0 & -a_q & b_q & 0 & 0 & & & \\ 0 & 0 & -a_{2w} & -1 & 0 & & & \\ 0 & 0 & -a_{1w} & 0 & 0 & & & \\ \hline & & & & & a_r & b_r & 0 \\ & & & & & 0 & a_{2v} & 1 \\ & & & & & 0 & 0 & a_p \\ & & & & & 0 & a_{1v} & 0 \end{array} \right] \begin{array}{c} w_1 \\ w_7 \\ w_3 \\ w_5 \end{array} + \begin{array}{c} \begin{array}{c} w_1 \\ w_7 \\ w_3 \\ w_5 \end{array} \quad \begin{array}{c} w_8 \\ w_2 \\ w_6 \\ w_4 \end{array} \\
 \left[\begin{array}{c|c|c|c} b_u & 0 & 0 & 0 \\ 0 & 0 & b_{2w} & b_{1w} \\ \hline & & & \end{array} \right] \begin{array}{c} \eta_u \\ \eta_w \\ \eta_v \\ \eta_p \end{array} \quad (6.66)
 \end{array}$$

$$\begin{array}{c}
 \begin{array}{c} u_g \\ q_g \\ w_g \end{array} \quad \begin{array}{c} w_1 \\ w_7 \\ w_3 \\ w_5 \end{array} \quad \begin{array}{c} w_7 \\ w_3 \\ w_5 \end{array} \quad \begin{array}{c} w_1 \\ w_7 \\ w_3 \\ w_5 \end{array} \quad \begin{array}{c} w_2 \\ w_6 \end{array} \quad \begin{array}{c} w_2 \\ w_6 \end{array} \quad \begin{array}{c} w_4 \\ w_4 \end{array} \\
 \left[\begin{array}{c|c|c|c|c|c|c|c} 1 & 0 & 0 & 0 & 0 & & & \\ 0 & 1 & d_q & 0 & 0 & & & \\ 0 & 0 & 1 & 0 & 0 & & & \\ \hline & & & & & 1 & d_r & 0 \\ & & & & & 0 & 1 & 0 \\ & & & & & 0 & 0 & 1 \end{array} \right] \begin{array}{c} u_g \\ q_g \\ w_g \end{array} = \begin{array}{c} \begin{array}{c} w_1 \\ w_7 \\ w_3 \\ w_5 \end{array} \quad \begin{array}{c} w_8 \\ w_2 \\ w_6 \\ w_4 \end{array} \\
 \left[\begin{array}{c|c|c|c} b_u & 0 & 0 & 0 \\ 0 & 0 & b_{2w} & b_{1w} \\ \hline & & & \end{array} \right] \begin{array}{c} \eta_u \\ \eta_w \\ \eta_v \\ \eta_p \end{array} \quad (6.67)
 \end{array}$$

Figure 32. Full-Gust Filter State Equations with Channeled State Component Assignment

$$\begin{bmatrix} \dot{w}_1 \\ \dot{w}_3 \\ \dot{w}_5 \\ \hline \dot{w}_2 \\ \dot{w}_4 \end{bmatrix} = \begin{bmatrix} w_1 & w_3 & w_5 & w_2 & w_4 \\ -a_u & 0 & 0 & 1 & 0 \\ 0 & -a_{2w} & 0 & a_{2w} & a_{1v} \\ 0 & -a_{1w} & 0 & 0 & 0 \\ \hline & & & & \end{bmatrix} \begin{bmatrix} w_1 \\ w_3 \\ w_5 \\ w_2 \\ w_4 \end{bmatrix} + \begin{bmatrix} \eta_u & \eta_w & \eta_v \\ b_u & 0 & 0 & b_{2v} & b_{1v} \\ 0 & b_{2w} & 0 & & \\ 0 & b_{1w} & 0 & & \\ \hline & & & & \end{bmatrix} \begin{bmatrix} \eta_u \\ \eta_w \\ \eta_v \end{bmatrix} \quad (6.68)$$

$$\begin{bmatrix} u_g \\ w_g \\ \hline v_g \end{bmatrix} = \begin{bmatrix} w_1 & w_3 & w_5 \\ 1 & 0 & 0 & 0 \\ 0 & 1 & 0 & 1 & 0 \\ \hline & & & & \end{bmatrix} \begin{bmatrix} w_1 \\ w_3 \\ w_5 \\ w_2 \\ w_4 \end{bmatrix} \quad (6.69)$$

Figure 33. Reduced-Gust Filter State Equations

SECTION VII

DEVELOPMENT OF THE NOMINAL STATE AND PARAMETER (TRIMMING)

The way the nominal state and parameters of a rigid body in flight are developed depends on whether the body is controlled or uncontrolled. When a prescribed nominal trajectory to be generated by a controlled body (i. e., aircraft, guided missile) is under consideration, one can find it either: (a) by simulation with an autopilot for given flight conditions and reading out the nominal values of state and control parameters during the flight; or (b) by assuming that a body is forced to fly in accordance with given flight conditions and computing the missing nominal states and parameters which produce that flight. The first technique is called "trimming with an autopilot" and the second "algebraic trimming."

When a body is uncontrolled (i. e., iron bomb, bullet) the nominal trajectory cannot be arbitrarily specified. It is obtained by integrating the differential equations of motion starting from a given initial condition.

In the following the development of the nominal state and parameters along a prescribed trajectory are treated for a controlled body first using the algebraic trimming approach. Then trimming with an autopilot is discussed. In ADAPS the latter approach is utilized.

ALGEBRAIC TRIMMING

Consider an aircraft represented by

$$\dot{x} = f(x, u) \quad (7.1)$$

$$y = h(x) \quad (7.2)$$

where

x = state vector

u = control vector

y = response vector

The response rate is then given by

$$\dot{y} = H(x) f(x, u) \quad (7.3)$$

where

$$H(x) = \frac{\partial h}{\partial x} \quad (7.4)$$

The response vector may consist of a set of trajectory variables such as

$$y = \begin{bmatrix} V \\ \gamma \end{bmatrix} = \begin{bmatrix} \sqrt{u^2 + v^2 + w^2} \\ \theta - \tan^{-1} \frac{w}{u} \end{bmatrix} \quad (7.5)$$

Most often, \dot{y} and some of the components of x , and \dot{x} are specified along the nominal trajectory.

For instance

$$\dot{y}_d = \begin{bmatrix} \dot{V} \\ \dot{\gamma} \end{bmatrix} = \begin{bmatrix} a \\ 0 \end{bmatrix} \quad (7.6)$$

indicates a quasi-steady motion with a constant acceleration and a constant flight-path angle (steep-dive bombing).

The trim problem is to find the missing state variables and controls such that the error defined by

$$e(t) = |H(x) f(x, u) - \dot{y}_d| \quad (7.7)$$

is small.

Algebraic Trimming for Dive and Pull-up Trajectory

The two-phase nominal trajectory considered here corresponds to a steady, symmetric, straight-path, dive-bombing maneuver [7], followed by a symmetric, steady-pitch (i. e., constant-g) pull-up maneuver.

In the first part of the nominal trajectory, it is assumed that the aircraft is in a steady flight with a constant velocity V_1 along a straight path with a flight-path angle γ , and altitude $h_0 \geq 2h_{pu}$ where h_{pu} is the pull-up altitude as shown in Figure 34. This type of flight is assumed to be accomplished by adjusting the elevator angle (i. e., stabilator in F-4 case) and the magnitude of the engine thrust.

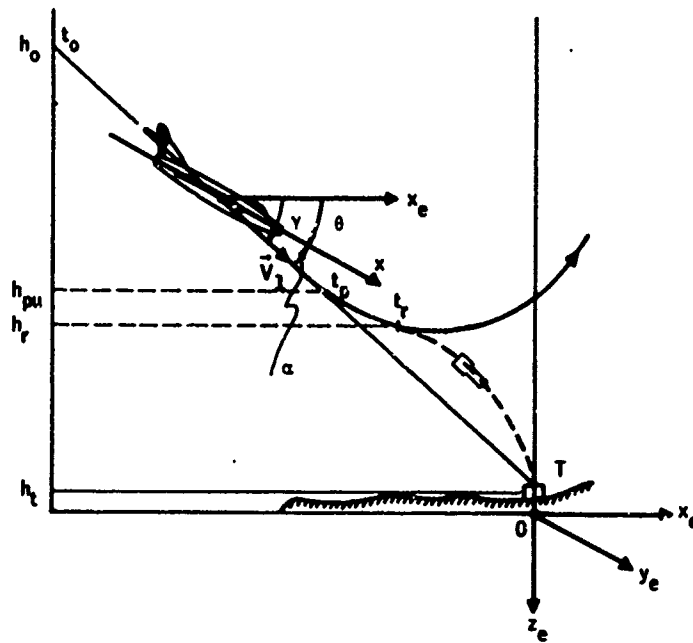


Figure 34. Nominal Dive and Pull-Up Trajectory

In the second part, it is assumed that the aircraft flies with a constant velocity \bar{V}_2 and a constant pitch rate Q_0 . Again this type of flight is assumed to be accomplished by adjusting the elevator angle and the magnitude of the engine thrust.

In the following, the trim equations for the dive phase of the maneuver are developed first. Then the constant-g pull-up case is treated.

Development of the Missing Nominal Values for a Dive Maneuver -- It follows from the above descriptions that the mathematical implications associated with the given conditions are:

$$\text{Constant Speed} \Rightarrow \dot{\bar{V}} = 0 \quad (7.8)$$

$$\text{Steady Flight} \Rightarrow \begin{pmatrix} \dot{u} \\ \dot{v} \\ \dot{w} \end{pmatrix} = 0 \text{ and } \begin{pmatrix} \dot{p} \\ \dot{q} \\ \dot{r} \end{pmatrix} = 0 \quad (7.9)$$

$$\text{Symmetric Flight} \Rightarrow \begin{pmatrix} u \\ v \\ w \end{pmatrix} = \begin{pmatrix} u(t) \\ 0 \\ w(t) \end{pmatrix}, \quad \begin{pmatrix} p \\ q \\ r \end{pmatrix} = \begin{pmatrix} 0 \\ q(t) \\ 0 \end{pmatrix}, \quad (7.10)$$

and

$$\begin{pmatrix} \theta \\ \phi \\ \psi \end{pmatrix} = \begin{pmatrix} \theta(t) \\ 0 \\ 0 \end{pmatrix} \text{ or equivalently } \begin{pmatrix} \lambda_0 \\ \lambda_1 \\ \lambda_2 \\ \lambda_3 \end{pmatrix} = \begin{pmatrix} \cos \theta/2 \\ 0 \\ \sin \theta/2 \\ 0 \end{pmatrix} \quad (7.11)$$

$$\text{Straight Flight} \Rightarrow \begin{pmatrix} p \\ q \\ r \end{pmatrix} = 0 \quad (7.12)$$

Finally,

$$\text{Controls} \Rightarrow \begin{pmatrix} \delta_a \\ \delta_s \\ \delta_r \end{pmatrix} = \begin{pmatrix} 0 \\ \delta_s(t) \\ 0 \end{pmatrix}, \quad T = T(t) \quad (7.13)$$

It is obvious at this point that the specified set of flight conditions does not give, directly, all the states and parameters along the trajectory. In the case treated here the missing state information is the angular position coordinate $\theta(t)$, and the missing parameters are the stabilator deflection δ_s and the thrust magnitude T .

Observation of the differential equations of motion reveals that

$$X + X_T - mg \sin \theta = m\dot{u} \quad (7.14)$$

$$Y \equiv \dot{v} \equiv 0 \quad (7.15)$$

$$Z + Z_T + mg \cos \theta = m\dot{w} \quad (7.16)$$

$$L \equiv \dot{p} \equiv 0 \quad (7.17)$$

$$M + M_T = I_y \dot{q} \quad (7.18)$$

$$N \equiv \dot{r} \equiv 0 \quad (7.19)$$

and

$$\begin{pmatrix} \dot{\theta} \\ \dot{\phi} \\ \dot{\psi} \end{pmatrix} = 0 \quad \text{or equivalently} \quad \begin{pmatrix} \dot{\lambda}_0 \\ \dot{\lambda}_1 \\ \dot{\lambda}_2 \\ \dot{\lambda}_3 \end{pmatrix} = 0 \quad (7.20)$$

Therefore the problem is to find $\theta(t)$, $\delta_g(t)$, and $T(t)$ such that

$$\dot{u} = \frac{X}{m} + \frac{X_T}{m} - g \sin \theta = 0 \quad (7.21)$$

$$\dot{w} = \frac{Z}{m} + \frac{Z_T}{m} + g \cos \theta = 0 \quad (7.22)$$

$$\dot{q} = \frac{M}{I_y} + \frac{M_T}{I_y} = 0 \quad (7.23)$$

Theoretically speaking, it is impossible to produce a steady flight during a dive motion due to changes in the altitude and Mach number parameters. However, for all practical purposes the contributions of \dot{u} , \dot{w} and \dot{q} terms are negligible.

It should be noted here that in the solutions of the above equations, an equivalent state α is used instead of θ , since the aerodynamic forces and moments are functions of this variable. After having found the value of α , $\theta(t)$ and $\lambda(t)$ are computed from

$$\theta = \alpha + \gamma \quad (7.24)$$

and

$$\begin{pmatrix} \lambda_0 \\ \lambda_1 \\ \lambda_2 \\ \lambda_3 \end{pmatrix} = \begin{pmatrix} \cos \theta/2 \\ 0 \\ \sin \theta/2 \\ 0 \end{pmatrix} \quad (7.25)$$

Development of the Missing Nominal Values for a Steady-Pitch Pull-Up Maneuver -- As discussed previously, symmetric, steady-pitch flight conditions imply a quasi-steady motion in which

$$\begin{pmatrix} \dot{u} \\ \dot{v} \\ \dot{w} \end{pmatrix} = \begin{pmatrix} \dot{u}(t) \\ 0 \\ \dot{w}(t) \end{pmatrix}, \quad \begin{pmatrix} \dot{p} \\ \dot{q} \\ \dot{r} \end{pmatrix} = 0 \quad (7.26)$$

and

$$\begin{pmatrix} u \\ v \\ w \end{pmatrix} = \begin{pmatrix} u(t) \\ 0 \\ w(t) \end{pmatrix}, \quad \begin{pmatrix} p \\ q \\ r \end{pmatrix} = \begin{pmatrix} 0 \\ q \\ 0 \end{pmatrix} \quad (7.27)$$

Similarly

$$\begin{pmatrix} \phi \\ \psi \end{pmatrix} = \begin{pmatrix} \theta(t) \\ 0 \\ 0 \end{pmatrix} \text{ or equivalently } \begin{pmatrix} \lambda_0 \\ \lambda_1 \\ \lambda_2 \\ \lambda_3 \end{pmatrix} = \begin{pmatrix} \cos \theta/2 \\ 0 \\ \sin \theta/2 \\ 0 \end{pmatrix} \quad (7.28)$$

with controls

$$\begin{pmatrix} \delta_a \\ \delta_s \\ \delta_r \end{pmatrix} = \begin{pmatrix} 0 \\ \delta_s(t) \\ 0 \end{pmatrix}, \quad T = T(t) \quad (7.29)$$

Observation of the differential equations of motion for this case reveals that

$$X + X_T - mg \sin \theta = m\dot{u} + mqw \quad (7.30)$$

$$Y \equiv \dot{v} \equiv 0 \quad (7.31)$$

$$Z + Z_T + mg \cos \theta = m\dot{w} - mqu \quad (7.32)$$

$$L \equiv \dot{p} \equiv 0 \quad (7.33)$$

$$M + M_T = I_y \dot{q} \quad (7.34)$$

$$\dot{N} \equiv \dot{r} \equiv 0 \quad (7.35)$$

$$\dot{\theta} = q \quad (7.36)$$

$$\dot{\phi} \equiv 0 \quad (7.37)$$

$$\dot{\psi} \equiv 0 \quad (7.38)$$

$$\dot{x}_e = (\cos \theta) u + (\sin \theta) w \quad (7.39)$$

$$\dot{y}_e \equiv 0 \quad (7.40)$$

$$\dot{z}_e = -(\sin \theta) u + (\cos \theta) w \quad (7.41)$$

Now, substituting $u = V \cos \alpha$, $w = V \sin \alpha$ into (7.30) and (7.32) yields

$$\frac{X}{m} + \frac{X_T}{m} - g \sin \theta - qV \sin \alpha = \dot{u} \quad (7.42)$$

$$\frac{Z}{m} + \frac{Z_T}{m} + g \cos \theta + qV \cos \alpha = \dot{w} \quad (7.43)$$

$$\frac{M}{I_y} + \frac{M_T}{I_y} = \dot{q} \quad (7.44)$$

which shows that the set (7.42), (7.43), and (7.44) reduces to set (7.21), (7.22), and (7.23) when q is set to zero. Here u and v are functions of t and $\dot{u} \neq 0$, $\dot{w} \neq 0$. If contributions due to \dot{u} and \dot{w} are neglected (this is a common procedure in algebraic trim), the set of equations to be solved becomes almost the same for the two parts of the nominal trajectory.

In practice, usually, pull-up maneuver is defined by specifying the so-called load factor. Assuming $\dot{w} \approx 0$ in (7.32), one can write

$$q = \frac{g}{u} \left[\frac{-(Z + Z_T)}{mg} - \cos \theta \right] \quad (7.45)$$

The load factor is defined as

$$n_z = \frac{-(Z + Z_T)}{mg} \quad (7.46)$$

In terms of this quantity the q terms in (7.42) and (7.43) become

$$qV \sin \alpha = g(n_z - \cos \theta) \tan \alpha \quad (7.47a)$$

$$qV \cos \alpha = g(n_z - \cos \theta) \quad (7.47b)$$

Now, for a symmetric flight, the engine thrust variables are given by

$$X_T = T(\cos \xi \cos \eta) \quad (7.48)$$

$$Z_T = -T(\cos \xi \sin \eta) \quad (7.49)$$

and

$$M_T = X_T \Delta z - Z_T \Delta x = T(\Delta z \cos \xi \cos \eta + \Delta x \cos \xi \sin \eta) \quad (7.50)$$

Observation of (7.48)-(7.50) together with (7.21)-(7.23), or, equivalently, (7.42)-(7.44), indicates that the total thrust, T , enters into the equations linearly. That is,

$$\dot{u} = c_1 \frac{T}{m} + \frac{X}{m} - g \sin \theta - qV \sin \alpha = 0 \quad (7.51)$$

$$\dot{w} = c_2 \frac{T}{m} + \frac{Z}{m} + g \cos \theta + qV \cos \alpha = 0 \quad (7.52)$$

and

$$\dot{q} = c_3 \frac{T}{I_y} + \frac{M}{I_y} = 0 \quad (7.53)$$

where

$$c_1 = \cos \xi \cos \eta \quad (7.54)$$

$$c_2 = -\cos \xi \sin \eta \quad (7.55)$$

$$c_3 = (\Delta z \cos \xi \cos \eta + \Delta x \cos \xi \sin \eta) \quad (7.56)$$

For this reason the number of equations to be solved can be reduced to two by eliminating T .

Solving (7. 51) for T yields

$$T = \frac{1}{c_1} [mg \sin \theta + mqV \sin \alpha - X] \quad (7. 57)$$

and substituting this into (7. 52) and (7. 53) one obtains

$$\begin{aligned} \dot{w} &= g(\cos \theta - c_4 \sin \theta) + qV(\cos \alpha - c_4 \sin \alpha) \\ &\quad + [(c_4 X + Z)/m] = 0 \end{aligned} \quad (7. 58)$$

$$\dot{q} = [c_5 (mg \sin \theta + mqV \sin \alpha - X) + M]/I_y = 0 \quad (7. 59)$$

where

$$\begin{aligned} c_1 &= \cos \xi \cos \eta \\ c_4 &= \tan \eta \\ c_5 &= (\Delta y - c_4 \Delta x) \end{aligned} \quad (7. 60)$$

Hence the problem is reduced to finding α and δ_g such that (7. 58) and (7. 59) are both zero.

To summarize, in the development of the trim equations it is assumed that the adjustable parameters are the magnitude of the engine thrust and the elevator deflection angle:

- Trim Equations -

$$\begin{aligned} \dot{w} &= g(\cos \theta - c_4 \sin \theta) + qV(\cos \alpha - c_4 \sin \alpha) \\ &\quad + \frac{(c_4 X + Z)}{m} \end{aligned} \quad (7. 58a)$$

$$\dot{q} = [M - c_5 (X - mg \sin \theta - mqV \sin \alpha)]/I_{yy} = 0 \quad (7. 59a)$$

where, neglecting $\dot{\alpha}$

$$\gamma = \gamma_0 + q\Delta T \quad (7. 61)$$

$$\theta = \gamma + \alpha \quad (7. 62)$$

and

$$q = \begin{cases} 0 & \text{dive} \\ \frac{g}{V \sin \alpha} [n_z - \cos \theta] & \text{pull-up} \end{cases} \quad (7.47a)$$

- Trim Value of Engine Thrust

$$T = (mg \sin \theta + mqV \sin \alpha - X)/c_1 \quad (7.57a)$$

- Trimmed Accelerations

$$\dot{u} = \frac{X_T + X}{m} - g \sin \theta - qV \sin \alpha \quad (7.63)$$

$$\dot{w} = \frac{Z_T + Z}{m} + g \cos \theta + qV \cos \alpha \quad (7.64)$$

$$\dot{q} = (M + M_T)/I_{yy} \quad (7.65)$$

In the following, a procedure is developed by which $\theta(t)$, $\delta_s(t)$ and $T(t)$ are found at time points $[t_k]$, $k = 1, 2, \dots$. The method is based on the concept of "finite number iterations."

Development of the Finite Iteration Algorithm

In short notation, (7.58) and (7.59) are expressed with the aid of (7.61) and (7.62) as

$$f_1(\text{Mach}, h, \alpha, \delta_s) = 0 \quad (7.66)$$

$$f_2(\text{Mach}, h, \alpha, \delta_s) = 0 \quad (7.67)$$

where mach number and altitude, h , are parameters and α , δ_s are the real solutions of these nonlinear algebraic equations [42, 43].

In the following, we shall formally develop a discrete version of the method given in [42], for solving (7.66) and (7.67) since the partial derivatives of f_1 and f_2 cannot be evaluated analytically as assumed in [42]. During this development, the parametric dependence of (mach, h) will be suppressed for the writing ease.

Define

$$\begin{bmatrix} \phi_1(\alpha, \delta_s, \tau_1, \tau_2) \\ \phi_2(\alpha, \delta_s, \tau_1, \tau_2) \end{bmatrix} = \begin{bmatrix} f_1(\alpha, \delta_s) - \tau_1 f_1(\alpha_o, \delta_{s_o}) \\ f_2(\alpha, \delta_s) - \tau_2 f_2(\alpha_o, \delta_{s_o}) \end{bmatrix} \quad (7.68)$$

where α_o, δ_{s_o} are initial estimates for α and δ_s , respectively, and τ_1, τ_2 are unknown parameters. Clearly for the initial values $\tau_1 = \tau_2 = 1$

$$\begin{bmatrix} \phi_1(\alpha_o, \delta_{s_o}, \tau_1, \tau_2) \\ \phi_2(\alpha_o, \delta_{s_o}, \tau_1, \tau_2) \end{bmatrix} = \begin{bmatrix} 0 \\ 0 \end{bmatrix} \quad (7.69)$$

Moreover, the values α and δ_s for which

$$\begin{bmatrix} \phi_1(\alpha, \delta_s, 0, 0) \\ \phi_2(\alpha, \delta_s, 0, 0) \end{bmatrix} = \begin{bmatrix} 0 \\ 0 \end{bmatrix} \quad (7.70)$$

are the solutions of (7.66) and (7.67). Hence, one can find the solution α, δ_s by gradually decreasing τ_1 and τ_2 to zero from the starting values $\tau_1 = \tau_2 = 1$, and at the same time determining α and δ_s so that $\phi_1 = \phi_2 = 0$ for every value of τ_1 and τ_2 .

Now let $\Delta\tau_1$ and $\Delta\tau_2$ be small perturbations about the initial values τ_1 and τ_2 . Then by expanding ϕ_1 and ϕ_2 about the initial point $(\alpha, \delta_s, \tau_1, \tau_2)$ it is possible to find small perturbations $\Delta\alpha$ and $\Delta\delta_s$ such that

$$\begin{bmatrix} \hat{\phi}_1 \\ \hat{\phi}_2 \end{bmatrix} = \begin{bmatrix} \phi_1(\alpha + \Delta\alpha, \delta_s + \Delta\delta_s, \tau_1 + \Delta\tau_1, \tau_2 + \Delta\tau_2) \\ \phi_2(\alpha + \Delta\alpha, \delta_s + \Delta\delta_s, \tau_1 + \Delta\tau_1, \tau_2 + \Delta\tau_2) \end{bmatrix} = \begin{bmatrix} 0 \\ 0 \end{bmatrix}$$

Ignoring the second- and higher-order terms and making use of (7.69) one obtains

$$\hat{\phi}_1 = \left(\frac{\partial f_1}{\partial \alpha} \right)_{\alpha, \delta_s} \Delta\alpha + \left(\frac{\partial f_1}{\partial \delta_s} \right)_{\alpha, \delta_s} \Delta\delta_s + f_1(\alpha_o, \delta_{s_o}) \Delta\tau_1 = 0 \quad (7.71)$$

$$\hat{\phi}_2 = \left(\frac{\partial f_2}{\partial \alpha} \right)_{\alpha, \delta_s} \Delta \alpha + \left(\frac{\partial f_2}{\partial \delta_s} \right)_{\alpha, \delta_s} \Delta \delta_s + f_2(\alpha_0, \delta_{s0}) \Delta \tau_2 = 0 \quad (7.72)$$

where indicated partials are obtained by divided differences. Now if these two equations are independent, then $\Delta \alpha$ and $\Delta \delta_s$ can be obtained in terms of given $\Delta \tau_1$ and $\Delta \tau_2$.

By continuing this procedure, the parameters τ_1 and τ_2 can be reduced to zero in a finite number of steps and the values of α and δ_s corresponding to $\tau_1 = \tau_2 = 0$ become the real solutions of (7.66) and (7.67). From the above formal treatment, a numerical algorithm for finding the values of α and δ_s emerges. The subroutine which implements the procedure is called SUBROUTINE NOMK.

In the following, finite iteration algorithm is compared with the Newton-Raphson process with respect to convergence.

Finite Iteration Algorithm versus Newton-Raphson Process

The development given above is closely tuned for solving a specific trim problem. However, the method of solution applies equally well to solving nonlinear vector equations of the form

$$f(x) = 0 \quad (7.73)$$

with a vector argument. In this case, one obtains the following vector equation with initial guess solution $x^{(0)}$:

$$\left(\frac{\partial f(x)}{\partial x} \right) \Delta x + f(x^{(0)}) \Delta \tau^{(0)} = 0 \quad (7.74)$$

Then for given value of $\Delta \tau^{(0)}$, Δx is found as

$$\Delta x = - \left[\frac{\partial f(x)}{\partial x} \right]^{-1} f(x^{(0)}) \Delta \tau^{(0)} \quad (7.75)$$

Provided that the inverse exists Starting with $x = x^{(0)}$ and $\tau = 1$, the variables are updated by

$$\begin{aligned} \tau &= \tau - \Delta \tau^{(0)} \\ x &= x + \Delta x \end{aligned} \quad (7.76)$$

and a new Δx is computed from (7.75). This process continues until $\tau = 0$, and at that point $x^{(1)} = x$ is the new solution.

To improve $x^{(1)}$, one may repeat the computations with the new initial vector $f(x^{(1)})$ and with possibly larger value of $\Delta\tau^{(1)}$, as illustrated in Figure 35. Note that as $\Delta\tau(i) \rightarrow 1$ this algorithm reduces to the Newton-Raphson process (Figure 36) in which the increments are computed [59] as,

$$\Delta x_k = - \left[\frac{\partial f}{\partial x} \right]_k^{-1} f(x_k) \quad (7.77)$$

and solution is corrected as

$$x_{k+1} = x_k + \Delta x_k \quad (7.78)$$

Note that, in the finite iteration algorithm, the solution is approached in small steps (i. e., $\Delta\tau \ll 1$) and corrected in small steps. Consequently, it is not so sensitive to the convergence problems as the Newton-Raphson process.

TRIMMING WITH AN AUTOPILOT

Figure 37 shows a trimming process by an autopilot. During the nonlinear simulation of aircraft, the error signal, (i. e., the difference between actual and desired trajectory variable) is used in a simple autopilot to generate a control input. If the gains are properly chosen, $e(t)$ can be maintained reasonably small while obtaining trim profile. The controller equation used for dive and pull-up is in the form:

$$\begin{aligned} \delta_s(t_{k+1}) = & \delta_s(t_k) + K_\gamma [\gamma_o - \gamma(t_k)] + K_{\dot{\gamma}} \dot{\gamma}(t_k) \\ & + K_q [q_o - q(t_k)] + K_{\dot{q}} \dot{q}(t_k) \end{aligned} \quad (7.79)$$

This equation is implemented as subroutine PILOT in ADAPS.

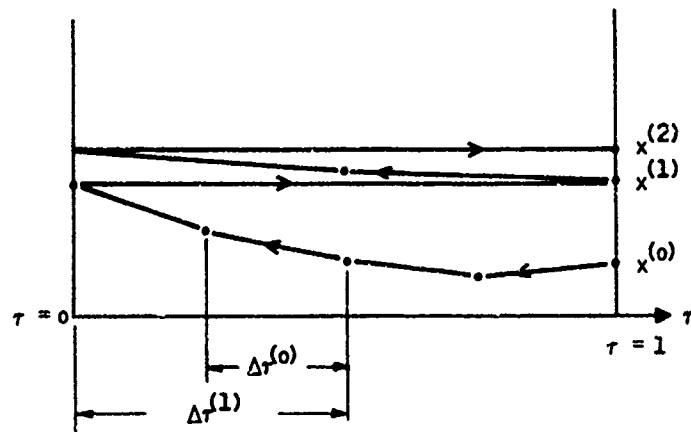


Figure 35. Finite Iteration Algorithm

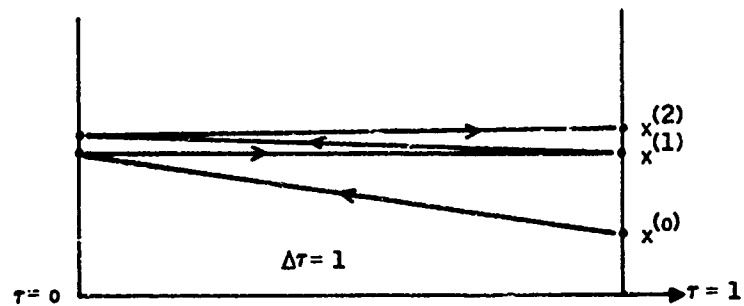


Figure 36. Newton-Raphson Process

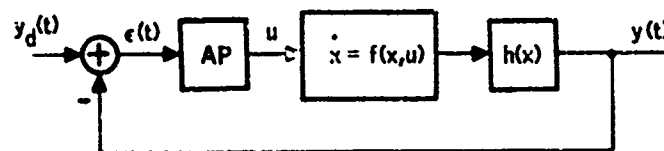


Figure 37. Trim by Autopilot

SECTION VIII

DEVELOPMENT OF A PERFORMANCE MEASURE FOR OPTIMAL WEAPON DELIVERY CONTROLLER DESIGN

In this section, a methodology is developed for determining weighting matrices for optimal weapon delivery controller design. Half probability area, HPA, is chosen as a measure of weapon delivery performance, and the effects of flight control parameters, airframe dynamics, measurement errors, and gust disturbances are related to this measure by using the over-all system model.

HPA is the area of a circle centered at the mean impact point with 0.5 hit probability. CEP is its radius (see Figure 45). For normal distributions with small cross correlations, this area can be closely approximated in terms of the impact covariance matrix of the bomb.

For this reason, performance analysis of a weapon delivery process can be reduced to linear covariance analysis. In the following, a model is developed for determining the initial perturbation state of bomb, and propagating the release point errors to impact. Next the expression for the HPA performance measure is developed and its approximation in terms of quadratic cost is given. The analysis is implemented as subprogram PERK which propagates the release errors to impact.

DEVELOPMENT OF THE INITIAL STATE OF BOMB

The statistical description of the perturbation state of bomb just after release is needed to propagate release-point errors to impact.

The state of bomb and the state of aircraft which carries the bomb are related to each other by a nonlinear algebraic equation

$$x_b = h_b (x, E_b, \Delta r_b) \quad (8.1)$$

where

x = state of aircraft

E_b = bomb orientation matrix (transformation from aircraft to bomb axes)

Δr_b = bomb position vector

The perturbation state of the bomb at $t = t_r$ for fixed E_b and Δr_b is given by

$$\delta x_b(t_r) = H_b \delta x(t_r) \quad (8.2)$$

where

$$H_b = \left. \frac{\partial h_b}{\partial x} \right|_{t_r} \quad (8.3)$$

In this work it will be assumed that

$$H_b = I \quad (8.4)$$

(i.e., the bomb is at the cg of the aircraft and oriented parallel to the aircraft axes). However, for completeness, the bomb station geometry will be given briefly in what follows.

Nominal State of Bomb at Release

The twelve components of the state of the plant undergo a jump at the release time (Figure 38). This is due to changing the plants, namely the transition of dynamics from the aircraft to the weapon and adding ejection velocities.

$$x_p \rightarrow x_b$$

To compute the nominal state of the bomb at release from the nominal state of the airplane, the bomb station geometry is considered.

It is assumed that the mass center O_b of bomb is located by a vector Δr_b from the mass center O of the aircraft (Figure 39). It is further assumed that ψ_b , θ_b are fixed azimuth and elevation angles from aircraft to bomb axes.

Then, as developed later in this section, the nominal state of the bomb at release is obtained as follows (see Figure 38):

• Transition of the Linear Velocity State -

$$x_1(t_{r+}) = E_b(\theta_b, \psi_b) \{ E'_s(t_r) x_{1s}(t_r) + W \Delta r \} \quad (8.5)$$

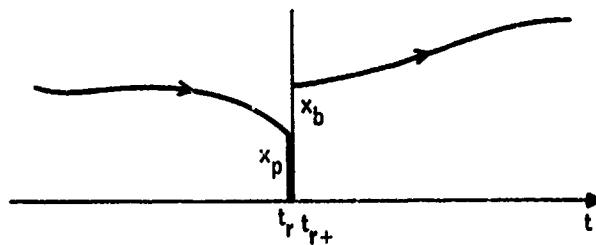


Figure 38. Discrete Nonlinear Transition of the State at Release

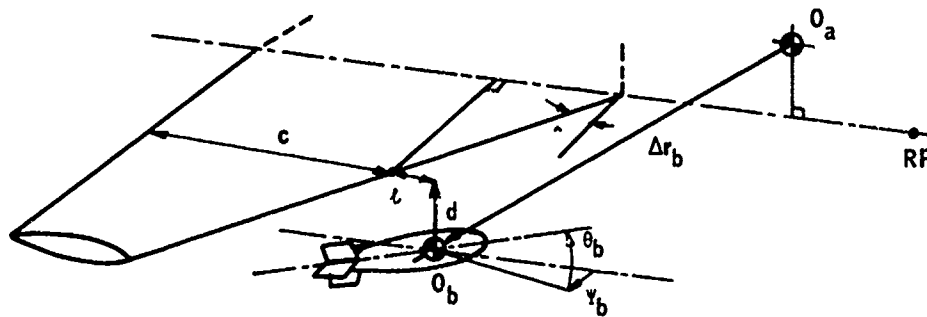


Figure 39. Bomb Station Geometry

where

$$x_{1s}(t_{r+}) = \text{col}(u_s, v_s, v_e)$$

$$u_s = \sqrt{u_a^2 + w_a^2}$$

$$v_s = v_a$$

$$v_e = \text{ejection velocity}$$

$$E_s = \text{transformation from aircraft body to stability axes}$$

$$E_b = \text{transformation from aircraft body axes to bomb body axes}$$

- Transition of the Angular Velocity State -

$$x_2(t_{r+}) = E_b(\theta_b, \psi_b) x_2(t_r) \quad (8.6)$$

- Transition of the Attitude State -

- (a) Transformation matrix from earth to bomb:

$$E(t_{r+}) = F_J(\theta_b, \psi_b) E(t_r) \quad (8.7)$$

- (b) Corresponding attitudes (Section III)

$$\theta(t_{r+})$$

$$\phi(t_{r+})$$

$$\psi(t_{r+})$$

- (c) Corresponding quaternions (Section III)

$$\lambda_0(t_{r+})$$

$$\lambda_1(t_{r+})$$

$$\lambda_2(t_{r+})$$

$$\lambda_3(t_{r+})$$

- Transition of the Position State -

$$x_4(t_{r+}) = x_4(t_r) + E'(t_r) \Delta r \quad (8.8)$$

where $\Delta \mathbf{r} = \begin{pmatrix} \Delta x_b \\ \Delta y_b \\ \Delta z_b \end{pmatrix}$ the distance vector from aircraft
cg to bomb cg in aircraft axes

$E(t_r)$ = transformation matrix from earth to aircraft body axes

The set of equations given above defines the nominal state of the bomb at $t = t_r$. The linearization of bomb dynamics at $t = t_r$ utilizes this nominal state.

Perturbation State of Aircraft at Release

To express the perturbation state of the aircraft at release, consider the nominal and perturbed release points represented by $[x(t_r), t_r]$ and $[\tilde{x}(\tilde{t}_r), \tilde{t}_r]$ respectively in Figure 40.

Define the release point error to be

$$\delta \tilde{x}(t_r) = [\tilde{x}(\tilde{t}_r) - x(t_r)] \quad (8.9)$$

with

$$\delta t_r = \tilde{t} - t_r \quad (8.10)$$

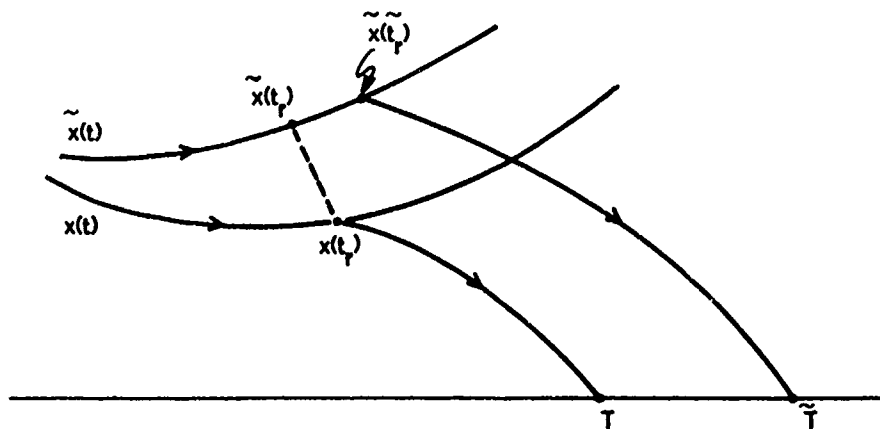


Figure 40. Linearization About the Nominal Release Point $[x(t_r), t_r]$

and

$$\delta x(t_r) = \tilde{x}(t_r) - x(t_r) \quad (8.11)$$

Let

$$\dot{\tilde{x}} = f(\tilde{x}, \tilde{u}) \quad (8.12)$$

be the equation of the evolution of \tilde{x} (i.e., perturbed state of the aircraft).

Then along the perturbed trajectory

$$\tilde{x}(\tilde{t}_r) = \tilde{x}(t_r) + \int_{t_r}^{\tilde{t}_r} f(\tilde{x}, \tilde{u}) dt \quad (8.13)$$

Making use of (8.11) and expanding the integrand into Taylor Series about the nominal yields

$$\tilde{x}(\tilde{t}_r) = [x(t_r) + \delta x(t_r)] + \int_{t_r}^{\tilde{t}_r} f(x, u) dt + \text{h.o.t.} \quad (8.14)$$

Using (8.10) and assuming small δt_r , it follows from (8.14) that

$$[\tilde{x}(\tilde{t}_r) - x(t_r)] = \delta x(t_r) + f(x(t_r), u(t_r))\delta t_r + \dots \quad (8.15)$$

Therefore the perturbation state of the aircraft at release in terms of terminal perturbation state and terminal time error is given by

$$\delta \tilde{x}(t_r) = \delta x(t_r) + f(x(t_r), u(t_r))\delta t_r \quad (8.16)$$

From (8.16) the mean error vector and the covariance matrix of the error can readily be obtained:

$$\overline{\delta \tilde{x}(t_r)} = \overline{\delta x(t_r)} + f(x(t_r), u(t_r))\overline{\delta t_r} \quad (8.17)$$

$$\tilde{X}(t_r) = X(t_r) + f_r E\{\delta t_r^2\} f_r' \quad (8.18)$$

Here f_r denotes the derivative of the aircraft state vector evaluated at the nominal release point $(x(t_r), t_r)$.

Equations (8.17) and (8.18) show that the statistics of δt_r (i.e., $E\{\delta t_r\}$, $E\{\delta t_r^2\}$) must be known to compute release point error statistics.

The release time error δt_r consists of two components: (a) timing error δt_d due to delays in the release mechanism, and (b) timing error δt_r in computing the release time.

For closed-loop fire control algorithms in which release time continuously depend upon the current state, the release time perturbation δt_r is a deterministic function of the state at the nominal release time t_r . That is

$$t_r = h[x(t)] \quad t \leq t_r \quad (8.19)$$

For small perturbations in state, Equation (8.19) yields

$$\delta t_r = \eta' \delta x(t_r) \quad (8.20)$$

where

$$\eta = \left. \frac{\partial h}{\partial x} \right|_{t_r} \quad (8.21)$$

Equation (8.20) is the linearized model of the release computer. If instead of δx , its estimate is available, then

$$\delta t_r = \eta' [\delta \hat{x}(t_r) + \epsilon(t_r)] \quad (8.22)$$

where $\epsilon(t_r)$ is the error in the state estimation, and $\delta \hat{x}(t_r)$ is the optimal estimate of $\delta x(t)$.

Thus, (8.16) and (8.22) define the release-point error in terms of the perturbations about the release point.

Perturbation State of Bomb at Release

The transition from the aircraft perturbation state to the bomb perturbation state is accomplished using equation (8.2). The nonsingular matrix H_b is obtained from the linearization of (8.5)-(8.8) at nominal release point $[x(t_r), t_r]$. Substituting (8.16) into (8.2) yields the perturbation state of the bomb at release:

$$\delta \tilde{x}_b(t_r) = H_b \{ \delta x(t_r) + f[x(t_r), u(t_r)] \delta t_r \} \quad (8.23)$$

As indicated before, in this work $H_b = I$ will be utilized.

Perturbation State Transition During Release Transient

Modeling of the state transition during the release transient phase (Figure 41) is outside the scope of this work. A detailed model is currently being developed in [9,10].

Since it is difficult to predict the bomb aerodynamics (i.e., aerodynamic forces acting on bomb) in the region of wing, the state transition during this phase is taken into account in a simplified manner by introducing an additive release transient error ξ_r with known statistics. (Ejection velocity is included in ξ_r .)

$$\tilde{\delta x}_b(t_{r+}) = \tilde{\delta x}_b(t_r) + H_r \xi_r \quad (8.24)$$

where H_r is the release transient input matrix. Thus, perturbation state of bomb just after release is given by

$$\tilde{\delta x}_b(t_{r+}) = H_b [\delta x(t_r) + f_r \delta t_r] + H_r \xi_r$$

Figure 42 shows its structure.

Statistical description of perturbation state of bomb at release, (mean and covariance), are given respectively as

$$\overline{\delta x_{bo}} = H_b [\overline{\delta x_r} + f_r \overline{\delta t_r}] + H_r \overline{\xi_r} \quad (8.25)$$

$$X_{bo} = H_b [X_r + f_r f_r' \overline{\delta t_r^2}] H_b' + H_r \Sigma_r H_r' \quad (8.26)$$

where X_r and Σ_r denote the covariance matrices of δx_r and ξ_r respectively.

In these equations $\overline{\delta x_r}$ and X_r are obtained by using the linear equations of the aircraft together with the deterministic and stochastic inputs (i.e., mean wind and gust).

The estimate of $\overline{\delta t_r}$ and $\overline{\delta t_r^2}$ involves basically, determining: (a) the contribution of the release computer and (b) the contribution of uncorrected delays in release mechanism.

The estimate of $\overline{\xi_r}$ and Σ_r involves the knowledge of ejection velocity, its uncertainties as well as transient effects. In this work they are considered to be arbitrary input parameters.

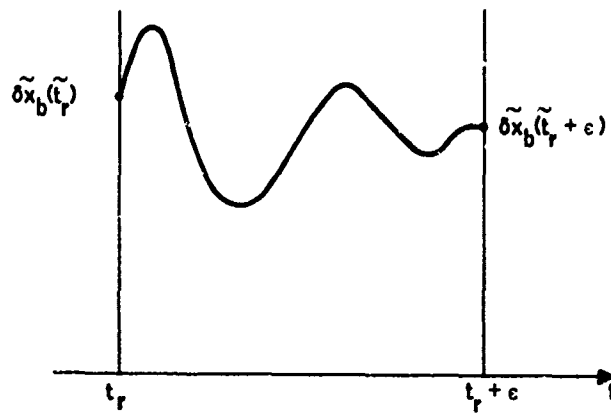


Figure 41. Weapon State Transition During Release Transient Phase

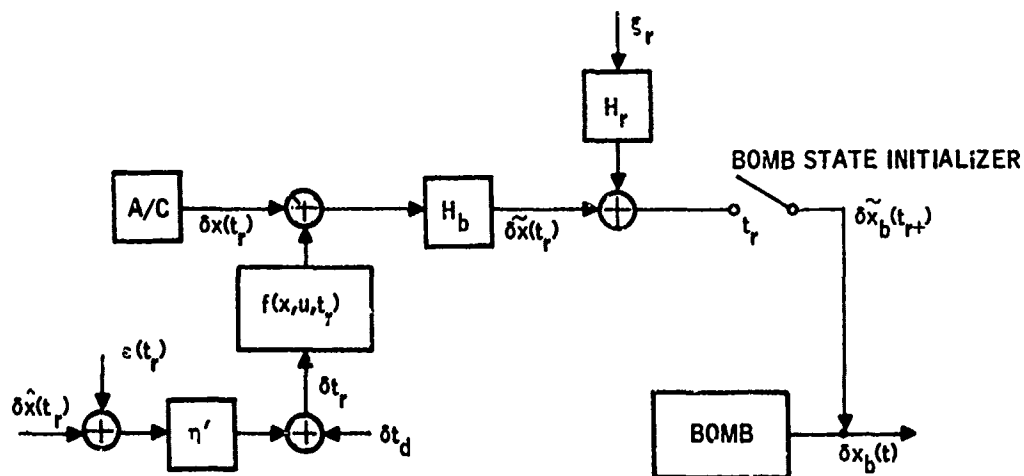


Figure 42. Structure of Perturbation State of Bomb Just After Release

Perturbation State of Bomb at Impact Planes

Consider the nominal and perturbed impact points represented by $[x(t_f), t_f]$ and $[\tilde{x}(t_f), \tilde{t}_f]$ respectively (Figure 43).

Analogous to (8.16) the impact error can be written as

$$\delta \tilde{x}(t_f) = \delta x(t_f) + f[x(t_f), u(t_f)] \delta t_f \quad (8.27)$$

where f is the derivative of the nonlinear bomb dynamics. In (8.27) δt_f is computed using horizontal or vertical impact planes. Horizontal impact occurs when the end point of the perturb trajectory lies in the xy plane ($\delta h = 0$). Similarly vertical impact occurs when the end point lies in the yh plane, ($\delta x_e = 0$).

These take place when

$$\delta t_{fh} = - \frac{\delta h(t_f)}{\dot{h}(t_f)} \quad \delta t_{fv} = - \frac{\delta x_e(t_f)}{\dot{x}_e(t_f)} \quad (8.28)$$

Substituting (8.28) into (8.27) yields the horizontal and vertical impact errors in terms of the nominal impact error:

$$\begin{aligned} \delta \tilde{x}_h(t_f) &= H_h \delta x(t_f) \\ \delta \tilde{x}_v(t_f) &= H_v \delta x(t_f) \end{aligned} \quad (8.29)$$

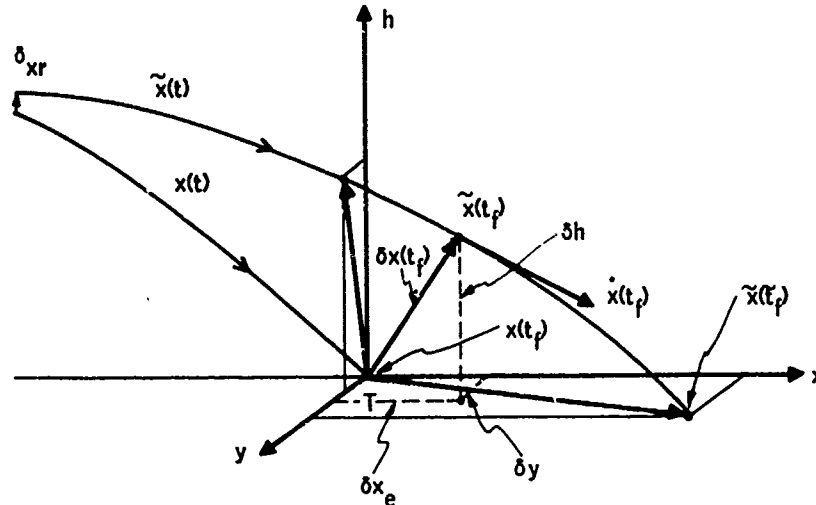


Figure 43. Linearization About the Nominal Impact Point $[x(t_f), t_f]$

where

$$H_h = \left[I - \frac{f(t_f)c'_h}{c'_h f(t_f)} \right] \quad (8.30)$$

$$H_v = \left[I - \frac{f(t_f)c'_{x_e}}{c'_{x_e} f(t_f)} \right]$$

where c_h and c_{x_e} are vectors which pick up h and x_e components out of full state vector x .

From (8.29) the mean error and the mean square error matrix can readily be obtained

$$\begin{aligned} \overline{\delta x_h(t_f)} &= H_h \overline{\delta x(t_f)} \\ \tilde{X}_h(t_f) &= H_h X(t_f) H_h' \end{aligned} \quad (8.31)$$

(Similar expressions apply to the vertical impact errors.)

DEVELOPMENT OF STATISTICAL PERFORMANCE MEASURE FOR WEAPON DELIVERY PROCESSES

For a linear system driven by a Gaussian white noise, the mean and the covariance of the state are described respectively by

$$\dot{\bar{x}} = F\bar{x} + G_1\bar{u} + G_2\bar{w} \quad (8.32)$$

$$\bar{y} = H\bar{x} \quad (8.33)$$

and

$$\tilde{X} = F\tilde{X} + \tilde{X}F' + G_1\tilde{U}G_1' + G_2\tilde{W}G_2' \quad (8.34)$$

$$\tilde{Y} = H\tilde{X}H' \quad (8.35)$$

where

$$\bar{x} = E\{x\}, \bar{u} = E\{u\}, \bar{w} = E\{w\}, \bar{y} = E\{y\}, \quad (8.36)$$

$$\tilde{X} = E\{(x-\bar{x})(x-\bar{x})'\}, \tilde{U} = E\{(u-\bar{u})(u-\bar{u})'\}, \tilde{Y} = E\{(y-\bar{y})(y-\bar{y})'\} \text{ and}$$

$$\tilde{W} = E\{ww'\}$$

Since the process is linear the state turns out to be Gaussian also. For this reason, the mean and the covariance (i.e., first and second moments) completely determine the statistical behavior of the state, and the output. The probability density function of the state vector x of size $n \times 1$ is given [47] by

$$f(x, t) = \frac{1}{\sqrt{(2\pi)^n \det \tilde{X}(t)}} e^{-\frac{1}{2} (x - \bar{x})' \tilde{X}^{-1}(t) (x - \bar{x})} \quad (8.36a)$$

The loci of constant probability densities at each time instant are families of concentric quadratic surfaces centered at \bar{x} and are described by

$$(x - \bar{x})' \tilde{X}^{-1}(t) (x - \bar{x}) = c \quad (8.36b)$$

The density is maximum at its center, and it equals

$$f(\bar{x}, t) = \frac{1}{\sqrt{(2\pi)^n \det \tilde{X}(t)}} \quad (8.36c)$$

For weapon delivery performance, the distribution of x_4 (i.e., position coordinates) are needed for computing the probability of an event described by $\{x_4 \in D\}$. In general the probability density function of x_4 in subspace R^3 , (i.e., marginal density) is obtained by integrating the joint density f_x :

$$f_{x_4}(x_4) = \int_{-\infty}^{+\infty} \int_{-\infty}^{+\infty} \int_{-\infty}^{+\infty} f_x(x_1, x_2, x_3, x_4) dx_1 dx_2 dx_3 \quad (8.36d)$$

However, for the case treated here this integral can be eliminated since the output is linear function of state and is therefore, normal (i.e., Gaussian). It follows that x_4 has a mean and covariance given respectively by

$$\bar{x}_4 = H\bar{x} \quad (8.37a)$$

$$\tilde{X}_4 = H\tilde{X}H' \quad (8.37b)$$

where H is a matrix of size $3 \times n$ which selects the position coordinates from the full state vector x of size $n \times 1$. Thus its density is described as

$$f_{x_4}(x_4) = \frac{1}{\sqrt{(2\pi)^3 \det \tilde{X}_4}} e^{-\frac{1}{2} (x_4 - \bar{x}_4)' \tilde{X}_4^{-1} (x_4 - \bar{x}_4)} \quad (8.38)$$

This shows that when components x_i are jointly normal, they are also marginally normal.

Now, consider a region D in R^3 , and an event described by

$$\{x_4 \in D\} \quad (8.39)$$

The probability of occurrence of this event is

$$P\{x_4 \in D\} = \int_D f_{x_4}(x_4, t) dx dy dh \quad (8.40)$$

where the integration extends over the region D .

Region D may be a cube or a ball. For weapon delivery performance against a specific target of dimensions $a \times b \times c$, hit probability P_H given by (8.40) is used with

$$D: = -\frac{a}{2} \leq x \leq \frac{a}{2}, -\frac{b}{2} \leq y \leq \frac{b}{2}, -\frac{c}{2} \leq z \leq \frac{c}{2} \quad (8.41)$$

If the shape of target is not specified, n -dimensional ball ($n = 1, 2, 3$) centered at the mean is used most often for region D . The probability that the weapon is within this ball at time t is also given by (8.40) with integration extending over the ball:

$$D: (x-\bar{x})^2 + (y-\bar{y})^2 + (h-\bar{h})^2 \leq (R)^2 \quad (8.41a)$$

The radius R for which $P = \frac{1}{2}$ is referred to as the "spherical probable error" and is denoted by SEP or SPE.

When the region D is circular, the radius of its boundary is referred to as CEP or CPE. (These are confusing names attached to a radius.)

Figure 44 demonstrates the evolution of the spherical region D as a function of time.

In air-to-air weapon delivery, SEP can be used to measure the delivery performance. For air-to-ground delivery, a simpler measure, CEP can be used effectively.

For horizontal targets, CEP_H is obtained from

$$\int_{D_H} f_{x,y}(x,y) dx dy = \frac{1}{2} \quad (8.42)$$

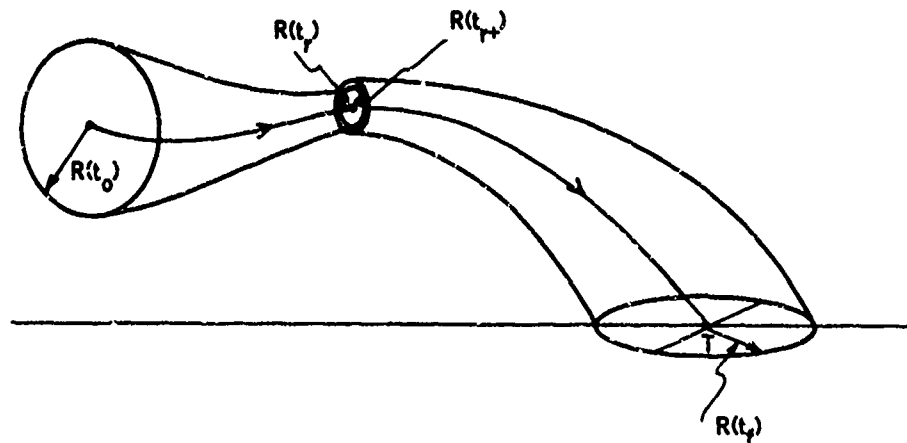


Figure 44. Evolution of the Region D

where the integration extends over the circular region defined by

$$D_H: (x-\bar{x})^2 + (y-\bar{y})^2 \leq (CEP_H)^2 \quad (8.43)$$

Similarly for vertical targets, CEP_V is obtained from

$$\int_{D_V} f_{yh}(x, h) dy dh = \frac{1}{2} \quad (8.44)$$

where the integration extends over the circular region defined by

$$D_V: (y-\bar{y})^2 + (h-\bar{h})^2 \leq (CEP_V)^2 \quad (8.45)$$

Regions D_H and D_V are illustrated in Figure 45.

Range error probable (REP), deflection error probable (DEP), and elevation error probable (EEP), are defined respectively as

$$\int_{D_R} f_x(x) dx = \frac{1}{2}, \quad D_R: |x-\bar{x}| \leq REP \quad (8.46)$$

$$\int_{D_D} f_y(y) dy = \frac{1}{2}, \quad D_D: |y-\bar{y}| \leq DEP \quad (8.47)$$

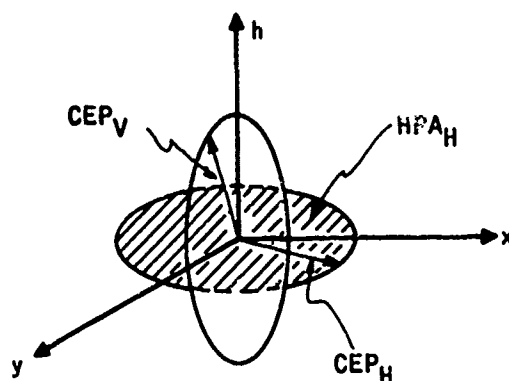


Figure 45. Regions for Horizontal and Vertical CEP Evaluations

and

$$\int_{D_H} f_h(h) dh = \frac{1}{2}, D_H: |h - \bar{h}| \leq EEP \quad (8.48)$$

Table III shows the terminology associated with the radius of the half probability ball for one-, two- and three-dimensional balls.

Table III. Terminology for the Radius of Half Probability Ball

Dimension of Ball (n)	Symbol for the Radius of Half Probability Ball	Name for the Radius of Half Probability Ball
3	SEP	Spherical Error Probable
2	CEP, (CEP _H , CEP _V)	Circular Error Probable (horizontal, vertical)
1	LEP, (REP, DEP, EEP)	Linear Error Probable (range, deflection, elevation)

In general, the integrals given by (8.40), (8.41a) and (8.43) cannot be evaluated analytically. The results from a computer solution for the case where x and y are independent stochastic processes is given in [44].

In [45, 46], CEP is expressed as

$$\text{CEP} = Q(\rho) \sigma_i \quad (8.49)$$

and this dependence is exhibited as shown in Figure 46, where $Q(\rho)$ is referred to as the CEP parameter and is a function of the ratio

$$0 \leq \rho = \frac{\sigma_j}{\sigma_i} \leq 1 \quad (8.50)$$

and σ_i greater of $\{\sigma_x, \sigma_y\}$, $\sigma_j = \text{smaller of } \{\sigma_x, \sigma_y\}$, and σ_x, σ_y are the cross-range and down-range variances, respectively.

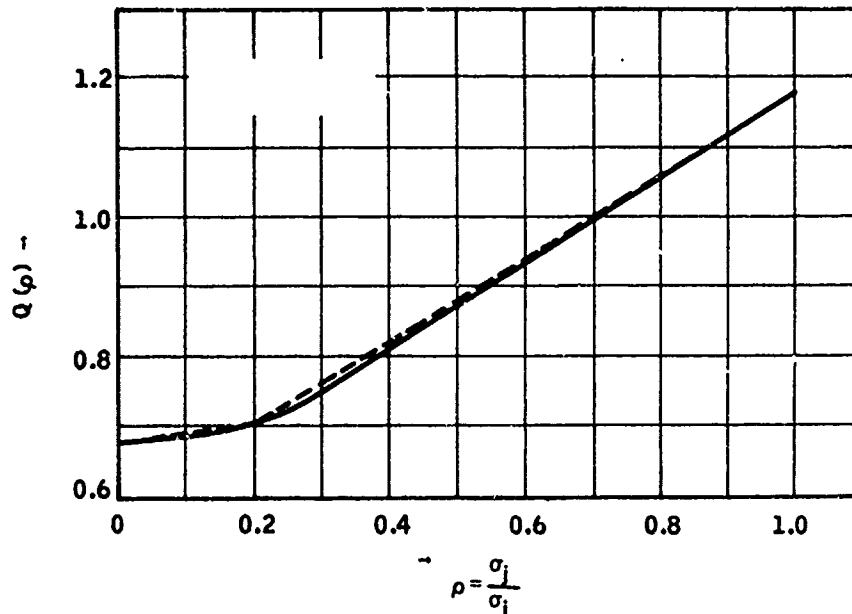


Figure 46. CEP Parameter versus Standard Deviation Ratio

Now, we shall introduce a modified performance measure, "Half-Probability-Area (HPA)" defined as

$$\text{HPA} \triangleq (\pi) (\text{CEP})^2 \quad (8.51)$$

and relate this to the quadratic measure described by

$$J = \text{tr} \{HX(t)H^T\} \quad (8.52)$$

where tr is the trace operator and H is the output matrix which selects and weighs appropriate elements (i. e., σ_x^2 , σ_y^2 , σ_h^2) of the covariance matrix. To be specific, we wish to find weighting parameters α and β such that the quadratic cost given by

$$J = (\pi) (\alpha) [1 + (\rho^2 \beta)] \alpha_i^2 \quad (8.53)$$

where

$$\rho = \frac{\sigma_j}{\sigma_i} \leq 1 \quad (8.54)$$

is a good approximation to HPA.

For a close fit, α and β should be functions of ρ . For simplicity, we shall assume constant α and β in the interval

$$0 \leq \rho \leq 1.$$

Approximation to Weapon Delivery Performance

The CEP parameter $Q(\rho)$ is approximated by two line segments

$$Q(\rho) \cong k_i (1 + \mu_i \rho) \quad i = 1, 2 \quad (8.55)$$

for the ranges $0 \leq \rho \leq 0.2$ and $0.2 \leq \rho \leq 1.0$, as shown by dotted lines in Figure 46. The values for k_i and μ_i are:

<u>$0 \leq \rho \leq 0.2$</u>	<u>$0.2 \leq \rho \leq 1.0$</u>
$k_1 = 0.6744$	$k_2 = 0.585$
$\mu_1 = 0.24$	$\mu_2 = 1$

Figure 47 shows the HPA parameter $\hat{Q}(\rho)$ defined by

$$\hat{Q}(\rho) \triangleq [Q(\rho)]^2 \quad (8.56)$$

Also shown is an almost-bound to $\hat{Q}(\rho)$ defined by

$$\tilde{Q}(\rho) = \alpha [1 + \beta \rho^2] \quad (8.57)$$

$$\text{where } \alpha = \frac{1}{2}, \text{ and } \beta = 2. \quad (8.58)$$

With these values, the quadratic cost becomes

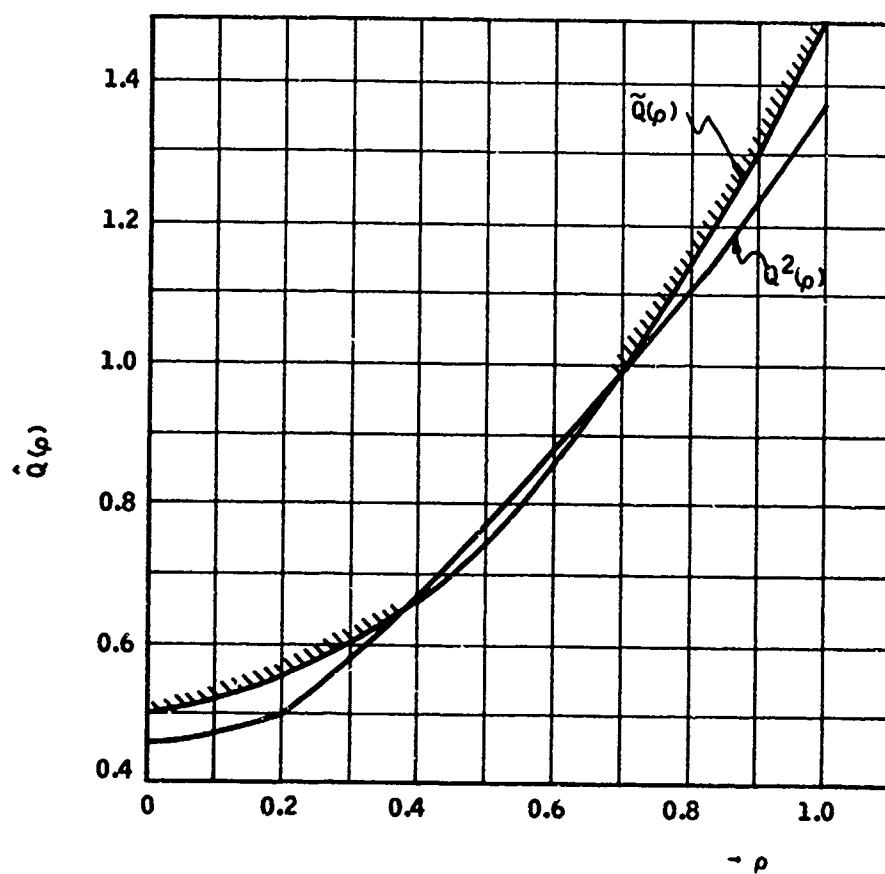


Figure 47. HPA Parameter versus Standard Deviation Ratio

$$J = \frac{\pi}{2} [1 + 2\rho^2] \sigma_i^2 \quad (8.59)$$

or

$$J = q_i \sigma_i^2 + q_j \sigma_j^2, \sigma_i > \sigma_j \quad (8.60)$$

where

$$q_i = \frac{\pi}{2}, \text{ and } q_j = \pi \quad (8.61)$$

Finally from this quadratic cost (i. e. half-probability area) approximate CEP can be computed as

$$\widetilde{\text{CEP}} = \sqrt{\frac{J}{\pi}} \quad (8.62)$$

Development of Design Performance Index

It was shown in the previous section that for normal distributions with small cross-correlations, the half-probability area HPA is almost bounded by the quadratic cost:

$$J = q_i \sigma_i^2 + q_j \sigma_j^2 \quad (8.63)$$

where

σ_x = downrange standard deviation

σ_y = crossrange standard deviation

σ_i = greater of $\{\sigma_x, \sigma_y\}$

σ_j = smaller of $\{\sigma_x, \sigma_y\}$

$q_i = \pi/2$

$q_j = \pi$

Equation (8.63) can be written in terms of the covariance matrix as

$$\text{HPA} \cong \text{tr} \{HX(t)H'\} = \text{tr} \{X(t)Q_0\} \quad (8.64)$$

where

$$Q_o = H'H = \begin{bmatrix} 0 & 0 & 0 \\ 0 & q_x & 0 \\ 0 & 0 & q_y & 0 \\ 0 & 0 & 0 \end{bmatrix} \quad (8.65)$$

which selects and weighs the downrange and cross-range variances out of the full weapon state covariance matrix.

DEVELOPMENT OF THE RELEASE ERROR PROPAGATION PROCESS

In this subsection the bomb covariance, CEP measures and the equivalent quadratic weighting matrices are developed in terms of the release state covariance, using the results of the initial-state development and the wind model. This analysis is implemented in subprogram PERK.

Figure 48 shows the vector state diagram of a linearized bomb model with a wind driver.

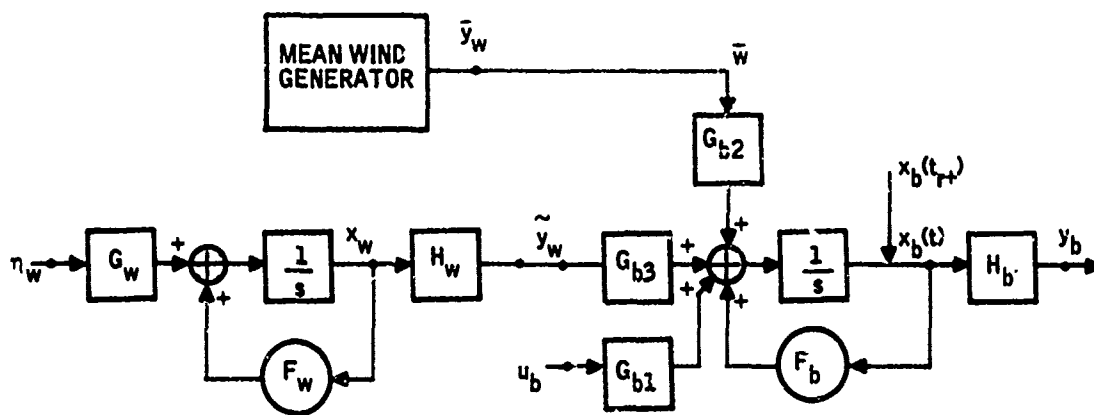


Figure 48. Bomb Dynamics with a Wind Driver

The state equations are given by

$$\dot{x}_w = F_w x_w + G_w \eta_w \quad (8.66)$$

$$\tilde{y}_w = H_w x_w \quad (8.67)$$

and

$$\dot{x}_b = F_b x_b + G_{b1} u_b + G_{b2} \bar{y}_w + G_{b3} \tilde{y}_w \quad (8.68)$$

$$y_b = H_b x_b \quad (8.69)$$

letting $x = \text{col}(x_b | x_w)$ and substituting (8.67) into (8.68) yields

$$\dot{x} = Fx + G_1 u_b + G_2 \bar{y}_w + G_3 \eta \quad (8.70)$$

$$y_b = Hx \quad (8.71)$$

where

$$F = \left[\begin{array}{c|c} F_b & (G_{b3})(H_w) \\ \hline 0 & F_w \end{array} \right], \quad G_1 = \left(\begin{array}{c} G_{b1} \\ 0 \end{array} \right), \quad G_2 = \left(\begin{array}{c} G_{b2} \\ 0 \end{array} \right), \quad G_3 = \left(\begin{array}{c} 0 \\ G_w \end{array} \right)$$

$$\text{and } H = (H_b | 0) \quad (8.72)$$

From (8.70), (8.71) and (8.72) the mean and covariance responses are determined using (8.32) through (8.35).

For convenience, the total state covariance matrix is separated into two components, (a) homogeneous and (b) forced. This enables one to evaluate an impact covariance matrix for arbitrary initial covariance matrices. Obviously, if only one initial covariance matrix is considered it is better to integrate (8.34) with nonzero initial conditions to obtain total covariance.

It should be noted that forced covariance component is obtained by integrating the differential equation (8.34) rather than evaluating the integral

$$X_f(t) = \int_{t_r}^t \phi(t, s) W(s) \phi'(t, s) ds \quad (8.73)$$

Where $\phi(t, s)$ is the state transition matrix.

The total covariance at any time instant is given by

$$X(t) = \phi(t, t_r) X_{r+} \phi'(t, t_r) + X_f(t), \quad t \geq t_r \quad (8.74)$$

As was shown previously, the quadratic approximation to HPA(t) is given by

$$\text{HPA}(t) \cong J(t) = \text{tr} \{X(t) Q_0\} \quad (8.75)$$

Substituting (8.74) into (8.75) yields

$$J(t) = \text{tr} \{(\phi X_{r+} \phi' + X_f(t)) Q_0\}$$

or

$$J(t) = \text{tr} \{(X_{r+}) (\phi' Q_0 \phi) + (X_f(t)) (Q_0)\} \quad (8.76)$$

The matrix defined by

$$Q \triangleq \phi' Q_0 \phi \quad (8.77)$$

where $\phi = \phi(t, t_r)$ will be referred to as the state covariance weighting matrix or the propagation matrix.

The approximate radius $\widetilde{\text{CEP}}(t)$ is computed from

$$\widetilde{\text{CEP}}(t) = \sqrt{\frac{J(t)}{\pi}}, \quad t \leq t_f \quad (8.78)$$

As developed previously, the non-zero elements of Q_0 ; (q_x, q_y) or (q_y, q_h) are determined from (σ_x^2, σ_y^2) or (σ_y^2, σ_h^2) by a simple test. Namely, in each pair, greater variance is associated with weighting value $\pi/2$ and smaller with π .

At impact it follows from (8.74) that

$$X(t_f) = \phi(t_f, t_r) X_{r+} \phi'(t_f, t_r) + X_f(t_f) \quad (8.79)$$

Substituting this into (8.31) yields the impact covariance

$$\widetilde{X}_h(t_f) = H_h [\phi X_{r+} \phi' + X_f] H_h' \quad (8.80)$$

where ϕ and X_f are matrices evaluated at impact time t_f .

HPA at impact is then given by

$$\text{HPA}(t_f) \cong J(t_f) = \text{tr} \{\widetilde{X}(t_f) Q_0\} \quad (8.81)$$

Substituting (8.80) into (8.81) yields

$$J(t_f) = \text{tr} \{ H_h (\phi X_{r+} \phi' + X_f) H_h' Q_o \} \quad (8.82)$$

or

$$J(t_f) = \text{tr} \{ X_{r+} [\phi' \tilde{Q}_o \phi] + X_f \tilde{Q}_o \} \quad (8.83)$$

where

$$\tilde{Q}_o = H_h' Q_o H_h \quad (8.84)$$

is called the "impact propagation matrix".

DEVELOPMENT OF THE VARIANCE CONTRIBUTION MATRIX

The variance contribution matrix, V , displays the effects of the perturbation state vector components onto the position error variances at impact. Its brief development is presented in what follows:

The diagonal elements of $X(t_f)$, can be expressed as:

$$x(t_f) = \psi_1 x_{1r+} + \psi_2 x_{2r+} + \dots + \psi_n x_{nr+} + x_f(t_f) \quad (8.85)$$

where

x_{1r+}, \dots, x_{nr+} are the column vectors of the X_{r+} matrix, that is

$$X_{r+} = \begin{bmatrix} x_{1r+} & | & x_{2r+} & | & \dots & | & x_{nr+} \end{bmatrix} \quad (8.86)$$

and $x(t_f)$, $x_f(t_f)$ are vectors made up from the diagonal elements of $X(t_f)$ and $X_f(t_f)$ matrices, respectively. The elements of the weighting matrices ψ_j and covariance vectors x_{jr+} for $j = 1, \dots, n$ are given by

$$\psi_j = \begin{bmatrix} \phi_{1j}\phi_{11} & \phi_{1j}\phi_{12} & \dots & \phi_{1j}\phi_{1n} \\ \phi_{2j}\phi_{21} & \phi_{2j}\phi_{22} & \dots & \phi_{2j}\phi_{2n} \\ \cdot & & & \cdot \\ \cdot & & & \cdot \\ \cdot & & & \cdot \\ \phi_{nj}\phi_{n1} & \phi_{nj}\phi_{n2} & \dots & \phi_{nj}\phi_{nn} \end{bmatrix}, \quad x_{jr+} = E \begin{bmatrix} \delta x_1 \delta x_j \\ \delta x_2 \delta x_j \\ \cdot \\ \cdot \\ \delta x_j \delta x_j \\ \cdot \\ \delta x_n \delta x_j \end{bmatrix} + \quad (8.87)$$

In the decomposition represented by (8.85), each vector in the sum, e. g.,

$$\psi_j x_{j_{r+}}$$

is identified as the contribution of the perturbation state component δx_j to the impact covariance vector. Note that in this identification the cross-variance terms are also included as given by (8.87).

If position error covariance, $(\sigma_{xe}^2, \sigma_{ye}^2, \sigma_h^2)$ about the nominal impact point are of interest only, the three rows of (8.85) need be evaluated.

The matrix which is made up of the vectors $\psi_j x_{j_{r+}}$ is called the variance contribution matrix:

$$V = \left[\psi_1 x_{1_{r+}} \mid \dots \mid \psi_j x_{j_{r+}} \mid \dots \mid \psi_n x_{n_{r+}} \right]$$

Each row sum of this matrix gives a component of the error variance about the nominal impact point. Dividing the elements in each row by their row sum gives a normalized variance contribution matrix, in which each element shows the relative contributions of state components onto position error variances about the impact.

The normalized variance contribution matrix is used to identify those state components which are important contributors to impact error variances.

SECTION IX

DEVELOPMENT OF A METHOD FOR NONSTATIONARY OPTIMAL WEAPON DELIVERY CONTROLLER DESIGN

In this section, a method is presented for designing an optimal non-stationary perturbation controller for the precision weapon delivery processes [47, 11].

The optimization problem considered here involves direct minimization of the CEP. Strictly speaking, CEP is the radius of a 0.5 probability circle centered at the mean impact point of a bomb at target. For normal distributions with small cross correlations, the area of this circle can be closely approximated in terms of the impact covariance matrix.

As shown in Section VIII, about a nominal trajectory, the impact covariance matrix can be expressed in terms of the state covariance matrix at bomb release. By this process, controller optimization for the precision bomb delivery is reduced to optimization with a terminal time performance index, in which the state deviations at the nominal release time are penalized by a weighting matrix which depends upon the nominal bomb trajectory sensitivities.

In the following, the statement and solution of the optimization problem corresponding to continuous time-varying processes are given first for completeness. Then the discretized model and its solution are developed. This solution is implemented as a program called DISCOP.

STATEMENT OF THE PROBLEM

Given the linear system

$$\begin{aligned}\dot{x}(t) &= F(t)x(t) + G_1(t)u(t) + G_2(t)\bar{v}_w(t) + G_3(t)\eta_1(t) \\ r(t) &= H_1(t)x(t) + D_1(t)u(t) + D_2(t)\bar{v}_w(t) \\ \eta(t) &= H_2(t)x(t) + \eta_2(t)\end{aligned}\tag{9.1}$$

where $u(t)$ is a deterministic (known) time function, the inputs $\eta_1(t)$ and $\eta_2(t)$ are independent white noise processes

$$\begin{aligned}E \{ \eta_1(t) \eta_1(t_1)' \} &= W_1(t) \delta(t-t_1) \\ E \{ \eta_2(t) \eta_2(t_1)' \} &= W_2(t) \delta(t-t_1) \\ E \{ \eta_1(t) \eta_2(t_1)' \} &= W_3(t) \delta(t-t_1)\end{aligned}\tag{9.2}$$

and the initial state mean and covariance are known

$$E \{x(o)\} = \bar{x}(o) \quad (9.3)$$

$$E \{(x(o) - \bar{x}(o)) (x(o) - \bar{x}(o))'\} = X(o)$$

Find the linear control functional of past and present measured outputs $m(t)$

$$u(t) = L(t, m[o, t]), \quad (9.4)$$

that minimizes the quadratic J

$$J = \text{tr} [Q(T)S(T) + V(T)R'(T) + \int_0^T (Q(t)S(t) + V(t)R(t))dt] \quad (9.5)$$

where $R(t)$ is the mean response matrix defined by

$$R(t) = \bar{r}(t)\bar{r}(t)' \quad (9.6)$$

$S(t)$ is the response covariance matrix defined by

$$S(t) = E \{(r(t) - \bar{r}(t)) (r(t) - \bar{r}(t))'\} \quad (9.7)$$

and $Q(t)$, $V(t)$ are the weighting matrices, assumed to be symmetric and non-negative definite for all $t \in [0, T]$, the matrices $D_1'Q(t)D_1$ and $D_1'V(t)D_1$ are assumed positive definite for all $t \in [0, T]$

$$Q(T)D_1(T) = V(T)D_1(T) = 0 \quad (9.8)$$

SOLUTION OF THE PROBLEM

In this subsection, solution to the optimization problem posed above is given in terms of differential equation formulation. It is shown [46] that the minimization of J can be separated into a deterministic problem and a stochastic problem, and that the solutions of these two problems can be combined to form the optimum controller.

Minimization of the Continuous Model

The J minimization problem can be divided into the control of the mean response $\bar{r}(t)$ and the control of the response deviation from the mean, $r(t) - \bar{r}(t)$.

By defining \bar{x} , \bar{m} , \bar{u} to be mean responses, and

$$\begin{aligned} x^* &= x - \bar{x} \\ m^* &= m - \bar{m} \\ u^* &= u - \bar{u} \\ r^* &= r - \bar{r}, \end{aligned} \tag{9.9}$$

to be deviations from the mean, there results the two sets of system equations

$$\begin{aligned} \dot{\bar{x}}(t) &= F(t)\bar{x}(t) + G_1(t)\bar{u}(t) + G_3(t)\bar{v}_w(t) \\ \bar{r}(t) &= H_1(t)\bar{x}(t) + D_1(t)\bar{u}(t) + D_2(t)\bar{v}_w(t) \\ \bar{m}(t) &= H_1(t)\bar{x}(t) \end{aligned} \tag{9.10}$$

and

$$\begin{aligned} \dot{x}^*(t) &= F(t)x^*(t) + G_1(t)u^*(t) + G_2(t)\eta_1(t) \\ r^*(t) &= H_1(t)x^*(t) + D_1(t)u^*(t) \\ m^*(t) &= H_2(t)x^*(t) + \eta_2(t) \end{aligned} \tag{9.11}$$

The cost J becomes

$$\begin{aligned} J &= [\bar{r}(T)' V(T) \bar{r}(T) + \int_0^T \bar{r}(t)' V(t) \bar{r}(t) dt] \\ &\quad + E[r^*(T)' Q(T) r^*(T) + \int_0^T r^*(t)' Q(t) r^*(t) dt] \end{aligned} \tag{9.12}$$

Since u^* in (9.11) does not in any way affect \bar{r} in (9.10), and \bar{u} in (9.10) does not in any way affect r^* in (9.11), the controls \bar{u} and u^* may be designed separately to minimize their respective contributions to J .

Development of the Optimal Mean Control Law -- The mean control \bar{u} will be determined first [47]. Given (9.10), the functional \bar{J} where

$$\bar{J} = \bar{r}(T)' V(T) \bar{r}(T) + \int_0^T \bar{r}(t)' V(t) \bar{r}(t) dt \tag{9.13}$$

is to be minimized.

Examination of the responses whose terminal behavior is to be controlled reveals that the equations for those responses do not contain the final control $u(T)$. It can therefore be assumed that the contribution of $\bar{u}(T)$ to $\bar{x}(T)' V(T) \bar{x}(T)$ is zero. That is

$$V(T) D_1(T) = 0 \quad (9.14)$$

The above problem is then a Bolza variational problem. By writing

$$\bar{J} = G_1 \bar{x}(T) + \int_0^T G_2(\bar{x}(t), \bar{u}(t), t) dt \quad (9.15)$$

The Hamiltonian for the problem is

$$H = G_2 + \lambda' \dot{\bar{x}} \quad (9.16)$$

and the control $\bar{u}(t)$ is defined by the equations

$$\begin{aligned} \frac{\partial H}{\partial \bar{u}(t)} &= 0 \\ \frac{\partial H}{\partial \bar{x}(t)} &= -\dot{\lambda}'(t) \end{aligned} \quad (9.17)$$

$$\frac{\partial G_1}{\partial \bar{x}(T)} = \lambda'(T)$$

With

$$\begin{aligned} H = [H_1(t) \bar{x}(t) + D_1(t) \bar{u}(t) + D_2(t) \bar{v}_w(t)]' V(t) [H_1(t) \bar{x}(t) + D_1(t) \bar{u}(t) \\ + D_2(t) \bar{v}_w(t)] + \lambda(t)' [F(t) \bar{x}(t) + G_1(t) \bar{u}(t) + G_3(t) \bar{v}_w(t)] \end{aligned} \quad (9.18)$$

then

$$\begin{aligned} \frac{\partial H}{\partial \bar{x}(t)} &= -\dot{\lambda}'(t) = F(t)' \lambda(t) + 2H_1(t)' V(t) [H_1(t) \bar{x}(t) + D_1(t) \bar{u}(t) \\ &\quad + D_2(t) \bar{v}_w(t)] \end{aligned}$$

$$\frac{\partial G_1}{\partial \bar{x}(T)} = \lambda'(T) = 2H_1(T)' V(T) [H_1(T)' \bar{x}(T) + D_2(T) \bar{v}_w(T)]$$

$$\frac{\partial H}{\partial \bar{u}(t)} = 0 = G_1(t)' \lambda(t) + 2D_1(t)' V(t) [H_1(t) \bar{x}(t) + D_1(t) \bar{u}(t) + D_2(t) \bar{v}_w(t)]$$

By making the additional substitutions [49]

$$\begin{aligned}\lambda(t) &= 2[P_V(t)\bar{x}(t) + g(t)] \\ \bar{u}(t) &= K_V(t)\bar{x}(t) + f_V(t),\end{aligned}\tag{9.19}$$

and assuming that the inverse $[D_1(t)' V(t) D_1(t)]^{-1}$ exists for $t \in [0, T]$, there results the familiar Riccati end conditions:

$$\begin{aligned}P_V(T) &= H_1(T)' V(T) H_1(T) \\ g(T) &= H_1(T)' V(T) D_2(T) \bar{v}_w(T),\end{aligned}\tag{9.20}$$

the backwards differential equations

$$\begin{aligned}-\dot{P}_V(t) &= F(t)' P_V(t) + P_V(t) F(t) + H_1(t)' V(t) H_1(t) \\ &\quad - [P_V(t) G_1(t) + H_1(t)' V(t) D_1(t)] [D_1(t)' V(t) D_1(t)]^{-1} \\ &\quad \cdot [G_1(t)' P_V(t) + D_1(t)' V(t) H_1(t)] \\ -\dot{g}(t) &= F(t)' g(t) + [P_V(t) G_2(t) + H_1(t)' V(t) D_2(t)] \bar{v}_w(t) \\ &\quad - [P_V(t) G_1(t) + H_1(t)' V(t) D_1(t)] [D_1(t)' V(t) D_1(t)]^{-1} \\ &\quad \cdot [G_1(t)' g(t) + D_1(t)' V(t) D_2(t) \bar{v}_w(t)],\end{aligned}\tag{9.21}$$

and the controller equations

$$\begin{aligned}K_V(t) &= - [D_1(t)' V(t) D_1(t)]^{-1} [G_1(t)' P_V(t) + D_1(t)' V(t) H_1(t)] \\ f_V(t) &= - [D_1(t)' V(t) D_1(t)]^{-1} [G_1(t)' g(t) + D_1(t)' V(t) D_2(t) \bar{v}_w(t)]\end{aligned}\tag{9.22}$$

These three sets of equations completely define the mean control $\bar{u}(t)$.

Development of the Optimal Stochastic Control Law -- Given the system equations, (9.11), it remains to find the controller

$$u^*(t) = L(t, m^*[0, t])$$

minimizing the quadratic J^*

$$J^* = E[r^*(T)' Q(T) r^*(T) + \int_0^T r^*(t)' Q(t) r^*(t) dt]\tag{9.23}$$

Let $x^*(t)$ be the sum

$$x^*(t) = x_1(t) + \tilde{x}(t)\tag{9.24}$$

where $x_1(t)$ is defined by the orthogonality condition

$$E[x_1(t)' \tilde{x}(t) | m^*(o, t), u^*(o, t)] = 0 \quad (9.25)$$

This is the expected value of the product $x_1(t)' \tilde{x}(t)$, given present and past output measurements $m^*(t)$ and past inputs $u^*(t)$. Let $K_Q(t)$ be the set of gains defined by (9.20), (9.21) and (9.22) when $V(t)$ is replaced by $Q(t)$. It is asserted that the controller $L(t, m^*(o, t))$ minimizing the quadratic J^* is

$$u^*(t) = K_Q(t)x_1(t)$$

That is, the optimum control input $u^*(t)$ is the product of the state estimate $x_1(t)$ defined by the orthogonality relation (9.25), and the gains $K_Q(t)$ defined by the Riccati equations, (9.20), (9.21) and (9.22).

This assertion is known as the "separability property". It permits separating the J^* minimization into two problems:

- The determination of the state estimate $x_1(t)$
- The determination of the controller gains $K_Q(t)$ that would be employed if the entire state $x^*(t)$ could be measured, and the system inputs $u_1(t)$ were known

State Estimation

The state estimate $x_1(t)$ must be generated to complete the controller design. The problem of generating state estimates $x_1(t)$ satisfying the orthogonality (9.25) has been completely resolved [50]. It is well known that the orthogonality condition (9.25) implies that, with $x^*(t)$ Gaussian, $x_1(t)$ is the conditional expectation

$$x_1(t) = E \{x^*(t) | m^*[o, t], u^*[o, t]\} \quad (9.26)$$

It can be shown that $x_1(t)$ could be generated by a linear transformation of $m^*(t)$ and $u^*(t)$

$$x_1(t) = L^* \{t, m^*[o, t], u[o, t]\} \quad (9.27)$$

In [49], the appropriate linear transformation L^* is developed for the case where

$$\text{rank}[W_2(t)] = \text{dim}[m^*(t)]$$

$$W_3(t) = 0$$

That is, every nonzero linear transformation of $m^*(t)$ contains white noise, and the inputs $u_1(t)u_2(t)$ in (9.11) are uncorrelated. In [52], the latter restriction ($W_3 = 0$) is removed.

Assuming the system is of the form (9.11), $x_1(t)$ could be generated from the linear system

$$\dot{x}_1(t) = [F(t) - L(t)H_2(t)]x_1(t) + L(t)m^*(t) \quad (9.28)$$

where $L(t)$ is the solution of the forward Riccati equation

$$\begin{aligned} \dot{P}_\eta(t) = & F(t)P_\eta(t) + P_\eta(t)F(t)' + G_2(t)W_1(t)G_2(t)' \\ & - [(P_\eta(t)H_2(t)' + G_1(t)W_3(t)] \\ & (W_2(t))^{-1} [W_3(t)'G_1(t) + H_2(t)P_\eta(t)] \end{aligned} \quad (9.29)$$

Then the estimator gains are given by

$$L(t) = [P_\eta(t)H_2(t)' + G_1(t)W_3(t)] W_2(t)^{-1}$$

where the initial conditions are

$$P_\eta(0) = \text{cov}[x^*(0)x^*(0)'] \quad (9.30)$$

Combining the Results

The optimum control is the sum of the deterministic and stochastic solutions

$$\begin{aligned} u(t) &= \bar{u}(t) + u^*(t) \\ &= K_V(t)\bar{x}(t) + f_V(t) + K_Q(t)x_1(t) \\ &= K_Q(t)[x_1(t) + \bar{x}(t)] + [K_V(t) - K_Q(t)]\bar{x}(t) + f_V(t) \\ &= K_Q(t)\hat{x}(t) + f(t) \end{aligned} \quad (9.31)$$

where $f(t)$ is the deterministic input given by

$$f(t) = [K_V(t) - K_Q(t)]\bar{x}(t) + f_V(t) \quad (9.32)$$

and $\hat{x}(t)$ is the conditional state expectation

$$\hat{x}(t) = x_1(t) + \bar{x}(t) = E[x(t)|m(0, t), u(0, t), \bar{v}_w(0, t)] \quad (9.33)$$

where \bar{x} and x_1 are generated by (9.10) and (9.28), respectively. Figure 49 shows the decomposition of the state vector.

DISCRETIZATION OF THE CONTINUOUS PROCESS AND OPTIMIZATION OF THE DISCRETIZED SYSTEM

For computational purposes the differential equations given above are approximated by difference equations. Also, the performance integral is



Figure 49. Decomposition of the State Vector

approximated by a sum. This is called the discretization of the continuous optimization problem. The discretized model is derived with two constraints in mind. Both of the constraints are based on the desire to achieve reasonable computation time for the optimization program and at the same time maintain a sufficiently accurate approximation of the differential equations, and the performance integral.

The simplest discretization is based on the rectangular rule. This approximation would be sufficiently accurate if Δt is chosen sufficiently small. But the computation time is inversely proportional to Δt ; to reduce computation time it is desirable to choose Δt to be as large as possible.

In the following discretization based on the rectangular rule is presented first. Then a more accurate discretization with matrix exponentials is given. The latter discretization can be used for the high-frequency dynamics of the overall system, and former for the low-frequency dynamics of the system.

Discretization by Rectangular Rule

Choose a large, finite integer N and let

$$\Delta t = \frac{T}{N}. \quad (9.34)$$

Define

$$\begin{aligned} A(n) &= I + \Delta t F(n\Delta t) & H_1(n) &= H_1(n\Delta t) & W_1(n) &= W_1(n\Delta t) \\ B_1(n) &= \Delta t G_1(n\Delta t) & D_1(n) &= D_1(n\Delta t) & W_2(n) &= W_2(n\Delta t) \\ B_2(n) &= \Delta t G_2(n\Delta t) & D_2(n) &= D_2(n\Delta t) & W_3(n) &= W_3(n\Delta t) \\ B_3(n) &= \Delta t G_3(n\Delta t) & H_2(n) &= H_2(n\Delta t) & Q(n) &= Q(n\Delta t) \\ \bar{v}_w(n) &= \bar{v}_w(n\Delta t) & & & V(n) &= V(n\Delta t). \end{aligned} \quad (9.35)$$

The above quadratic problem may then be restated: given the linear system

$$\begin{aligned}x(n+1) &= A(n)x(n) + B_1(n)u(n) + B_2(n)\bar{v}_w(n) + B_3(n)\eta_1(n) \\r(n) &= H_1(n)x(n) + D_1(n)u(n) + D_2(n)\bar{v}_w(n) \\m(n) &= H_2(n)x(n) + \eta_2(n)\end{aligned}\tag{9.36}$$

where

$$\begin{aligned}E\{\eta_1(i)\eta_1(j)'\} &= (\Delta t)^{-1} W_1(i)\delta_{ij} \\E\{\eta_2(i)\eta_2(j)'\} &= (\Delta t)^{-1} W_2(i)\delta_{ij} \\E\{\eta_1(i)\eta_2(j)'\} &= (\Delta t)^{-1} W_3(i)\delta_{ij}\end{aligned}\tag{9.37}$$

$$\begin{aligned}\delta_{ii} &= 1, \delta_{ij} = 0 \text{ if } i \neq j \\E\{x(o)\} &= \bar{x}(o) \\E\{(x(o) - \bar{x}(o))(x(o) - \bar{x}(o))'\} &= X(o)\end{aligned}\tag{9.38}$$

find the linear functional (i. e., piecewise constant controller)

$$u(n) = \sum_{i=0}^N L(n, i) m(i)\tag{9.39}$$

that minimizes the quadratic J

$$J = \text{tr} \left[Q(N)S(N) + V(N)R(N) + \sum_{n=0}^{N-1} \Delta t (Q(n)S(n) + V(n)R(n)) \right].\tag{9.40}$$

where

$$\begin{aligned}R(n) &= \bar{r}(n)\bar{r}(n)' \\S(n) &= E\{(r(n) - \bar{r}(n))(r(n) - \bar{r}(n))'\}\end{aligned}\tag{9.41}$$

It is assumed that $Q(n)$ and $V(n)$ are symmetric and nonnegative definite for $n=0, \dots, N$, and $D_1(n)'Q(n)D_1(n)$ and $D_1(n)'V(n)D_1(n)$ are positive definite for $n < N$, and

$$Q(N)D_1(N) = V(N)D_1(N) = 0\tag{9.42}$$

Discretization by a Matrix Exponential

For a given value of Δt a more accurate approximation to equation (9.1) is given by the sample-data form

$$x[(k+1)\Delta t] = e^{\Delta t F(k\Delta t)} \left\{ x(k\Delta t) + F^{-1}(k\Delta t) [I - e^{-\Delta t F(k\Delta t)}] \cdot [G_1(k\Delta t)u(k\Delta t) + G_2(k\Delta t)\eta(k\Delta t) + G_3(k\Delta t)\bar{v}_w(k\Delta t)] \right\} \quad (9.43)$$

This form is approximate in that the various coefficients are not constant over the Δt intervals, and the control $u(t)$ is continuous and not piecewise constant. The major disadvantage of equation (9.43) is that almost all of the elements of the coefficient matrices are nonzero, whereas in equation (9.35) the majority of the elements of the coefficient matrices are zero. Computation time increases at least linearly with the number of nonzero elements [11].

SOLUTION FOR THE DISCRETIZED MODEL WITH PIECEWISE CONSTANT CONTROLLER

The solution to the above discretized model problem follows that presented for the continuous-model problem. The optimum control is of the form

$$u(n) = K_Q(n)\hat{x}(n) + [K_V(n) - K_Q(n)]\bar{x}(n) + f_V(n) \quad (9.44)$$

where $\bar{x}(n)$ is the a priori mean state

$$\bar{x}(n) = E \{x(n)\} \quad (9.45)$$

and $\hat{x}(n)$ is the conditional estimate

$$\hat{x}(n) = E \{x(n) | m(0), \dots, m(n), u(0), \dots, u(n-1), \bar{v}_w(0), \dots, \bar{v}_w(n-1)\}$$

The gains $K_V(n)$ and input $f_V(n)$ are the solutions of the backwards difference equations

$$P_V(N) = H_1(N)' V(N) H_1(N) \quad (9.46)$$

$$g(N) = H_1(N)' V(N) D_2(N) \bar{v}_w(N) \quad (9.47)$$

$$K_V(n) = - [B_1(n)' P_{V(n+1)} B_1(n) + \Delta t D_1(n)' V(n) D_1(n)]^{-1} \cdot [B_1(n)' P_{V(n+1)} A(n) + \Delta t D_1(n)' V(n) H_1(n)] \quad (9.48)$$

$$f_V(n) = - [B_1(n)' P_{V(n+1)} B_1(n) + \Delta t D_1(n)' V(n) D_1(n)]^{-1} \cdot \{B_1(n)' [g(n+1) + P_{V(n+1)} B_2(n) \bar{v}_w(n)] + \Delta t D_1(n)' V(n) D_2(n) \bar{v}_w(n)\} \quad (9.49)$$

$$P_V(n) = [A(n) + B_1(n) K_V(n)]' P_{V(n+1)} [A(n) + B_1(n) K_V(n)] + \Delta t [H_1(n) + D_1(n) K_V(n)]' V(n) [H_1(n) + D_1(n) K_V(n)] \quad (9.50)$$

$$g(n) = [A(n) + B_1(n)K_V(n)]' [g(n+1) + P_V(n+1)(B_1(n)f(n) + B_2(n)\bar{v}_w(n))] \\ + \Delta t [H_1(n) + D_1(n)K_V(n)]' V(n) [D_2(n)\bar{v}_w(n) + D_1(n)f(n)] \quad (9.51)$$

The gain $K_Q(n)$ is the solution to the above where $V(n)$ is replaced by $Q(n)$. A major simplification which has been found satisfactory in [46] and [11] is setting

$$V(n) = Q(n), \quad 0 \leq n \leq N \quad (9.51a)$$

This is assumed in the implementation of the above equations.

The solution to the state estimation problem is

$$\hat{x}(n) = x_1(n) + \bar{x}(n) \quad (9.52)$$

$$x_1(n+1) = (A(n) - \Delta t L(n) H_2(n)) x_1(n) + \Delta t L(n) m(n) \quad (9.53)$$

where $L(n)$ is obtained from the solution of the forward Riccati equation

$$P_\eta(0) = X(0) \\ \Delta t L(n) = \left[A(n) P_\eta(n) H_2(n)' + B_3(n) \frac{W_3(n)}{\Delta t} \right] \\ \left[H_2(n) P_\eta(n) H_2(n)' + \frac{W_2(n)}{\Delta t} \right]^{-1} \quad (9.54)$$

$$P_\eta(n+1) = A(n) P_\eta(n) A(n)' + B_3(n) \frac{W_1(n)}{\Delta t} B_3(n)' \\ - \Delta t L(n) \left[H_2(n) P_\eta(n) H_2(n)' + \frac{W_2(n)}{\Delta t} \right] L(n)' \Delta t. \quad (9.55)$$

The matrix $P_\eta(n)$ in these equations is the covariance matrix of the estimation error $\tilde{x}(n)$ given by

$$\tilde{x}(n) = x(n) - \hat{x}(n) \quad (9.56)$$

$$P_\eta(n) = \text{cov}\{\tilde{x}(n)\tilde{x}(n)'\} \\ = E\{\tilde{x}(n)\tilde{x}(n)'\} \quad (9.57)$$

The estimation error $\tilde{x}(n)$ has zero mean

$$E\{\tilde{x}(n)\} = 0 \quad (9.58)$$

A state covariance transition matrix can be derived from this property.

With

$$\begin{aligned} \mathbf{x}(n+1) &= \mathbf{A}(n)\mathbf{x}(n) + \mathbf{B}_1(n)\mathbf{K}(n)\hat{\mathbf{x}}(n) + \mathbf{B}_2(n)\bar{\mathbf{v}}_w(n) + \mathbf{B}_3(n)\eta_1(n) \\ \bar{\mathbf{x}}(n+1) &= \mathbf{A}(n)\bar{\mathbf{x}}(n) + \mathbf{B}_1(n)\mathbf{K}(n)\bar{\mathbf{x}}(n) + \mathbf{B}_2(n)\bar{\mathbf{v}}_w(n) \end{aligned} \quad (9.59)$$

then

$$\begin{aligned} \mathbf{x}(n+1) - \bar{\mathbf{x}}(n+1) &= \mathbf{A}(n)(\mathbf{x}(n) - \bar{\mathbf{x}}(n)) + \mathbf{B}_1(n)\mathbf{K}(n)(\hat{\mathbf{x}}(n) - \bar{\mathbf{x}}(n)) + \mathbf{B}_3(n)\eta_1(n) \\ &= (\mathbf{A}(n) + \mathbf{B}_1(n)\mathbf{K}(n))(\hat{\mathbf{x}}(n) - \bar{\mathbf{x}}(n)) + \mathbf{A}(n)\tilde{\mathbf{x}}(n) \\ &\quad + \mathbf{B}_3(n)\eta_1(n) \end{aligned} \quad (9.60)$$

Then

$$\begin{aligned} \text{cov} \{ \mathbf{x}(n+1)\mathbf{x}(n+1)' \} &\stackrel{\Delta}{=} \mathbf{E} \{ (\mathbf{x}(n+1) - \bar{\mathbf{x}}(n+1))(\mathbf{x}(n+1) - \bar{\mathbf{x}}(n+1))' \} \\ &= (\mathbf{A}(n) + \mathbf{B}_1(n)\mathbf{K}(n))\mathbf{E} \{ (\hat{\mathbf{x}}(n) - \bar{\mathbf{x}}(n))(\hat{\mathbf{x}}(n) - \bar{\mathbf{x}}(n))' \} (\mathbf{A}(n) + \mathbf{B}_1(n)\mathbf{K}(n))' \\ &\quad + (\mathbf{A}(n) + \mathbf{B}_1(n)\mathbf{K}(n))\mathbf{E} \{ (\hat{\mathbf{x}}(n) - \bar{\mathbf{x}}(n))\tilde{\mathbf{x}}(n)' \} \mathbf{A}(n)' \\ &\quad + (\mathbf{A}(n) + \mathbf{B}_1(n)\mathbf{K}(n))\mathbf{E} \{ (\hat{\mathbf{x}}(n) - \bar{\mathbf{x}}(n))\eta_1(n)' \} \mathbf{B}_3(n)' \\ &\quad + \mathbf{A}(n)\mathbf{E} \{ \tilde{\mathbf{x}}(n)(\hat{\mathbf{x}}(n) - \bar{\mathbf{x}}(n))' \} (\mathbf{A}(n) + \mathbf{B}_1(n)\mathbf{K}(n))' \\ &\quad + \mathbf{A}(n)\mathbf{E} \{ \tilde{\mathbf{x}}(n)\tilde{\mathbf{x}}(n)' \} \mathbf{A}(n)' \\ &\quad + \mathbf{A}(n)\mathbf{E} \{ \tilde{\mathbf{x}}(n)\eta_1(n)' \} \mathbf{B}_3(n)' \\ &\quad + \mathbf{B}_3(n)\mathbf{E} \{ \eta_1(n)(\hat{\mathbf{x}}(n) - \bar{\mathbf{x}}(n))' \} (\mathbf{A}(n) + \mathbf{B}_1(n)\mathbf{K}(n))' \\ &\quad + \mathbf{B}_3(n)\mathbf{E} \{ \eta_1(n)\tilde{\mathbf{x}}(n)' \} \mathbf{A}(n)' \\ &\quad + \mathbf{B}_3(n)\mathbf{E} \{ \eta_1(n)\eta_1(n)' \} \mathbf{B}_3(n)' \end{aligned} \quad (9.61)$$

Since $\mathbf{x}(n)$, $\hat{\mathbf{x}}(n)$, and hence $\tilde{\mathbf{x}}(n)$, are functions of past inputs, they are independent of the current (white) input $\eta_1(n)$, and

$$\mathbf{E} \{ (\hat{\mathbf{x}}(n) - \bar{\mathbf{x}}(n))\eta_1(n)' \} = \mathbf{E} \{ \tilde{\mathbf{x}}(n)\eta_1(n)' \} = 0 \quad (9.62)$$

From the above

$$\begin{aligned} \mathbf{E} \{ (\hat{\mathbf{x}}(n) - \bar{\mathbf{x}}(n))\tilde{\mathbf{x}}(n)' \} &= \mathbf{E} \{ \hat{\mathbf{x}}(n)\tilde{\mathbf{x}}(n)' \} - \bar{\mathbf{x}}(n)\mathbf{E} \{ \tilde{\mathbf{x}}(n)' \} \\ &= 0 - 0 = 0 \end{aligned} \quad (9.63)$$

Hence

$$\begin{aligned} \text{cov} \{x(n+1)x(n+1)\}' &= (A(n) + B_1(n)K(n))E \{(\hat{x}(n) - \bar{x}(n))(\hat{x}(n) - \bar{x}(n))'\} \\ &\quad (A(n) + B_1(n)K(n))' + A(n)E \{\tilde{x}(n)\tilde{x}(n)'\} A(n)' + B_3(n)E \{\eta_1(n) \\ &\quad \eta_1(n)'\} B_3(n) \end{aligned} \quad (9.64)$$

With $\hat{x} - \bar{x} = x - \bar{x} - \tilde{x}$, (see Figure 49.)

$$\begin{aligned} E \{(\hat{x}(n) - \bar{x}(n))(\hat{x}(n) - \bar{x}(n))'\} &= E \{(x(n) - \bar{x}(n))(x(n) - \bar{x}(n))'\} \\ &\quad - E \{(x(n) - \bar{x}(n))\tilde{x}(n)'\} - E \{\tilde{x}(n)(x(n) - \bar{x}(n))'\} \\ &\quad + E \{\tilde{x}(n)\tilde{x}(n)'\} \\ &= \text{cov} \{x(n)x(n)'\} - 2E \{\tilde{x}(n)\tilde{x}(n)'\} + E \{\tilde{x}(n)\tilde{x}(n)'\} \end{aligned} \quad (9.65)$$

then

$$\begin{aligned} \text{cov} \{x(n+1)x(n+1)'\} &= [(A(n) + B_1(n)K(n))] \\ &\quad \cdot [\text{cov} \{x(n)x(n)'\} - P_\eta(n)](A(n) + B_1(n)K(n))' \\ &\quad + A(n)P_\eta(n)A(n)' + B_3(n) \frac{W_1(n)}{\Delta t} B_3(n)'. \end{aligned} \quad (9.66)$$

Thus the optimal state covariance matrix

$$X(n) = E \{[x(n) - \bar{x}(n)][x(n) - \bar{x}(n)]'\}$$

satisfies the difference equation

$$\begin{aligned} X(n+1) &= [A(n) + B_1(n)K(n)][X(n) - P_\eta(n)][A(n) + B_1(n)K(n)]' \\ &\quad + A(n)P_\eta(n)A(n)' + (\Delta t)^{-1}B_3(n)W_1(n)B_3(n)' \end{aligned} \quad (9.67)$$

with $X(0) = X_0$.

The response covariance matrix, $S(n) = E \{[r(n) - \bar{r}(n)][r(n) - \bar{r}(n)]'\}$, may be obtained as follows:

$$\begin{aligned} r(n) - \bar{r}(n) &= H_1(n)[x(n) - \bar{x}(n)] + D_1(n)K(n)[\hat{x}(n) - \bar{x}(n)] \\ &= [H_1(n) + D_1(n)K(n)][x(n) - \bar{x}(n)] - D_1(n)K(n)[x(n) - \hat{x}(n)] \end{aligned}$$

$$\begin{aligned}
S(n) &= [H_1(n) + D_1(n)K(n)]X(n)[H_1(n) + D_1(n)K(n)]' \\
&\quad + D_1(n)K(n)P_\eta(n)K'(n)D_1'(n) - [H_1(n) + D_1(n)K(n)] \\
&\quad \cdot E\{[x(n) - \bar{x}(n)][x(n) - \hat{x}(n)]'\} K'(n)D_1'(n) - D_1(n)K(n) \\
&\quad \cdot E\{[x(n) - \hat{x}(n)][x(n) - \bar{x}(n)]'\} [H_1(n) + D_1(n)K(n)]' \\
&= [H_1(n) + D_1(n)K(n)]X(n)[H_1(n) + D_1(n)K(n)]' \\
&\quad + D_1(n)K(n)P_\eta(n)K'(n)D_1'(n) - [H_1(n) + D_1(n)K(n)] \\
&\quad \cdot P_\eta(n)K'(n)D_1'(n) - D_1(n)K(n)P_\eta(n)[H_1(n) + D_1(n)K(n)]'
\end{aligned}$$

Thus the response covariance matrix is given by

$$\begin{aligned}
S(n) &= [H_1(n) + D_1(n)K(n)][X(n) - P_\eta(n)][H_1(n) + D_1(n)K(n)]' \\
&\quad + H_1(n)P_\eta(n)H_1'(n)
\end{aligned} \tag{9.68}$$

For the special case in which it is assumed that the complete state can be measured exactly, $m(n) = x(n)$ and the above results are simplified since $\hat{x}(n) = x(n)$ and $P_\eta(n) = 0$. The mean optimal response vector is obtained by substituting (9.44) into (9.36) and averaging the resulting equation. It is given by

$$\bar{r}(n) = H_1(n)\bar{x}(n) + D_1(n)[K(n)\bar{x}(n) + f(n)] + D_2(n)\bar{v}_w(n) \tag{9.69}$$

where

$$\bar{x}(n+1) = A(n)\bar{x}(n) + B_1[K(n)\bar{x}(n) + f(n)] + B_2(n)\bar{v}_w(n) \tag{9.70}$$

This finishes the discussion on the development of the optimal control and estimation algorithms. These algorithms are implemented as program DISCOP. The discretized dynamics of the overall system is shown in Figure 50.

The gains and performance values obtained from the equations are functions of sampletime Δt . As Δt goes to zero, the values obtained by DISCOP approach to the continuous model solutions.

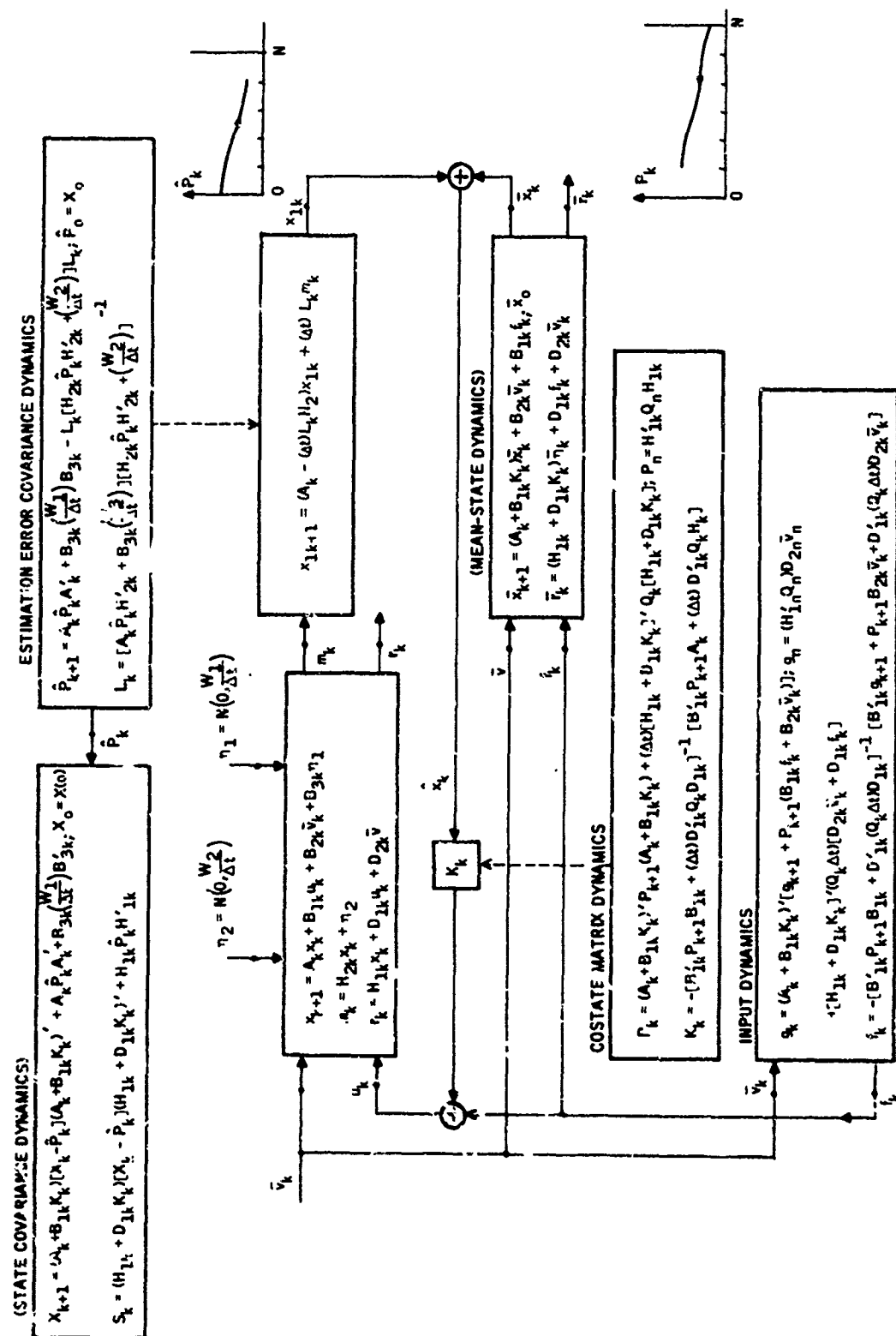


Figure 50. Discretized Dynamics of Overall System

SECTION X

DEVELOPMENT OF A METHOD FOR STATIONARY OPTIMAL CONTROLLER DESIGN

As developed in Section IX, the computation of optimal controllers involves integration of Riccati differential equations backward for the controller gains and forward for the estimator gains together with state covariance differential equations.

If the dynamics are stationary, and constant gains are used, very substantial savings can be achieved by directly computing steady-state solutions of the covariance and Riccati equations [57].

In the following, the development of stationary design equations and the description of algorithms for solving these equations are briefly presented.

DESCRIPTION OF ALGORITHM LYAK

The LYAK is an iterative algorithm for solving either of the following matrix equations for the unknown matrix X given the matrices A and Q

$$XA + A'X + Q = 0 \quad (10.1)$$

$$XA' + AX + Q = 0 \quad (10.2)$$

In what follows the method for solution is briefly stated. Next the convergence criteria is explained.

Method of Solution

The method used to solve the equations is iterative and based on conformal mapping and matrix functions [53, 57]. Given the matrices A and Q where A is a stability matrix (real parts of all eigenvalues of A are negative), let $\psi = (A - \alpha I)^{-1}$ where α is a positive constant $\alpha \geq 1$, define

$$\phi_0 = I + 2\alpha\psi \quad (10.3)$$

$$X_0 = 2\alpha\psi' Q \psi \quad (10.4)$$

then the iterative algorithm is given by the following set of equations:

$$\Delta X_i = \phi_i' X_i \phi_i \quad (10.5)$$

$$X_{i+1} = X_i + \Delta X_i \quad (10.6)$$

$$\phi_{i+1} = \phi_i \phi_i \quad (10.7)$$

Choice of the Parameter α

It is shown in [53] that there is an optimal value for the parameter α (i.e., optimal in the sense that the algorithm will converge in a minimum number of iterations), call it α^* . Calculation of α^* requires solving for the eigenvalues of A. This cannot be considered because it is too expensive computationally. It is also shown in [53], however, that a good suboptimal choice of α , call it $\hat{\alpha}$, is the arithmetic-mean of the eigenvalues of A. Since the sum of the eigenvalues of A is just the trace of A

$$\alpha = |\text{tr}\{A\}|/N \quad (10.8)$$

where tr is the trace operator and N is the order of the matrix A.

Convergence Criteria

The convergence criteria for this algorithm is a ratio test which is performed at the end of each iteration. The absolute value of the ratio $\Delta X_i / X_{i+1}$, for each element in the upper triangle of the two matrices ΔX_i and X_{i+1} , is tested to see if it is less than or equal to some small constant ϵ . (The value of ϵ currently being used is 0.01.) If this test is passed X_{i+1} is accepted as the converged solution. If the test is not passed the iterative process will continue.

DESCRIPTION OF ALGORITHM DIAK

The DIAK is a doubly iterative algorithm for solving the algebraic Riccati equation

$$P\tilde{A} + \tilde{A}'P + PEP + \tilde{Q} = 0 \quad (10.9)$$

where

$$\tilde{A} = (A - EP) \quad (10.10)$$

In the following, first, equivalence relations are developed between (10.9) and the optimization problem posed. Then the method of solution is given.

Stationary Optimization Problem for Controller Gains

Given the time-invariant matrices F, G_1 , G_2 , H, D, Q defining the controlled system

$$\dot{x} = Fx + G_1 u + G_2 \eta_1 \quad (10.11)$$

$$r = Hx + Du \quad (10.12)$$

where r is the vector of controlled responses, u is the control-input vector, and η is white noise

$$E\{\eta_1(t) \eta_1(\tau)'\} = W_1 \delta(t-\tau) \quad (10.13)$$

Let the cost of control be

$$J = E\{r' Q r\} \quad (10.14)$$

where $Q \geq 0$, $D' Q D > 0$, (F, G_1) controllable and (F, H) observable [47].

The problem is to find the gain matrix K such that the controller $u = Kx$ will minimize the cost J .

The covariance equation for this problem is

$$0 = (F + G_1 K)X + X(F + G_1 K)' + G_2 W_1 G_2' \quad (10.15)$$

where

$X = E\{xx'\}$ is the covariance matrix

$R = E\{rr'\} = (H + DK)X(H + DK)'$ is the response covariance matrix (10.16)

The cost is

$$J = \text{tr} \{ (H + DK)' Q (H + DK) X \} \quad (10.17)$$

where tr is the trace operator. Appending the covariance equation to J via the Lagrange multipliers P yields the Hamiltonian

$$|H| = \text{tr} \{ (H + DK)' Q (H + DK) X \} + \text{tr} \{ P [(F + G_1 K)X + X(F + G_1 K)' + G_2 W_1 G_2'] \} \quad (10.18)$$

Taking derivatives

$$\frac{\partial |H|}{\partial P} = 0 = (F + G_1 K)X + X(F + G_1 K)' + G_2 W_1 G_2' \quad (10.19)$$

$$\frac{\partial |H|}{\partial X} = 0 = (F + G_1 K)' P + P(F + G_1 K) + (H + DK)' Q (H + DK) \quad (10.20)$$

$$\frac{\partial |H|}{\partial K} = 0 = \{ D' Q (H + DK) + G_1' P \} X \quad (10.21)$$

The optimal controller K , for this problem, is the solution to the pair of equations (10.20) and (10.21). Solving (10.21) for K results in:

$$K = -(D'QD)^{-1} [G_1'P + D'QH] \quad (10.22)$$

Substituting this into equation (10.20) yields the Riccati equation in P

$$0 = (F - G_1 [D'QD]^{-1} D'QH)'P + P(F - G_1 [D'QD]^{-1} D'QH) - P \{ G_1 [D'QD]^{-1} G_1' \} P + H'QH - H'QD [D'QD]^{-1} D'QH \quad (10.23)$$

Equating matrices in equations (10.23) and (10.9) gives the following relationships:

$$A = (F - G_1 [D'QD]^{-1} D'QH) \quad (10.24)$$

$$E = (G_1 [D'QD]^{-1} G_1') \quad (10.25)$$

$$\bar{Q} = H'QH - H'QD [D'QD]^{-1} D'QH \quad (10.26)$$

Method of Solution

Equation (10.9) is rewritten as

$$P\tilde{A} + \tilde{A}'P + \tilde{Q} = 0 \quad (10.27)$$

where

$$\tilde{A} = (A - EP) \quad (10.28)$$

$$\tilde{Q} = (\bar{Q} + PEP) \quad (10.29)$$

Starting with P_0 such that $\tilde{A} = (A - EP_0)$ is a stability matrix, equation (10.27) is solved by the iterative algorithm LYAK. The solution to (10.27) is substituted into (10.28) and (10.29) and then equation (10.27) is solved again for the updated values of \tilde{A} and \tilde{Q} [54]. This process is continued until two successive solutions to equation (10.27) are the same to a certain number significant figures (i. e., the same convergence test as is used in the algorithm LYAK).

STATIONARY OPTIMIZATION PROBLEM FOR THE ESTIMATOR GAINS

Consider the following time-invariant plant, measurement and estimator equations:

$$\dot{x} = Fx + G_1 u + G_2 \eta_1 \quad (10.30)$$

$$m = H_2 x + \eta_2 \quad (10.31)$$

$$\dot{\hat{x}} = (F - LH_2) \hat{x} + G_1 u + Lm \quad (10.32)$$

where η_1 and η_2 are stationary white noises with

$$E\{\eta_1(t) \eta_1(\tau)'\} = W_1 \delta(t-\tau) \quad (10.33)$$

$$E\{\eta_2(t) \eta_2(\tau)'\} = W_2 \delta(t-\tau) \quad (10.34)$$

$$E\{\eta_1(t) \eta_2(\tau)'\} = W_3 \delta(t-\tau) = 0 \quad (10.35)$$

and L is the estimator gain matrix, (F, G_2) controllable and (F, H_2) observable.

Define the estimation error to be

$$\tilde{x} = x - \hat{x} \quad (10.36)$$

Then the differential equation of the estimation error is obtained from

$$\dot{\tilde{x}} = \dot{x} - \dot{\hat{x}} \quad (10.37)$$

Substituting (10.14) and (10.16) into (10.37) yields

$$\dot{\tilde{x}} = (F - LH_2) \tilde{x} + G_2 \eta_1 - L\eta_2 \quad (10.38)$$

The covariance of the estimation error is given by

$$\dot{P}_\eta = (F - LH_2)P_\eta + P_\eta(F - LH_2)' + LW_2L' + G_2W_1G_2', \quad P_\eta(0) = X(0) \quad (10.39)$$

The minimization of P_η with respect to L yields optimal estimator gain as

$$L = P_\eta H_2' W_2^{-1} \quad (10.40)$$

Substituting (10.40) into (10.39) results in

$$\dot{P}_\eta = (F - P_\eta \dot{I}) P_\eta + P_\eta (F - P_\eta \dot{I})' + P_\eta \dot{I} P_\eta + G_2 W_1 G_2' \quad (10.41)$$

where

$$\dot{I} = H_2' W_2^{-1} H_2 \quad (10.42)$$

is called the "information rate".

The steady-state value of the estimation error covariance is given by

$$\hat{A} P_\eta + P_\eta \hat{A}' + \hat{Q} = 0 \quad (10.43)$$

where

$$\hat{A} = (F - P_\eta \dot{I}) \quad (10.44)$$

$$\hat{Q} = (G_2 W_1 G_2' + P_\eta \dot{I} P_\eta) \quad (10.45)$$

Note that the set of equations (10.43), (10.44) and (10.45) have the same structure (i. e., duals) of the equations (10.27), (10.28) and (10.29). Therefore, the steady-state estimation covariance and the estimator gains are obtained also by using the algorithm DIAK.

THE STEADY-STATE COVARIANCE WITH THE OPTIMAL ESTIMATOR

The covariance of the controlled system with the estimator is obtained from the definition given by (10.36):

$$x = \hat{x} + \tilde{x} \quad (10.46)$$

where

\hat{x} = the state of the estimator dynamics

\tilde{x} = the estimation error

Clearly,

$$X = \hat{X} + P_\eta + Y + Y' \quad (10.47)$$

where

$$X = E\{xx'\}, \hat{X} = E\{\hat{x}\hat{x}'\}, P_\eta = E\{\tilde{x}\tilde{x}'\} \text{ and } Y = E\{\hat{x}\tilde{x}'\}$$

We remark here that for the optimal estimator gains

$$Y = Y' = 0 \quad (10.48)$$

so that (10.47) reduces to

$$X = \hat{X} + P_{\eta} \quad (10.49)$$

Now using the feedback law given by

$$u = -K\hat{x} \quad (10.50)$$

and substituting (10.31) into (10.32) yields

$$\dot{\hat{x}} = (F - G_1 K)\hat{x} + LH_2 \tilde{x} + L\eta_2 \quad (10.51)$$

From (10.51) and (10.38) one obtains

$$\begin{pmatrix} \dot{\hat{x}} \\ \dot{\tilde{x}} \end{pmatrix} = \left[\begin{array}{c|c} (F - G_1 K) & LH_2 \\ \hline 0 & (F - LH_2) \end{array} \right] \begin{pmatrix} \hat{x} \\ \tilde{x} \end{pmatrix} + \begin{bmatrix} L\eta_2 \\ G_2\eta_1 - L\eta_2 \end{bmatrix} \quad (10.52)$$

This yields the following set of differential equations:

$$\dot{\hat{X}} = (F - G_1 K)\hat{X} + \hat{X}(F - G_1 K)' + (LH_2 Y' + YH_2' L') + LW_2 L' \quad (10.53)$$

$$\dot{Y} = (F - G_1 K)Y + Y(F - LH_2)' - L(W_2 L' - H_2 P_{\eta}) \quad (10.54)$$

$$\dot{P}_{\eta} = (F - LH_2)P_{\eta} + P_{\eta}(F - LH_2)' + LW_2 L' + G_2 W_1 G_2' \quad (10.55)$$

The initial conditions are given by

$$\hat{X}(0) = 0 \quad (10.56)$$

$$Y(0) = E\{\hat{x}(0) \tilde{x}'(0)\} = 0 \quad (10.57)$$

$$P_{\eta}(0) = X(0) \quad (10.58)$$

On the account of the optimality the last term in (10.54) vanishes so that with equation (10.57) one concludes that

$$Y(t) \equiv 0 \quad (10.59)$$

Also noting that

$$LW_2L' = P_\eta \dot{I}P_\eta \quad (10.60)$$

equation (10.53) can be written as:

$$\dot{\hat{X}} = (F-G_1K)\hat{X} + \hat{X}(F-G_1K)' + P_\eta \dot{I}P_\eta \quad (10.61)$$

The steady-state value of \hat{X} is obtained from

$$\tilde{A}\hat{X} + \hat{X}\tilde{A}' + \tilde{Q} = 0 \quad (10.62)$$

where

$$\tilde{A} = (F-G_1K) \quad (10.63)$$

$$\tilde{Q} = P_\eta \dot{I}P_\eta \quad (10.64)$$

Once P_η and \hat{X} are found X is obtained from (10.49).

An alternate way of computing X can be developed by writing (10.55) as

$$\dot{P}_\eta = FP_\eta + P_\eta F' - P_\eta \dot{I}P_\eta + G_2W_1G_2' \quad (10.65)$$

This can be written as

$$\begin{aligned} \dot{P}_\eta = & (F-G_1K)P_\eta + P_\eta(F-G_1K)' + G_1KP_\eta + P_\eta K'G_1' \\ & - P_\eta \dot{I}P_\eta + G_2W_1G_2' \end{aligned} \quad (10.66)$$

Summing (10.61) and (10.66) yields

$$\dot{\hat{X}} = (F-G_1K)\hat{X} + \hat{X}(F-G_1K)' + G_2W_1G_2' + [G_1KP_\eta + P_\eta K'G_1'] \quad (10.67)$$

Equation (10.67) indicates that the estimator error covariance acts as a driver in the state covariance differential equation. The steady-state value of X is computed from

$$\tilde{A}X + X\tilde{A}' + \tilde{Q} = 0 \quad (10.68)$$

where

$$\tilde{A} = (F - G_1 K) \quad (10.69)$$

$$\tilde{Q} = (G_2 W_1 G_2' + G_1 K P_\eta + P_\eta K' G_1') \quad (10.70)$$

In ADAPS, the total covariance, X , is computed from (10.49) by solving \hat{X} from equations (10.62), (10.63) and (10.64) using the algorithm LYAK.

SECTION XI

CONCLUSIONS AND RECOMMENDATIONS

The overall objectives of this study were threefold: (1) development of theoretical analyses and mathematical models for precision weapon delivery, (2) development and documentation of computer analysis programs, and (3) demonstration of their use.

These objectives were primarily met. In the following, qualitative results and recommendations for future studies pertaining to the work reported in this volume are discussed.

SIGNIFICANT QUALITATIVE RESULTS

The following aspects of the technique developed in this study are considered significant:

The stochastic formulation of the weapon delivery problem is meaningful and tractable. It incorporates into the design the stochastic nature of the incident winds, the time-varying aircraft and weapon dynamics, and the finite-time nature of the weapon delivery control problem. It develops the full impact error covariance matrix using the overall system model. It handles high-order system descriptions, arbitrary sensor arrangements, arbitrary sensor noise levels, and arbitrary control points. The formulation defines an optimum controller, and it provides a criterion for measuring the quality of any linear controller. Its basis minimizing the CEP at impact is a meaningful and appealing design motivation. The technique makes the physical nature of the weapon delivery problem evident. The release covariance of the airframe and the impact propagation matrix of the weapon show where the control and measurement emphasis should be placed for the best delivery.

RECOMMENDATIONS FOR FUTURE ANALYSIS AND MODELING WORK

Many interesting issues came up in the course of the study:

- Optimal steering of aircraft from an arbitrary target acquisition point to weapon release. This can be posed as an optimal control problem with a nonlinear cost functional. It can be treated using iteratively quadratic control in the quadratic equivalence theory of Skelton.
- Although no simulation was required in this study, the developed model can simulate nonlinear aircraft and nonlinear weapons. To increase the simulation capability to automatic weapon

delivery a model of the nonlinear weapon release state predictor based on the current state of aircraft should be developed and incorporated into the program.

- For efficient piloted-weapon delivery analysis, the model of the operator should be incorporated into the program.
- The nominal trajectories for the linearization are generated by using a soft autopilot. The selection of suitable gains in the autopilot depends on past experience and trial-and-error process. To increase the versatility of the program, the algorithm designed for algebraic trim should be programmed, tested and incorporated into the program.
- In this study, an exact probability density function of the overall system is developed as a function of time. Therefore, the universally used assumption of small correlations in the CEP evaluation should be removed by using this density function. A good approximation to HPA should be developed using the full covariance matrix.

CONCLUSIONS

A reasonably powerful technique for the analysis and design of precision weapon delivery systems is developed in this study. The technique employs nonlinear modeling, linearization, stochastics, quadratics and a significant amount of digital computation. The optimum controller it produces minimizes the CEP at impact. Optimal time-varying as well as time-invariant gains can be evaluated for various airframes, control points, measurement points, and weapons.

The value of the approach lies in its mathematical models and algorithms. They provide total system analysis and design capability by a digital computer.

APPENDIX I

DEVELOPMENT OF A METHOD FOR FIXED-FORM OPTIMAL CONTROLLER DESIGN

A method is presented in this appendix which designs optimal algebraic controllers with limited number of states (i. e., fixed-form controllers) [55].

The method is based on the concept of orderly reduction of the elements of optimal full gain matrix to zero for the states which are not measured. This is achieved by adjusting the remaining elements (i. e., elements corresponding to measured states) while maintaining the optimality. It tacitly assumes the existence of solutions.

The program which implements the technique is called "PROGRAM PAPS". It enables one, among other things, to assess the performance degradations which occur when the complexity of a full set of optimal gains and a Kalman filter cannot be permitted.

In the following, the problem statement is given first. The method of solution is treated next.

PROBLEM STATEMENT

Given a time-invariant stochastic control system

$$\dot{x} = Fx + G_1 u + \xi \quad (I-1)$$

$$r = Hx + Du$$

x = vector of state variables

u = vector of controls

r = response vector

ξ = vector of disturbances such that

$$E\{\xi\} = 0 \quad E\{\xi(t) \xi'(\tau)\} = N\delta(t-\tau)$$

The problem is to minimize the performance index

$$J(K^1 + K^3) = \{ \text{tr} [H + D(K^1 + K^3)] Q [H + D(K^1 + K^3)]' x x' \} \quad (I-2)$$

with a controller of the form

$$u = (K^1 + K^3)x \quad (I-3)$$

In (I-3), K^1 is an $(m \times n)$ matrix with the following zero elements:

$$(K^1)_{ij} = 0 \quad j \in \Omega, \quad i = 1, 2, \dots, m$$

The set Ω denotes a prespecified collection of integers which define the unmeasured states. K_3 is an arbitrary fixed matrix.

METHOD OF SOLUTION

A gain matrix K corresponding to full-state measurement can be decomposed into the following components:

$$K = K^1 + \lambda K^2 + K^3, \quad \lambda = 1$$

λ is a scalar parameter with

$$\begin{aligned} K_{ij}^1 &= \begin{cases} K_{ij}(ij) & i \in \Omega_1 \\ 0 & i \notin \Omega_1 \end{cases} \\ K_{ij}^2 &= \begin{cases} K_{ij}(ij) & i \in \Omega_2 \\ 0 & i \notin \Omega_2 \end{cases} \\ K_{ij}^3 &= \begin{cases} K_{ij}(ij) & i \in \Omega_3 \\ 0 & i \notin \Omega_3 \end{cases} \end{aligned} \tag{I-4}$$

where the sets Ω_1 , Ω_2 , and Ω_3 denote preselected collections of integers which define the row and column indices of K^1 , K^2 and K^3 .

The necessary condition for the optimality of K^1 is

$$\left. \frac{\partial}{\partial K^1} J(K^1 + \lambda K^2 + K^3) \right|_{\lambda = 0} = 0 \tag{I-5}$$

To express K^1 as a function of λ , (I-5) can be written as

$$\frac{\partial}{\partial K^1} J(K^1 + \lambda K^2 + K^3) = 0 \quad (\text{with } K^2 \text{ and } K^3 \text{ constant and } \lambda \text{ arbitrary})$$

which implies $K^1 = K^1(\lambda)$.

Then by the Implicit Function Theorem $K^1(\lambda)$ is defined by the following differential equation:

$$\frac{dK^1(\lambda)}{d\lambda} = - \left[\frac{\partial^2 J(K^1 + \lambda K^2 + K^3)}{\partial K^1 \partial \lambda K^{1T}} \right]^{-1} \frac{\partial^2 J(K^1 + \lambda K^2 + K^3)}{\partial K^1 \partial \lambda} \quad (I-6)$$

A solution to equation (I-1) can be obtained by starting with any known terminal condition $K = K^1 + \lambda K^2 + K^3$ for $\lambda = 1$ and integrating (I-6) backwards to $\lambda = 0$. In the program the terminal condition used is the global optimum of the performance index J (i.e., the solution of the perfect sensing optimal quadratic control problem). In order to integrate (I-6), one must develop the indicated partials and select a numerical integration algorithm.

NUMERICAL INTEGRATION ALGORITHM

The numerical integration algorithm used to solve (I-6) is a predictor-corrector scheme [55] which employs the following equations:

(Predictor)

$$K^P = K^1(\lambda_K) + \frac{\Delta\lambda}{24} \left[55 \frac{dK^1}{d\lambda}(\lambda_K) - 59 \frac{dK^1}{d\lambda}(\lambda_{K-1}) + 37 \frac{dK^1}{d\lambda}(\lambda_{K-2}) - 9 \frac{dK^1}{d\lambda}(\lambda_{K-3}) \right] \quad (I-7)$$

(Corrector)

$$K^1(\lambda_{K+1}) = K^P - \left[\frac{\partial^2 J(K^P + \lambda_{K+1} K^2 + K^3)}{\partial K^1 \partial K^{1T}} \right]^{-1} \frac{\partial J(K^P + \lambda_{K+1} K^2 + K^3)}{\partial K^1} \quad (I-8)$$

where $\lambda_0 = 1$; $\lambda_K = \lambda_0 + K\Delta\lambda$, ($K = 1, 2, \dots, \frac{1}{\Delta\lambda}$).

In order to obtain enough "back information" to use (I-7), the first three predictor steps employ the following equation

$$K^P = K^1(\lambda_K) + \Delta\lambda \frac{dK^1}{d\lambda}(\lambda_K) \quad K = 1, 2, 3 \quad (I-9)$$

The major computational task is to evaluate the first and second partial derivatives in (I-6) and (I-8). A method to evaluate these partials is given in the next subsection.

METHOD OF EVALUATING PARTIAL DERIVATIVES

Let X denote the covariance matrix of system (I-1) with the controller $u = Kx$

$$(F+GK)X + X(F+GK)' + N = 0 \quad (I-10)$$

and corresponding to X , define an adjoint matrix S as follows:

$$(F+GK)'S + S(F+GK) + (H+DK)'Q(H+DK) = 0 \quad (I-11)$$

The performance index $J(K)$ of (I-2) is given by

$$J(K) = \text{tr} \{ (H+DK)' Q (H+DK) X \} + \text{tr} \{ SN \} \quad (I-12)$$

The first partial of J [55] is:

$$\frac{\partial J}{\partial K_{ij}} = 2 \text{tr} \{ [H+DK]' Q D + S G E^{ij} X \} \quad (I-13)$$

where

$$E^{ij} \triangleq \frac{\partial K}{\partial K_{ij}}$$

The second partials of J are

$$\begin{aligned} \frac{\partial^2 J}{\partial K_{ij} \partial K_{lm}} = 2 \left\{ (D' Q D)_{li} X_{jm} + \sum_a [(H+DK)' Q D + S G]_{ai} \left(\frac{\partial X}{\partial K_{lm}} \right)_{ja} \right. \\ \left. + \sum_a [(H+DK)' Q D + S G]_{al} \left(\frac{\partial X}{\partial K_{ij}} \right)_{ma} \right\} \quad (I-14) \end{aligned}$$

where $\frac{\partial X}{\partial K_{ij}}$ is defined by

$$(F+GK) \frac{\partial X}{\partial K_{ij}} + \frac{\partial X}{\partial K_{ij}} (F+GK)' + (G E^{ij}) X + X (G E^{ij})' = 0 \quad (I-15)$$

$$\frac{\partial^2 J}{\partial K_{ij} \partial \lambda} = 2 \text{TR} \left\{ (K D^2)' Q D E^{ij} X + [(H+DK)' Q D + S G] \left(K^2 \frac{\partial X}{\partial K_{ij}} + E^{ij} \frac{\partial X}{\partial \lambda} \right) \right\} \quad (I-16)$$

where $\partial X / \partial \lambda$ is defined by (I-15) with E^{ij} replaced by K^2 . Therefore, if the number of non-zero elements in K^1 is ℓ the partials required to solve (I-6) and (I-8) can be computed by solving $\ell + 3$ covariance equations for the matrices S , S

$$\frac{\partial X}{\partial K_{ij}} \quad (j \in \Omega \text{ a total of } \ell) \quad \text{and} \quad \frac{\partial X}{\partial \lambda}$$

The program PAPS implements these analytic developments.

APPENDIX II

DEVELOPMENT OF THE NOMINAL RELEASE EQUATIONS

In the analysis and design of weapon delivery systems, for a given attack maneuver and a slant range, the prediction of the nominal weapon release time is needed.

With a high-power airborne computer, the prediction of release time for hitting a target can be based on the six-degree-of-freedom weapon trajectory, computed on line, taking into account all miss-producing effects, and the current states of the aircraft. This may be referred to as "release with a perfect computer." To reduce demand on high computing power, however, a simplified model is usually used.

Since no real-time simulation is involved in ADAPS, the prediction of nominal release time is based on the integration of six-degree-of-freedom trajectory equations (i. e., perfect computer). For determining the magnitude of timing errors in release, the release model must be developed separately by the user as it depends heavily on the fire control system being evaluated. In the following one such model is developed for completeness.

DEVELOPMENT OF NOMINAL WEAPON RELEASE EQUATIONS

It is assumed that the position vector of the bomb's trajectory is given by

$$\vec{r}_w(\tau) = \vec{r}_r + \int_0^\tau \vec{v}_r d\tau + \int_0^\tau \int_0^s \dot{\vec{v}} ds d\tau \quad (\text{II-1})$$

where

\vec{v}_r = weapons velocity at $\tau = 0$

$\dot{\vec{v}}$ = weapons acceleration

The acceleration term can be decomposed into contributions due to gravity, aerodynamic drag per unit mass, lift per unit mass, rotational effects per unit mass, etc. In order to avoid line integrals given by (II-1), it will be assumed that all these effects can be lumped into the form of [56]

$$\vec{g}_e = k \vec{g} \quad (\text{II-2})$$

That is, the bomb "sees" gravity as equivalent to \vec{g}_e . In addition, the drag terms affecting the forward velocity are neglected. With these assumptions, (II-1) can be written as

$$\vec{r}_w(\theta, \tau) = \vec{r}_r(\theta) + \vec{v}_r(\theta)\tau + \frac{1}{2}\vec{g}_e\tau^2 \quad (\text{II-3})$$

Referring to Figure 51, the miss-vector, $\vec{\tilde{r}}$, (i.e., the position vector from target to weapon) can be expressed as

$$\vec{\tilde{r}}(\theta, \tau) = \vec{r}_w(\theta, \tau) - \vec{r}_T \quad (\text{II-4})$$

$$= \vec{r}_r(\theta) + \vec{v}_r(\theta)\tau + \frac{1}{2}\vec{g}_e\tau^2 - \vec{r}_T \quad (\text{II-5})$$

Now the problem becomes finding θ and τ such that

$$\vec{\tilde{r}}(\theta, \tau) = 0 \quad (\text{II-6})$$

Equation (II-6) forms the basic part of the so-called fire control equations.

This algebraic problem can be solved in various ways. One approach is to evaluate

$$J^{**} = \min_{\theta} \min_{\tau} |\vec{\tilde{r}}(\theta, \tau)| \quad (\text{II-7})$$

which overrides the questions of existence of solutions to (II-6).

In the following the existence of solutions to (II-6) is assumed and a solution algorithm is developed as given in [42] (see Section VII also).

In matrix notation (II-6) is expressed as

$$\begin{pmatrix} \tilde{x} \\ \tilde{z} \end{pmatrix} = \begin{bmatrix} f_1(\theta, \tau) \\ f_2(\theta, \tau) \end{bmatrix} = \begin{pmatrix} 0 \\ 0 \end{pmatrix} \quad (\text{II-8})$$

where

$$\begin{bmatrix} f_1(\theta, \tau) \\ f_2(\theta, \tau) \end{bmatrix} = \begin{bmatrix} \vec{r}_r(\theta) \\ \vec{z}_r(\theta) \end{bmatrix} + \begin{bmatrix} \vec{u}_r(\theta) \\ \vec{w}_r(\theta) \end{bmatrix} \tau + \frac{1}{2} \begin{bmatrix} 0 \\ \text{kg} \end{bmatrix} \tau^2 - \begin{bmatrix} \vec{x}_T \\ \vec{z}_T \end{bmatrix} \quad (\text{II-9})$$

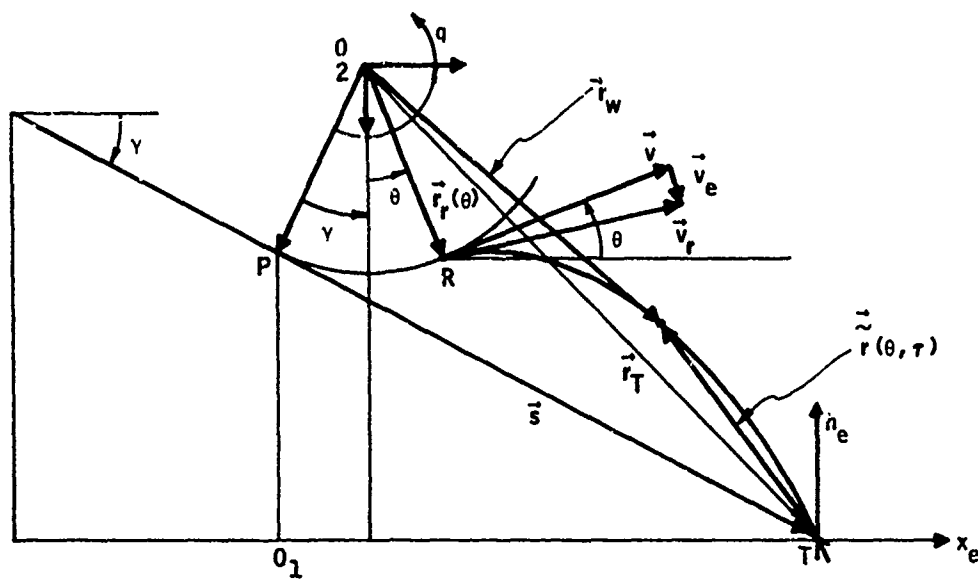


Figure 51. Weapon-Release Geometry in the x_e - z_e Plane

With ejection velocity \vec{v}_e along \vec{r}_r , the velocity term in II-9 becomes

$$\begin{pmatrix} u_r \\ w_r \end{pmatrix} = \begin{bmatrix} v_e & V \\ -V & v_e \end{bmatrix} \begin{pmatrix} \sin \theta \\ \cos \theta \end{pmatrix} \quad (\text{II-10})$$

On the other hand, letting

$$r(\theta) = \begin{bmatrix} \sin \theta \\ \cos \theta \end{bmatrix}, \quad q = \frac{V}{R}, \quad \text{and} \quad q_e = \frac{v_e}{R} \quad (\text{II-11})$$

one can write

$$\begin{pmatrix} x_r \\ z_r \end{pmatrix} = R r(\theta) \quad (\text{II-12})$$

Substituting (II-10), (II-11) and (II-12) into (II-9), collecting terms and dividing throughout by R yields the normalized miss-vector equation

$$\bar{f}(\theta, \tau) = \begin{bmatrix} \bar{f}_1(\theta, \tau) \\ \bar{f}_2(\theta, \tau) \end{bmatrix} = \{ [I + Q\tau] r(\theta) + \frac{g_e}{2R} \tau^2 - \eta_T \} = \begin{bmatrix} 0 \\ 0 \end{bmatrix} \quad (\text{II-13})$$

where

$$Q = \begin{bmatrix} q_e & q \\ -q & q_e \end{bmatrix} \quad (\text{II-13a})$$

and

$$\eta_T = \frac{\vec{r}_T}{R} \quad (\text{II-13b})$$

with

$$r_T = \begin{pmatrix} x_T \\ z_T \end{pmatrix} = \begin{bmatrix} -R & S \\ S & R \end{bmatrix} \begin{pmatrix} \sin \gamma \\ \cos \gamma \end{pmatrix} \quad (\text{II-13c})$$

DEVELOPMENT OF THE FIRE CONTROL ALGORITHM

Let $\xi \triangleq \begin{bmatrix} \theta \\ \tau \end{bmatrix}$ and define

$$\phi(\xi, h) = \bar{f}(\xi) - \bar{f}(\xi_0)(1-h) = 0$$

For $h = 0$ and $\xi = \xi_0$ one gets $\phi(\xi_0, 0) = 0$.

For $h = 1$, $\phi(\xi, 1) = \bar{f}(\xi) = 0$. This implies that if one can maintain $\phi(\xi, h) \equiv 0$ by properly choosing the values of ξ while increasing h from zero to one, the value of ξ at $h = 1$ becomes the solution vector to $\bar{f}(\xi) = 0$.

Using the implicit function theorem:

$$\frac{\partial \phi}{\partial \xi} \delta \xi + \frac{\partial \phi}{\partial h} \delta h = 0 \quad (\text{II-15})$$

If $(\partial \phi / \partial \xi)$ is invertible then

$$\frac{d\xi}{dh} = - \left(\frac{\partial \phi}{\partial \xi} \right)^{-1} \left(\frac{\partial \phi}{\partial h} \right) \quad (\text{II-16})$$

But

$$\frac{\partial \phi}{\partial \xi} = \frac{\partial \bar{f}}{\partial \xi} \quad \text{and} \quad \frac{\partial \phi}{\partial h} = \bar{f}(\xi_0) \quad (\text{II-17})$$

Therefore

$$\frac{d\xi}{dh} = - \left(\frac{\partial \bar{f}}{\partial \xi} \right)^{-1} \bar{f}(\xi_0) \quad (\text{II-18})$$

With the given h_0 and ξ_0 this differential equation is integrated up to $h = 1$ to get ξ . Now

$$\bar{f}(\xi) = [I + Q\tau] r(\theta) + \frac{g_e}{2R} \tau^2 - \eta_T \quad (\text{II-19})$$

and

$$\frac{\partial \bar{f}}{\partial \xi} = F(\xi) = \begin{pmatrix} \frac{\partial \bar{f}}{\partial \theta} & \frac{\partial \bar{f}}{\partial \tau} \end{pmatrix}$$

where

$$\begin{bmatrix} f_{11} & f_{12} \\ f_{21} & f_{22} \end{bmatrix} = [(I + Q\tau) P r(\theta) \mid Q r(\theta) + a\tau] \quad (\text{II-20})$$

with

$$P = \begin{bmatrix} 0 & 1 \\ -1 & 0 \end{bmatrix}, \quad a = \begin{pmatrix} 0 \\ kg \end{pmatrix} \quad (\text{II-21})$$

If Euler's integration algorithm is used, one can write from (II-18)

$$\begin{pmatrix} \theta \\ \tau \end{pmatrix}_{k+1} = \begin{pmatrix} \theta \\ \tau \end{pmatrix}_k - F^{-1}(\theta_k, \tau_k) b \quad (\text{II-22})$$

where

$$b = \bar{f}_0 \Delta h$$

and (II-20) is iterated from $k = 0$ to $k = \frac{1}{\Delta h} = N$.

To establish startup values for the fire control algorithm, select

$$\theta_0 = \tan^{-1} \frac{V_e}{V} \quad (\text{I-23})$$

and compute τ_0 so that $\tilde{z}_0 = f_2(\theta_0, \tau) = 0$. This gives

$$\tau_0 = \sqrt{\frac{2(z_T - R)}{kg}} \quad (\text{II-24})$$

Substituting this into f_1 in (II-9) gives the normalized range error at the beginning of the iteration

$$\tilde{x}_0 = f_1(\theta_0, \tau_0) = V_r \tau_0 - x_T \quad (\text{II-25})$$

Thus, following equations are used to start up the iterations:

$$\left(\frac{\theta_o}{\tau_o}\right) = \left(\frac{\tan^{-1} \frac{V_e}{V}}{\sqrt{\frac{2(z_{\tau} - R)}{\tau_{kg}}}}\right) \text{ and } \bar{f}_o = \frac{1}{R} \left(\frac{V_r \tau_o - x_{\tau}}{0}\right) \quad (\text{II-26})$$

After having found ξ_p so that (II-13) is satisfied, the predicted time during "pullup" is given by

$$t_{pu} = \frac{\gamma + \theta_p}{q} \quad (\text{II-27})$$

Due to simplifications used in the modeling of the weapon trajectory, the predicted nominal release time t_{pu} must be corrected. This correction is in the form of

$$t_r = k_c t_{pu} + \Delta t_c - \Delta t \quad (\text{II-28})$$

where

k_c = algorithmic error correction multiplier

Δt_c = algorithmic error correction bias

Δt = known delay in the release mechanism

Obviously, the actual nominal release will occur at

$$t_{ra} = k_c t_{pu} + \Delta t_c \quad (\text{II-29})$$

The correction multiplier k_c and bias Δt_c are obtained from numerical experiments with actual six-degree-of-freedom weapon model.

REFERENCES

1. Paskin, H. M., Exhibit A, RFP No. F33615-70-R-2259, USAF, Aeronautical Systems Division, Wright-Patterson AFB, Ohio, June 1970.
2. Rankine, Jr., R. R., "The Effects of Aircraft Dynamics and Pilot Performance on Tactical Weapon Delivery Accuracy," PhD Thesis, UCLA, 1970.
3. Allen, R. W., W. F. Clement, and H. R. Jex, "Research on Display Scanning, Sampling, and Reconstruction Using Separate Main and Secondary Tasks," Systems Technology, Inc., Technical report 170-2, July 1969.
4. McRuer, D. T., D. Graham, E. Krendel, and W. Reisener, Jr., "Human Pilot Dynamics in Compensatory Systems: Theory, Models, and Experiments with Controlled Element and Forcing Function Variations," Air Force Flight Dynamics Laboratory, Technical report AFFDL-TR-65-15, July 1965.
5. McRuer, D. T. and H. R. Jex, "A Review of Quasi-Linear Pilot Models," Institute of Electrical and Electronics Engineers. Trans. on Human Factors in Electronics, 8: p. 231-49, September 1967.
6. Geers, D. C., and W. L. Maberry, "Accuracy Analysis of F-4D Weapon Delivery System," Report A563, Vol. II, McDonnell Aircraft Corporation, June 1965.
7. New, N. C., "Bomb Delivery Maneuvers," NAVWEPS Report 9004, U. S. Naval Ordnance Test Station, March 1966.
8. Development of Weapon Delivery Models and Analysis Programs, Document 6D-A-5, Systems and Research Division, Honeywell, July 1970.
9. Epstein, C. S., "The Application of Weapon Compatibility Technology to Present and Future USAF Aircraft," 1969 Aircraft/Stores Compatibility Symposium Proceedings, Vol. I, p. 1-1.
10. Epstein, C. S., "Aircraft/Munitions Compatibility -- USAF Project SEEK EAGLE," paper No. 43, 8th Navy Symposium on Aeroballistics, May 1969.
11. Harvey, C. A., "Application of Optimal Control Theory to Launch Vehicles -- Final Technical Report," prepared for NASA Contract NAS8-21063, July 1968.

12. Bean, H.E., "General-Purpose Aircraft Simulation System," Honeywell Aerospace Division, Minneapolis, AM-173, 22 April 1968.
13. Brown, R.C., et al, "Six-Degree-of-Freedom Flight Path Study Generalized Computer Program, Part I, Problem Formulation, WADD Technical Report 60-781.
14. Churchyard, J.N., "Homine Six-Degree-of-Freedom Flight Path Study Generalized Computer Program," Report No. 7920-03, U.S. Army Mobility Equipment Research and Development Command, Fort Belvoir, Virginia.
15. Thelander, J.A., "Aircraft Motion Analysis," Technical Documentary Report TDL-IDR-64-70, March 1965.
16. Etkin, P., Dynamics of Flight Stability and Control, John-Wiley Sons, Inc., New York, 1959.
17. Cohen, C.J., and D. Werner, "A Formulation of the Equations of Motion of a Four-Finned Missile," NPG Report No. 1474, September 27, 1956.
18. Goldstein, E., Classical Mechanics, Addison-Wesley Publishing Co., Inc., Cambridge, Massachusetts.
19. Tait, P.G., An Elementary Treatise on Quaternions, The University Press, Cambridge.
20. Mitchell, E.E.L., and A.E. Rogers, "Quaternion Parameters in the Simulation of a Spinning Rigid Body," Simulation, June 1965.
21. Whittaker, E.E., A Treatise on the Analytical Dynamics of Particles and Rigid Bodies, Fourth Edition, Dover Publications, 1944.
22. Hildebrand, F.B., Introduction to Numerical Analysis, McGraw-Hill Book Company, Inc., New York, 1965.
23. Hakanson, H., "Simstab Computer Program," Ordnance Division, Honeywell Inc., Hopkins, Minnesota.
24. Autio, G., "Hot Impact Bomb Sight Program," Systems and Research Division, Honeywell Inc., Roseville, Minnesota.
25. Rhodes, C.W., and J.H.W. Shannon, "Results and Conclusions of the Joint R.A.E./W.R.E. Research Program on the Flight Dynamics and Ballistic Consistency of Freely Falling Missiles," Royal Aircraft Establishment Technical Report No. 65200, December 1965.

26. Lehner, Paul, "Static Stability Tests of the M-117 Bomb at Mach Numbers from 0.55 to 1.30 with Seven Tail-Fin Configurations," AEDC-TR-68-103, May 1968.
27. Homan, M. L., "Static Stability Characteristics of the M-117 Bomb at Mach Numbers from 0.60 to 1.40 with Three Tail Configurations," AEDC-TR-162, July 1968.
28. Murphy, C. H., "Fire Flight Motion of Symmetric Missiles," BRL Report No. 12106 RDT and E, Project No. 17010501A005, July 1963.
29. MK-82 Aerodynamic Coefficients, Air Force Armament Laboratory, Eglin Air Force Base, Florida.
30. Skelton, G. B., "Investigation of the Effects of Gusts on V/STOL Craft in Transition and Hover," AFTDL-TR-68-85, June 1968.
31. Atmospheric Disturbances, Mil. Spec. MIL-F-8785B, Section 3.7.
32. Lappe, U. O. and J. Clodman, "On Developing a Low-Altitude Turbulence Model for Aircraft Gust Loads," ASD-TDR-62-152. Aeronautical Systems Division of the Air Force Systems Command, Wright-Patterson AFB, Ohio, March 1962.
33. Lappe, U. O., R. H. Thuillier, and R. W. Reeves, "Development of a Low-Altitude Turbulence Model for Estimating Gust Loads on Aircraft," ASD-TDR-63-318. Aeronautical Systems Division of the Air Force Systems Command, Wright-Patterson AFB, Ohio, July 1963.
34. Lappe, U. O., "Design of a Low-Altitude Turbulence Model for Estimating Gust Loads on Aircraft," AFFDL-TR-64-170. Air Force Flight Dynamics Laboratory, Research and Technology Division of the Air Force Systems Command, Wright-Patterson AFB, Ohio, March 1965.
35. Lappe, U. O., "Low-Altitude Turbulence Model for Estimating Gust Loads in Aircraft," AIAA Journal of Aircraft, Vol. 3, No. 1, January-February 1966.
36. Yore, E. E., "Requirements for Minimum Backup Flight Control Systems," AFFDL-TR-70-48, June 1970.
37. Air Data Computer, Document PSD-102-A, Honeywell, Minneapolis, Minnesota, September 1970.
38. Livingstone, S. P., and W. Gracey, "Tables of Airspeed, Altitude, and Mach Number," Technical Note D-822, NASA.
39. Graham, K. D., "Kinematic Model for Fire Control," MR 10757, Honeywell Systems and Research Division, Research Department, Minneapolis, Minnesota, August 7, 1969.

40. Coddington, E.A. and N. Levinson, Theory of Ordinary Differential Equations, McGraw-Hill Book Co., Inc., New York, 1955.
41. Traub, J.F., "Iterative Methods for the Solution of Equations," Prentice Hall, Inc., Englewood Cliffs, N.J., 1964.
42. Kane, T.R., "Real Solutions of Sets of Nonlinear Equations," AIAA Journal, Vol. 4, No. 10, 1966.
43. Booth, A.D., Numerical Methods, Butterworth's Scientific Publications, Ltd., London, 1965.
44. Peterson, E.L., Statistical Analysis and Optimization of Systems, John Wiley and Sons Co., New York, 1961.
45. Papoulis, A., Probability, Random Variables, and Stochastic Processes, McGraw-Hill Book Co., New York, 1965.
46. Edinger, L.D., et al, "Design of a Load-Relief Control System," NASA Contractor Report CR-61169, April 21, 1967.
47. Kalman, R.E., "Contributions to the Theory of Optimal Control," Bol. Soc. Mat. Mex., 1961.
48. Bliss, G.A., Lectures on the Calculus of Variations, University of Chicago Press, Chicago, Illinois, 1946, Part II.
49. Ward, M.D., "Application of Optimal Control Theory to Launch Vehicles Computer Program Documentation," NAS8-21063.
50. Kalman, R.E., and R.S. Bucy, "New Results in Linear Filtering and Prediction Theory," ASME Trans. (J. of Basic Eng.), Vol. 83D, March 1961, pp. 95-108.
51. Kalman, R.E., "A New Approach to Linear Filtering and Prediction Problems," ASME Trans. (J. of Basic Eng.), Vol. 83D, March 1960, pp. 35-45.
52. Kalman, R.E., "New Methods and Results in Linear Prediction and Estimation Theory," Tech. Report 61-1, Research Inst. for Advanced Studies, Baltimore, Md., 1961.
53. Konar, A.F., "Improved-Iterative-Algorithm for Solving the Lyapunov Equation," memo to D.L. Markusen, 16 June 1969, MR 10702.
54. Kleinman, D.L., "On an Iterative Technique for Riccati Equation Computations," IEEE Trans. on AC, February 1968.

55. Stein, G., "Practicalization Algorithms," memo to G. B. Skelton, 13 January 1970, MR 10861.
56. Wrigley, W., and J. Hovorka, "Encyclopedia of Fire Control, Vol. 1, Fire Control Principles," Instrumentation Laboratory, MIT, June 1957.
57. Konar, A. F., "Synthesis of Optimal Hybrid Control Systems," PhD Thesis, Center for Control Sciences, University of Minnesota, March 1969.